CORROSION INHIBITORS FOR CONCRETE CORROSION - AN OVERVIEW

M. Pandiarajan[a]*, S. Rajendran[a],[b]*, J. Sathiyabama[a], J. Lydia Christy[c], J. Jeyasundari[d], P. Prabhakar[e]

Keywords: corrosion inhibitors, concrete.

Reinforced concrete is widely used for building materials and plays a significant role in economic development. However, the premature degradation of reinforced concrete structures due to the reinforcing steel corrosion has become a serious problem in modern society, which results in a huge economic loss. Under normal conditions, reinforcing steel in concrete can be protected from corrosion by forming a compact passive film on its surface in concrete pore solution with high alkalinity (pH 12.5-13.5). However, the passive film can be locally damaged and the localized corrosion of reinforcing steel takes place when pH and/or the chloride concentration at the steel/concrete interface reach the critical values for corrosion. Corrosion behaviour of metals and alloys in concrete solution has been investigated in presence and absence of inorganic and organic inhibitors. Usually carbon steel and steel rebars have been used. Sometimes galvanized steel and SS316L have been used. Organic inhibitors, inorganic inhibitors, and natural products have been used as inhibitors along with concrete admixture. Corrosion resistance of metals has been evaluated by weight loss method, electrochemical studies such as polarization study and AC impedance spectra. Galvanostatic pulse technique has also been employed. The protective film formed on the metal surface have been analyzed by SEM, FTIR spectroscopy, XPS, AFM and EDAX. The protective film consists of metal-inhibitor complex, calcium carbonate and calcium hydroxide. Experiments have been carried out at room temperature. Corrosion inhibitors fill up the pores and prevent the penetration chloride ion towards the metal surface. Passive films formed on the metal surface also increase the life time of concrete rebars.

* Corresponding Authors

[a] Corrosion Research Centre, PG and Research Department of Chemistry, G.T.N Arts College, Dindigul- 624 005, India. E-mail: pandiarajan777@gmail.com
[b] Corrosion Research Centre, R.V.S. School of Engineering and Technology, Dindigul- 624 005, India. E-mail: srmjoany@sify.com
[c] Department of Chemistry,VSB Engineering College, Karur-639 111, India.
[d] PG Department of Chemistry, SVN College, Madurai, India.
[e] PG and Research Department of Chemistry, APA College of Arts and Culture, Palani, Dindigul, India.

Introduction

Corrosion behaviour of metals and alloys in concrete solution has been widely studied[1–65]. In the past, most of the design studies in the literature and research in reinforced concrete assumed that the durability of reinforced concrete structures could be taken for granted. However, many reinforced concrete structures are exposed during their lifetimes to environmental stress (for example, corrosion and expansive aggregate reactions) which attacks the concrete or steel reinforcement[66]. Researchers and engineers are continuously in search of cost-effective means to prevent the corrosion of reinforcing steel for the duration of a concrete structure's design life. The cement paste in concrete is alkaline with a pH typically between 12 and 14. This paste forms a passive film surrounding reinforcing steel in concrete which further thicken iron oxide layer on the steel surface. Many researchers believe this alkaline environment facilitates the protective passive film around the steel[67,68]. The passive film is not invulnerable, though it can be damaged both chemically and mechanically. Some examples of chemical damage are carbonation, chloride ingress (seawater, de-icing salt, unwashed sea sand, admixtures etc) and sulphate attack. Proper design and preparation of concrete in accordance with relevant standards and timely maintenance of the structures under those conditions would guarantee them a long and efficient life in aggressive media. However, these requirements are not always met and adhered to. Preventive measures being used in the construction industry to salvage the service life of steel reinforcement in concrete structures are cathodic protection, inhibitors, coatings, penetrating sealers and chloride removal[69]. One of the practiced methods popularly used for the control of steel corrosion in concrete is the corrosion inhibitors either preventive or curative.

In recent years, the use of these inhibitors in producing high performance concrete has increased significantly. Inhibitors are chemical substance that decreases the corrosion rate when present in the corrosion system at suitable concentration without significantly changing the concentration of any other corrosion agent[70]. Many synthetic compounds (inhibitors) were developed to combats this endemic corrosion problem, but most of them are highly toxic to both human beings and environment[71]. Inhibitors toxicity according to ref. [72] is measured as lethal dose (LD) and lethal concentration (LC). LD_{50} is the lethal dose of a chemical at which 50% of a group of animals are killed for 24 h exposure time, whilst LC_{50} is lethal concentration in air or water which kills 50% of test population. Inhibitor biodegradation or biological oxygen demand (BOD) should at least be 60%. The BOD is a measure of how long the inhibitor will persist in the environment. Hence it becomes imperative to review the current inhibitors in order to find more appropriate, suitable and sustainable inhibitor.

Metals

Corrosion resistance of various metals in concrete solution has been investigated. Corrosion resistance of various metals such as Fe[3,4,5,6,7,8,10,11,12,13,17], carbon steel[9,54,62], mild steel[1,15,16,18,20,24,25,29,30,31], stainless steel[19,40,44,65] and galvanized steel[14,19,22,50,57] has been investigated.

Inhibitors

Among various inhibitors which have been used along with concrete admixtures, mention may be made of trisodium citrate[2], phosphate, nitrite[37], sodium gluganate[4], calcium nitrate, calcium nitrite[5], sodium molybdate[6], di-2 ethylhexyl sebacate[11], and uracil derivatives[13]. Organic inhibitors[2,4,8,9,11,12,13,48,61] have been used to control the corrosion of various metals and its alloy in various medium.

Medium

The inhibition efficiency of various inhibitor is controlling corrosion of metals and its alloys in SCPS medium [1,2,3,7,8,9,10,11,12,13,14], concrete medium[5,15,16,17,19,20,21,22,23,25] and alkaline medium[3,6,30,34,36,38] have been investigated.

Methods

Various methods have been used to evaluate the inhibition efficiency of corrosion inhibitors. Usually weight loss method[1,2,15,30,39,47,52,53,60], Electrochemical studies (polarization and AC impedance)[3,4,5,6,7,8,9,,12,13,14,15,18] and Galvanostatic pulse technique[34], and Gravimetric measurement[46] studies have been employed.

Surface analysis

The protective film formed on the metal surface, during the process of corrosion protection of various metals by inhibitors have been analyzed by various surface analysis technique such as SEM[3,10,14,62,64], FTIR[3,13,51], XPS[13,33], AFM[64], and EDAX[14,29]. In general it has been observed that the protective film consists of the metal-inhibitor complex along with $CaCO_3$ and $Ca(OH)_2$.

Temperature

The inhibition efficiency of various inhibitors has been evaluated at room temperature[29].

Mechanism of enhanced corrosion resistance

It is observed that when inhibitors are used along with simulated concrete pore solution, the corrosion resistances of metals increase. In general, it is due to adsorption of these inhibitors on the metal surface and forming metal-inhibitor complex. It is also due to strengthening of $CaCO_3$ and $Ca(OH)_2$ deposits on the metal surface. The inhibitors may fill up the pores in the concrete structures, which are formed in the absence of inhibitors[59]. The inhibitors may further prevent the penetration of corrosive ions such as chlorides and sulphate towards the metal surface[59]. Organic inhibitors are specially used for this purpose. The inhibitors may be hydrophobic in nature[57] and prevent the water molecules reaching the metal surface. However after long time exposure (two years) the chloride ions break the protective film formed on the metal surface, in presence of phosphate and nitrite[3]. When calcium nitrate is used 3% dosage is enough to protect the rebar against corrosion[5]. When sodium molybdate is used passive film is formed on steel rebar[5,6]. The aggressiveness of chloride ion in concrete structures has been minimized by addition of inhibitors such as sodium nitrite[7] and disodium mono fluorophosphate[12]. The improved corrosion resistance in presence of uracil derivative is due to Langmuir adsorption isotherm of inhibitor on the metal surface[13]. Apart from inhibitors addition of red mud along with concrete structures improve corrosion resistance of metals. This has been confirmed by electrochemical measurements and electrical resistivity[17].

Zinc coating[23], and Epoxy coating on the steel rebar have improved the bond strength. Fluoride ion even in very low concentration (< 25 ppm) is found to be more corrosive than chloride ion[30]. Hence care must be taken to avoid presence of fluoride ion in water used to prepare concrete admixture. Zinc phosphate coating considerably reduced the corrosion rate of mild steel even in chloride medium[36].This has been confirmed by electrochemical studies. When sodium nitrite is used as inhibitor, the stability of the protective film increases[37]. Among the oxyanions, the use of dichromate has been found to be very effective for mild steel[43]. Corrosion resistance of mild steel has been investigated in carbonated and non-carbonated concrete, in presence of sodium monosulphate[46]. Use of steel wire mesh reinforcement in ferrocement has been investigated. Addition of inhibitors such as calcium nitrite and tannic acid improved the corrosion resistance. Sodium nitrite has the ability to fill up the pits formed during corrosion process, by formation of passive films, in carbonated concrete pore solution. This has been confirmed by electrochemical noise measurement[54]. The use of inhibitors along with, concrete admixture improved the corrosion resistance of metals. Various inhibitors and various metals and alloys used in this line are summarized in Table 1.

Conclusion

Corrosion behaviour of metals and alloys in concrete solution has been investigated in presence and absence of inorganic and organic inhibitors. Usually carbon steel and steel rebars have been used. Sometimes galvanized steel and SS316L have been used. Organic inhibitors, inorganic inhibitors and natural products have been used as inhibitors along with concrete admixture.

Corrosion resistance of metals has been evaluated by weight loss method, electrochemical studies such as polarization study and AC impedance spectra. Galvanostatic pulse technique has also been employed. The protective film formed on the metal surface have been analyzed by SEM, FTIR spectroscopy, XPS, AFM, and EDAX. The protective film consists of metal-inhibitor complex, calcium carbonate and calcium hydroxide. Experiments can be carried out at room temperature. Corrosion inhibitors fill up the pores and present the penetration chloride ion towards the metal surface passive films formed on the metal surface also increase the life time concrete rebars.

Table 1. Inhibitors used to improve the corrosion resistance of metals in concrete admixture

Sl. No	Metal	Medium	Inhibitor	Additive	Method	Findings	Ref
1.	Mild steel, Galvanized steel, SS316L	Simulated concrete pore solution	-	-	Weight loss, Polarization, AC Impedance	Corrosion resistance decrease in scp solution in the order of SS316L>GS>MS	1
2.	SS316L	Simulated concrete pore solution	Tri sodium Citrate	-	Weight loss, Polarization, AC Impedance	Corrosion resistance of SS316L decrease in presence of Tri sodium citrate	2
3.	Steel	Alkaline medium	Phosphate and Nitrite	-	EIS, PC, OCP, SEM, XRD, FTIR	The efficiency of the tested inhibitors decreases with time after two years of immersion in chloride solution.	3
4.	Steel	Simulated concrete pore solution	D-Sodium glucanate	-	EIS	Formation of an adsorptive film on the steel surface	4
5.	rebar	Concrete	Calcium Nitrate, Calcium Nitrire, Potassium Nitrate	-	Electro chemical measurements	Inhibitor dosage on 3-4% of cement weight seems sufficient to protect the rebar against corrosion	5
6	Steel	5% NaCl SCP	Sodium Molybdate	-	Polarization, AC Impedance, Mott- Schotty Analysis Technique	Passive film formed on steel rebar surface in the presence of sodium molybdate	6
7.	Steel	SCP	Sodium Nitrite	-	Linear Polarization resistance, electrochemical impedance spectroscopy	The corrosion rate of Reinforcing Steel decreased with NO_2^- increasing concentration in SCP with Cl^-	7
8.	Steel	SCP	N-Laruroyl Sarcosine Sodium	-	Polarization, AC Impedance	Best inhibition effect on reinforcing steel in SCP	8
9.	Carbon Steel	SCP	Benzotriazol	-	Polarization, AC Impedance	Benzotriazol is a potentially attractive alternative to nitrites for inhibiting corrosion of reinforced in concrete	9
10.	Steel	SCP	Sodium Nitrate and D-Sodium GluGanate	-	SEM	The inhibition efficiency of the inhibitor was 99%	10
11.	Steel	SCP	di-2 ethyl hexyl sebacate	-		Anodic reaction of steel electrode was suppressed	11
12.	Steel	SCP	Disodium Mono flouro Phosphate	-	Polarization, AC Impedance, EIS	The Electrochemical reaction can be suppressed by forming a disposition film in the steel concrete. interface which retards the attack by aggressive Cl^-	12
13.	Steel	SCP	Uracil derivative	-	Polarization, FITR, XPS	Langmuir adsorption isotherm	13
14.	Hot dip Galvanized coated rebar	SCP	Molybdenum-Phosphorus	-	EIS, Raman Spectroscopy, SEM, EDXA, XRD	These Studies are expected to provide a new area in development of lesser polluting protective passive layer on galvanized coatings	14
15.	Mils Steel	Concrete	Zinc oxide	-	Weight loss, Potential time behavior and anodic polarization technique	The passivity of steel maintained by the addition of zinc oxide	15
16.	Zinc, Galvanized Steel, Mild steel	Concrete	-	-	Microscopy and X-ray micro analysis	Corrosion behavior of Zinc, Galvanised steel, Mild steel in concrete studied	16
17.	Steel	Concrete	-	Red mud	Conductivity of the anolyte electro chemical measurements, Electrical resistivity	The addition of the red mud is beneficial to concrete	17
18.	Mild Steel	Ferro cement	-	Cement Slurry Coating	Impedance, Anodic polarization	Cement slurry coating give better protection efficiency	18
19.	Bare mild Galvanized Epoxy coated Stainless Steel	Concrete	-	-	Reinforcing material and chloride content Studied	Among corrosion resisting Steels, the best durability performance is exhibited by the Stainless-clad reinforcing bars	19

DOI: 10.17628/ECB.2013.2.1

Table 1. (cont.) Inhibitors used to improve the corrosion resistance of metals in concrete admixture

Sl. No	Metal	Medium	Inhibitor	Additive	Method	Findings	Ref
20.	Mild steel	Concrete	-	5% NaCl	AC impedance, Linear polarization	Formation of Surface layer on the rods	20
21.	Steel	Concrete	-	-	Resistance measurement	Corrosion current, corrosion potential values measured	21
22.	Galvanized Steel	Concrete	-	-	X-ray diffraction	All Zn must corrode before any of the underlying steel. Corroded	22
23.	Steel	Concrete	Zinc coating	-	-	The coated reinforcement has also been found to result in about 50 percent greater bond Strength as compared to Similar but uncoated plain mild steel	23
24.	Mild Steel	Dilute Sodium Nitrate, Chloride Contaminated concrete	Cathodic current	-	-	Cathodic System is to induce passivation	24
25.	Mild Steel	Concrete	Epoxy Coating	-	-	The coated Steel rebar improved the bond Strength.	25
26.	Steel	Concrete	-	-	Linear Polarization Resistant, Zero resistant ammeter	Decreasing the frequency of cracking leads to a decrease in corrosion	26
27.	1. Polished Steel 2. Unpolished Steel	SCP	Calcium Nitrite	-	-	Evaluated for their apparent influence on passivity and corrosion rate.	27
28.	Steel	SCP	Hydroxy alkyl amine	-	-	The efficiency of migrating corrosion inhibitor in reducing corrosion of steel has been investigated.	28
29.	Mild steel	SCP	-	-	Polarization, Impedance. SEM, EDAX	Protective film formed on the reinforcing steel	29
30.	Mild Steel	0.01 N NaOH, Saturated lime water, Cement Slurry, and embedded mortars	-	-	Weight loss, Electrochemical DC cyclic polarization and polarization resistance, Surface topographic and X-ray diffraction	Accelerating effect of fluoride (<25 ppm) has almost double corrosive effect than noted for equal concentration of chloride ion	30
31.	Mild Steel	SCP	-	-	Polarization, AC impedance	R_{ct}, R_f ,ci values measured	31
32.	Mild steel, Low alloy Steel	Concrete	-	-	DC polarization, AC impedance, acoustics emission, and SEM	The rate of increase in corrosion rate with chloride content in mortars is considerably higher for MS than the LAS	32
33.	Mild Steel	SCP	-	-	Polarization, EDS, XRD, XPS	At the free corrosion potential in an aerated solution, a decrease of the carbonate content increases the corrosion rate	33
34.	Mild Steel	Alkali activated cement	-	NaCl	Galvanostatic pulse method	Oxidation of sulphide anions to sulphur prevents potential rising into the pitting regime and leads to inhibition of the oxygen cathode reaction	34
35.	Mild steel	concrete	Cement polymer composite, Interpenetrating polymer network coating and epoxy coating	-	Open circuit potential measurement	Corrosion performance measured	35
36.	Mild steel	Concrete	Zinc Phosphate	-	Potentio dynamic polarization, cronoamperometry and EIS, XRD, SEM	Corrosion rate is considerably lowered by this phosphate coating	36
37.	Mild Steel	SCP	Sodium nitrate	NaCl	Polarization and Zero Resistance ammetery	The Stability and Improvement of the passive film	37
38.	Mild Steel	Concrete	Extracts of Kola Plant and Tobacco	-	Potential Monitoring Technique	Protective film formed on the surface	38
39.	Steel	Concrete	Calcium Nitrite	-	Weight loss, electro chemical measurement	Calcium Nitrite based treatment applicable only to carbonated concrete without chloride.	39

DOI: 10.17628/ECB.2013.2.1

Table 1. (cont.) Inhibitors used to improve the corrosion resistance of metals in concrete admixture

Sl. No	Metal	Medium	Inhibitor	Additive	Method	Findings	Ref
40.	Duplex Stainless Steels	SCP	-	-	Polarization, SEM	The lean duplex 2304 has clearly better corrosion behavior than the 304 grade in simulated concrete pore solution	40
41.	Mild steel	Cement Paste	Stannous tin Sn(II)	-	Linear polarization, Analytical electron Microscopy.	Corrosion performance of Stannous tin (Sn(II)) is measured.	41
42.	Steel	SCP	Sodium Nitrate	-	EIS	Sodium Nitrate Reduce the corrosion Level	42
43.	Mild Steel	Concrete	Potassium dichromate	-	Electrochemical Potential Monitoring Method	The potassium dichromate inhibitor was Most effective amongst other inhibitor concentration	43
44.	Low Nickel Stainless Steel, AISI 304 SS Carbon Steel	SCP	-	5%NaCl	Cyclic anodic Polarization curve and EIS	Nickel Stainless Steel High corrosion resistance then carbon Steel	44
45.	Steel	-	Calcium Nitrite, Calcium nitrate, Amino alcohol, DMEA, Cyclo hexyl ammonium benzoate, Di isopropyl ammonium benzoate	3% NaCl	-	The chemical reactions of the corrosion process in concrete and of the most commonly used as inhibitors and discussed	45
46.	Steel	Concrete	Sodium mono sulphate	-	Gravimetric Measurement	Sodium mono fluoro phosphate had very little on the corrosion rates of steel in both non carbonated and carbonated concrete under the conditions studied.	46
47.	Steel	Concrete M15,M20, M30,M35	-	5% NaCl	Weight loss, Linear polarization, Galvanostatic pulse technique	The Galvano static pulse technique is able to give reliable corrosion rate values of steel in concrete	47
48.	Steel	Concrete	Alkyl amino alcohol	-	Electro chemical measurement	The inhibitor is able to reduce the corrosion rate	48
49.	Steel	Concrete	Chromate	-		Repassivation as pH raised	49
50.	Galvanized steel	SCP	Zn	-	Potentio dynamic Polarization tests, Polarization resistance	Galvanized Steel is a very good alternative to avoid the early damage of the structure.	50
51.	Steel	Portland Pozzolona Slag cement	0.5%Sodium Citrate+0.5% Sodium Stannate Migrating inhibitor amino alcohol, Amines, Nitrides	-	FTIR	The better corrosion resistance of steel embedded in migrating corrosion inhibiting system	51
52.	Steel	concrete	Calcium Nitrite and tannic acid	-	Weight loss, potentiodynamic polarization	The dose of these inhibitors for the protection of steel wire mesh reinforce Ment in Ferro cement	52
53.	Rebar	Acidified concrete pore solution	Sodium molybdate, Sodium tungstate, Sodium Nitrite Sodium phytate	-	Weight loss, Anodic polarization measurements, EIS	The concentration is above 0.5% Sodium phytate shows inhibitive effect and passivation is promoted. Molybdate and tungstate are present on the steel surface.	53
54.	Carbon Steel	Carbonated concrete pore solution	Sodium nitrite	-	Electrochemical Noise Measurement	High concentration of nitrite can inhibit the nucleation of meta stable pits around the rust cover and accelerate the repassivation of stable pits	54
55.	Steel	SCP	Nitrite	-	Weight loss, Polarization, EIS	The dosage of high amounts of nitrites on concrete can be unfavorable.	55

DOI: 10.17628/ECB.2013.2.1

Table 1. (cont.) Inhibitors used to improve the corrosion resistance of metals in concrete admixture

Sl. No	Metal	Medium	Inhibitor	Additive	Method	Findings	Ref
56.	Steel	Concrete	Calcium Nitrite	-	Polarization Resistance	The presence of nitrite ion efficient passivation of the rebar that maintain with time	56
57.	Galvanized Steel	Concrete	Surface and Bulk Hydrophobic	-	Water Absorption, electro chemical measurements, Chlorides penetration, Visual observation	Hydrophobic treatment is the most effective treatment to improve the corrosion resistance of Galvanized steel reinforcement in concrete	57
58.	Steel	Concrete	Sodium nitrite, Resorcinol, Phloroglucinol, Sodium Phosphate, Sodium gluconate, Calcium gluconate, zinc oxide, urotropin	-	Corrosion potential, polarization resistance	None of the alternative inhibitors studied was comparable to nitrite in terms of protective efficiency	58
59.	steel	Concrete	Sodium mono fluro phosphate, alkanolamines, amines, Zinc oxide molibdates, borates, Stannates	-	Potentio dynamic, potentiostatic measurement	The organic commercial inhibitors reduce the ingress of chlorides by filling concrete pores and blocking the porosity of concrete by the formation complex compound	59
60.	Steel	Concrete	-	-	Weight loss, linear polarization resistance	The technique can be used as qualitative measure of the corrosion rate of reinforcing steel in concrete	60
61.	Steel	Concrete	Alkyl amino alcohol	-	EIS	The inhibitor was able to reduce the corrosion rate only when the iniated chloride was below 0.16 wt %	61
62.	Carbon steel	Concrete	-	-	EIS,SEM	compressive stress produces more severe degradation of the passive film than does the tensile stress.	62
63.	Steel	Concrete	-	-	Embedded capacitor sensor (ECS)	Embedded sensor is robust and suitable for installation in reinforced concrete, hence capable of detecting changes in the immediate vicinity of the steel for a longer period.	63
64.	Steel	Concrete	-	-	SEM, AFM, EIS	AFM images revealed detail of the localized corrosion behavior	64
65.	Stainless steel	SCP	-	-	Potentio dynamic polarization, alternating current impedance	The Cl^- concentration had little effect on Stainless Steel.	65

DOI: 10.17628/ECB.2013.2.1

Acknowledgments

The authors are thankful to their management and St.Joseph's Research and Community Development Trust, Dindigul for their help and encouragement.

References

[1]Rajendran, S.; Muthumegala, T.S.; Krishnaveni, A.; Manivannan, M., *Zastita Mater.*, **2011**, *52(1)*, 35.

[2]Rajendran, S.; Muthumegala, T.S.; Pandiarajan, M.; Nithya devi P., *Zastita Mater.*, **2011**, *52(2)*, 85.

[3]Dhouibi, L.; Triki, E.; Rodrigues, M.; p.Raharinaivo, A., *Mater.d Struct.*, **2003,** *33*, 530.

[4]Li, J-H.; Zhao, B.; Du, R-G.; Lin, C-J., *J. Functional Mater.*, **2007,** *3*, 148.

[5]Ostoner, T.A.; Justness, H., *Adv. Appl. Ceram.*, **2011,** *110*, 131.

[6]Zhou. X.; Yang, H.-Y.; Wang, F-H., *Corros. Sci. Protect. Technol.*, **2010**, *22*, 343.

[7]Zhu, Y.; Lin C., *Metallurgica Sinica*, **2010**, *46(2)*, 245.

[8]Qiao, B.; Du, R.-G.; Lin, C.-J., *J. Functional Mater.*, **2009**, 40, 1496.

[9]Mennucci, M.M.; Banczek, E.P.; Rodrogues, P.R.P. Costa, *Cement and Concrete Composites*, **2009**, *31* , 418.

[10]Chen, W.; Wu, Q.; Du, R.-G.; Lin, C-J.; Sun, L, *J. Functional Mater.*, **2009**, *40*, 611.

[11]Chen, Y.; Wang, W., Yang, J., *J. Univ. Sci. Technol.*, **2007**, *29*, 21.

[12]Zhang, D-Q.; Zhang, W-P.; Wang, W.; Zhou, G.-D., *Corros. Protect.*, **2007**, *28*, 55.

[13]Nakayama, N., *Electrochemistry*, **2002**, *70*, 322.

[14]Singh, D.D.N.; Ghosh, R., *Surface and Coating Technol.*, **2008**, *202*, 4687.

[15]Ha, T.H.; Bae, J- H.; Ha, Y-C.; Lee, H.G.; Park, K-W.; Kim, D.-K., *Trans. Soc. Advancement of Electrochem. Sci. Technol.*, **2004**, *39*, 1.

[16]Blaszczynski, T.; Lowin-Kluge, A., *Corrosion*, **2007**, *63*, 1063.

[17]Riberio, D. V.; Labrincha, J.A.; Moreli, M.R, *Cement and Concrete Res.*, **2012**, *42*, 124.

[18]Rengaswamy, N.S.; Saraswathy, V.; Balakrishnan, K., *J. Ferrocement*, **1992**, *22*, 359.

[19]Rasheeduzzafar, Fahd H.; Dakhil, Fahd. Bader; Maher, A., Khan, Mohammed Mukarramt, *ACI Mater. J.*, **1992**, *89*, 439.

[20]Sagoe-Crentsil, K.K.; Glasser, F.P.; Irvine, T.T.S., *Brit. Corros. J.*, **1992**, 27, 113.

[21]Flis, J.; Sabol, S.; Pickering, H.W.; Sehgal, A.; Osseo-Asare, K.; Caddy, P.D. *Corrosion*, **1993**, *49*, 601.

[22]Hime, W.G.; Machin, M., *Corrosion*, **1993**, *49*, 858.

[23]Kapse, G.W.; Jain, V.K, *Indian Concrete J.*, **1984**, *58*, 354.

[24] Chadwick, G.K.Jr., *Corros. Sci.*, **1992**, *36*, 2193.

[25]Thangavel, K.; Rengaswamy, N.S.; Balakrishnan, K., *Indian Concrete J.*, **1995**, *69*, 289.

[26]Arya, C.; Ofori-darko, F.K., *Cement and Concrete Res.*, **1996**, *26*, 345.

[27]Martin,Farrel.Olek,Jan, *Proc. Mater. Eng. Conf.*, **1996**, *2*, 1111.

[28]Elsener, B., *Corrosion*, **2000**, *56*, 727.

[29]Velva, L.P.; Cebada, M.C., *ASTM Spec. Techn. Publ.*, **2000**, *1399*, 170.

[30]Ghosh, D.D.N.; Singh, B.K., *Corros. Sci.*, **2002**, *44*, 1713.

[31]Sieber, J.; Broton, D.; Fales, C.; Leigh, S.; MacDonald, B.; Marlow, A.; Nelles, S.; Yen. J., *Cement and Concrete Res.*, **2002**, *32*, 1915.

[32]Ghosh, R.; Singh, R,J.; Singh, D.D.N, *Corros. Prevent. Control*, **2003**, *50*, 94.

[33]Huet, B.L.; Hostis,V.; Miserque, F.; Idrissi, H., *Electrochim. Acta*, **2005**, *51*, 172.

[34]Holloway, M.; Sykes, J.M., *Corros. Sci.*, **2005**, *47*, 3097.

[35]Venkatesan, P.; Palaniswamy, N.; Rajagopal, K., *Progress in Org. Coating*, **2006**, *56*, 8.

[36]Simescu, F.; Idrissi, H., *Sci. Technol. Adv. Mater.*, **2008**, *9*, Art No.045009.

[37]Moayed, M.H., Abbaspour, Z.; Sadegian, M., *Int. J. Eng. Trans. B. Applications*, **2009**, *22*, 369.

[38]Loto, C.A.; Loto, R.T.; Popoola, *Int. J. Electrochem. Sci.*, **2011**, *6*, 3452.

[39]Ngala, V.T.; Page C.L.; Page, M., *Corros. Sci.*, **2002**, *44*, 2073.

[40]Alvarez, S.M.; Bautista, A.; Velasco, F., *Corros. Sci.*, **2011**, *53*, 1748.

[41]Sagoe–Crentsil, K.K.; Glasser, F.P.; YilMaz, V.T., *Cement and Concrete Res.*, **1994**, *24(2)*, 313.

[42]Saura. P.; Zomoza, E.; Andrade, C.; Garces.P., *Corrosion*, **2011**, 67.

[43]Loto. C.A.; Omotosho, O.A.; Popoola, A.P., *Int. J. Phys. Sci.*, **2003**, *6*, 2275.

[44]Fajardo, S.; Bastidas, D.M.; Criado, M.; Romero, M.; Bastidas, J.M., *Construction and Building Mater.*, **2011**, *25*, 4190.

[45]Gaidis, J. M., *Cement and Composites*, **2004**, *26*, 181.

[46]Nagala, V.T., Page, C.L., Page, M.M, *Corros. Sci.*, **2003**, *45*, 1523.

[47]Sathyanarayanan, S.; Panjali Natarajan, K.; Saravanan, S.; Srinivasan, G.; Venkatachari, *Cement and Concrete Composites*, **2006**, *28*, 630.

[48]Morris, W.; Vazquez, M., *Cement and Concrete Res.*, **2002**, *32*, 259.

[49]Schieb, P.; Mayer, T.F.; Osterminski, K., *Mater. Corros.*,**2008**, *59*, 115.

[50]Farina, S.B.; Duffo, S., *Electrochim. Acta*, **2007**, *52*, 5131.

[51]Thangavel, K.; Muralidharan, S.; Saraswathy, V.; Quraishi, M.A.; Ha-Won Song, *Arabian J. Sci. and Eng.*, **2009**, *34*, 83.

[52]Akhtar, S.; Quaraishi, M. A.; Arif, M., *Arabian J. Sci. and Eng.*, **2009**, *34*, 107.

[53]Tang, Y.; Zhang, G.; Zuo, Y., *Construction and Building Mater.*, **2012**, *28*, 327.

[54]Ze, Hua; Dong. Wei; Shi, Xing; Peng, Guo, *Corros. Sci.*, **2011**, *53*, 1322.

[55]Garces, P,; Saura, P.; Zornoza, E.; Andrade, C., *Corros. Sci.* **2011**, *53*, 3991.

[56]Sanchez, M.; Alonso, M.C., *Construction and Building Mater.*, **2011**, *25*, 873.

[57]Tittarelli, F.; Moriconi, G., *Cement and Concrete Res.*, **2011**, *41*, 609.

[58]Gonzalez, J.A., Ramirez, E. Bautista, *Cement and Concrete Res.*, **1998**, *28*, 577.

[59]Ormellese, M.; Berra, M.; Bolozoni, F.; Pastore, T., *Cement and Concrete Res.*, **2006**, *36*, 536.

[60]Law, D.W.; Cairns, J.; Millard, S.G.; Bungey, J.H.; *NDT&E Int.*, **2004**, 37, 381.

[61]Morris, A.; Vazquez, Vico M., *J. Appl. Electrochem.*, **2003**, 33, 1183.

[62]Feng, X.; Zuo, Y.; Tang, Y.; Zhao, X., Lu, X. *Electrochim. Acta*, **2011**, *58*, 258.

[63]Rahman, S.F.A.; Ismail, M., Muhammad, B.; Md Noor, N.; Bakhtiar, H., *Malaysian J. Civil Eng.*, **2011**, 23, 1.

[64]Zhang, F.; Pan, J.; Lin, C., *Corros. Sci.*, **2009**, *51*, 2130.

[65]Gong, L.; Zhu, L.-L, *Corros. Sci. Protection Technol.*, **2007**, 19, 397.

[66]Ormellese, M.; Lazzari, L.; Goidanich, S.;, Fumagalli, G.; Brenna, A., *Corros. Sci.*, **2009**, *51*, 2959.

[67]Broomfield, J.P., *Corrosion of Steel in Concrete: understanding, investigation and repair*, Taylor and Francis, **2003.**

[68]Soeda, K.; Ichimura, T., *Cement Concrete Compos*., **2003**, 25, 117.

[69]Ormellese, M.; Berra, M.; Bolzoni, F.; Pastore T., *Cement Concrete Res*., **2006**, *36*, 536.

[70]Saraswathy, V.; Song, H.W., *Build. Environ*., **2007**, *42*, 464.

[71] So¨ylev, T.A.; Richardson, M.G., *Constr. Build. Mat.*, **2008**, *22*, 609.

[72] Satapathy, A.K.; Gunasekaran, G.; Sahoo, S.C.; Kumar A.; Rodrigues, P.V., *Corros. Sci.*, **2009**, *51*, 2848.

[73] Uhlig, H., *Corrosion and Control*, George Harrap and Co. Ltd., **2004**; Wang, X.; Li, G.; Li, A.; Zhang, Z., J. *Mater. Process. Technol*., **2007**, *186*, 259.

Received: 07..11.2012.
Accepted: 01.12.2012.

EFFECTS OF THE DIFFERENT REACTION CONDITIONS ON SYNTHESIZING OF ISOPROPYL CHLOROACETATE

Liu Shu[a]* and You Hongjun[b]

Keywords: effect; reaction conditions; synthesizing; isopropyl chloroacetate

In the present article the effects of different reaction conditions on the synthetic method of isopropyl chloroacetate have been reviewed. Different catalysts that consist of inorganic salt like ($Ce(SO_4)_2{\cdot}4H_2O$ and $NaHSO_4$) and PCl_3 have also been introduced. The reaction conditions include the reaction time, the molar ratio of chloroacetic acid to isopropanol, the amount of the catalyst and the number of reusable catalyst. The optimized reaction time, the molar ratio of chloroacetic acid to isopropanol and the amount of the catalyst are beneficial to improve the yield of isopropyl chloroacetate.

* Corresponding Author
Fax: 86-24-56860869
E-Mail: youhongjun@hotmail.com
[a] Liaoning Shihua University, Fushun, Liaoning, P.R. China
[b] SAIT Polytechnic, Calgary AB, Canada.

INTRODUCTION

Isopropyl chloroacetate is one of the important organic chemical materials and intermediates. Isopropyl chloroacetate is used as an organic solvent and as an intermediate for synthesis of pharmaceuticals, mainly non-steroid anti-inflammatory drugs such as naproxen and ketoprofen[2]. Its molecular formula, boiling point, relative density (25 °C), refractive index n_D^{20} and flash point are $C_5H_9O_2Cl$, 149.5 °C, 1.0812, 1.0423 and 56 °C.[1] Requirements for isopropyl chloroacetate are gradually increased in *China*. The main manufacturing process has two types of methods. The first method is that chloroacetic acid and isopropanol as feedstocks and BF_3 as a catalyst are used to produce isopropyl chloroacetate. In the other method the catalyst is concentrated sulphuric acid. These methods have a lot of disadvantages, such as more secondary reaction taking place, low yield and purity of isopropyl chloroacetate. [3]

In the present paper, different catalysts such as inorganic salt ($Ce(SO_4)_2{\cdot}4H_2O$ and $NaHSO_4$) and PCl_3 have been evaluated in the synthesis of isopropyl chloroacetate. Effects of different reaction conditions, such as the reaction time, the molar ratio of chloroacetic acid to isopropanol, the amount of the catalyst and the number of reusable catalyst, on the synthetic method of isopropyl chloroacetate have been reviewed. Furthermore, the optimized reaction conditions are also pointed out.

DISCUSSION

Effects of the reaction time on the yields of isopropyl chloroacetate by the addition of $Ce(SO_4)_2{\cdot}4H_2O$ as a catalyst

Yang Liangzhun [4] developed a method for the preparation of isopropyl chloroacetate and effects of the reaction conditions on its yield were discussed. Using $Ce(SO_4)_2{\cdot}4H_2O$ as a catalyst and chloroacetic acid and isopropanol as feedstocks, isopropyl chloroacetate was generated. It was observed that the molar ratio of chloroacetic acid to isopropanol and the amount of $Ce(SO_4)_2{\cdot}4H_2O$ were kept constants and were 1.0:1.3 and 3.5 % of chloroacetic acid weight, respectively. Effects of the reaction time on the yields of isopropyl chloroacetate had also been discussed. Table 1 showed the effect of reaction time on the yield of isopropyl chloroacetate. The experimental results showed that the yield of isopropyl chloroacetate increased with an increase of the reaction time. When the reaction time was 4 h, the maximum yield of isopropyl chloroacetate was 98.62%, so the optimized reaction time was proved to be 4 h.

Table 1. Effect of the reaction time on the yield of isopropyl chloroacetate

Reaction time, h	1.0	2.0	2.5	3.0	4.0
Yield, %	57.42	79.12	84.29	97.50	98.62

The effect of the molar ratio of chloroacetic acid to isopropanol on the yield of isopropyl chloroacetate by the addition of $NaHSO_4$ as a catalyst

Zhang Jie [5] explained why $NaHSO_4$ as a catalyst could occupy the concentrated sulfuric acid to generate isopropyl chloroacetate. The reaction time and the amount of $NaHSO_4$ were kept at constants at 3.0 h and 1.0 % of chloroacetic acid weight, respectively. Effects of the molar ratio of chloroacetic acid to isopropanol on the yield of isopropyl chloroacetate had been discussed. Table 2 showed the effect of molar ratio of chloroacetic acid to isopropanol on the yield of isopropyl chloroacetate. The yield of isopropyl chloroacetate firstly increased and then decreased with an increase in the molar ratio of chloroacetic acid to isopropanol. When the molar ratio of chloroacetic acid to isopropanol was 1.0:1.2, the maximum yield of isopropyl chloroacetate reached the value of 82.4%. $NaHSO_4$ can be used to produce isopropyl chloroacetate because it was very cheap, stable and insoluble in organic acids and organic alcohol. After the reaction was done, $NaHSO_4$ as insoluble material can easily be separated from the reaction system.

Table 2. Effect of the molar ratio of chloroacetic acid to isopropanol on the yields of isopropyl chloroacetate

Molar ratio	1.0:1.0	1.0:1.1	1.0:1.2	1.0:1.3	1.0:1.4
Yield, %	60.6	72.7	82.4	77.3	72.1

Effects of the amount of PCl_3 on the yields of isopropyl chloroacetate by the addition of PCl_3 as a catalyst

Liang Chugen[6] described the principles of isopropyl chloroacetate synthesis and discussed the effect of reaction conditions on the yield of isopropyl chloroacetate. The reaction time and the molar ratio of chloroacetic acid to isopropanol were kept to be constant at 2.0 h and 1.0:1.4, respectively. Effects of the amount of PCl_3 on the yield of isopropyl chloroacetate had been discussed. The effect of the amount of PCl_3 on the yields of isopropyl chloroacetate is presented in Table 3. The yield of isopropyl chloroacetate firstly increased and then decreased with an increase in the amount of PCl_3. When the amount of PCl_3 was 6.7 % of chloroacetic acid weight, the maximum yield of isopropyl chloroacetate reached the value of 89.5%.

Table 3. The effect of PCl_3 amount on the yields of isopropyl chloroacetate

Amount of PCl_3, ml	0.5	1.0	2.0
Yield, %	71.0	89.5	82.0

Effects of the number of reusable $Ce(SO_4)_2{\cdot}4H_2O$ on the yields of isopropyl chloroacetate by the addition of $Ce(SO_4)_2{\cdot}4H_2O$ as a catalyst

Yang Liangzhun [4] introduced a synthetic method of isopropyl chloroacetate and evaluated the effect of reaction conditions on the yield of isopropyl chloroacetate. Chloroacetic acid was reacted with isopropanol to produce isopropyl chloroacetate with $Ce(SO_4)_2{\cdot}4H_2O$ as catalyst. The reaction time, the molar ratio of chloroacetic acid to isopropanol and the amount of $Ce(SO_4)_2{\cdot}4H_2O$ were kept to be constants at 4 hours, 1.0:1.3 and 3.5 % of chloroacetic acid weight, respectively. $Ce(SO_4)_2{\cdot}4H_2O$ as the catalyst was reused five times. Table 4 showed the relationship between the yield of isopropyl chloroacetate and the number of $Ce(SO_4)_2{\cdot}4H_2O$ reusing. When $Ce(SO_4)_2{\cdot}4H_2O$ was reused 5 times, the yield of isopropyl chloroacetate still kept at above 92.0 %, so $Ce(SO_4)_2{\cdot}4H_2O$ was proved to be the best catalysts.

Table 4. The relationship between the yield of isopropyl chloroacetate and the number of recycling of $Ce(SO_4)_2{\cdot}4H_2O$

The number of recycling	1	2	3	4	5
Yield, %	97.90	96.43	96.21	94.64	92.50

CONCLUSION

Based on the above discussion and review, using chloroacetic acid and isopropanol as feedstocks and $Ce(SO_4)_2{\cdot}4H_2O$, $NaHSO_4$ and PCl_3 as catalysts, the effect of the reaction time, the molar ratio of chloroacetic acid to isopropanol, the amount of the catalyst and the number of catalyst reusing on the yields of isopropyl chloroacetate have been discussed. The experimental results obtained are the following:

(1) The maximum yield of isopropyl chloroacetate reached at 98.62% in 4 h by the addition of $Ce(SO_4)_2{\cdot}4H_2O$.

(2) The maximum yield of isopropyl chloroacetate reached at 82.4% at chloroacetic acid/isopropanol ratio=1.0:1.2 when $NaHSO_4$ used as the catalyst

(3) The maximum yield of isopropyl chloroacetate was proved to be 89.5% when the amount of used PCl_3 catalyst was 6.7 % of chloroacetic acid weight.

(4) The maximum yield of isopropyl chloroacetate was still kept 92.50% even after 5 recycling of $Ce(SO_4)_2{\cdot}4H_2O$ catalyst.

REFERENCES

[1] You, H. J. *Journal of Liaoning University of Petroleum & Chemical Technology*, **2004**, 24(3), 35.

[2] Lai, J. L., Cheng, Y. L., Liu, C. S. and Luo, G. X. *Chemical Agents*, **2009**, 31(3), 197.

[3] Gao, X. H., Gao, J., Zhang, H. F. and Lin, L. *Chemical Industry and Engineering*, **2011**, 28(6), 6.

[4] Yang, L. Z., Chu, L. F., Li, F. and Zhang, D. H. *Speciality Petrochemicals*, **2000**, 3, 27.

[5] Zhang, J. Xu, J. S. and Qian, J. H. *Science Technology and Engineering*, **2011**, 11(11), 2519.

[6] Liang, C. G., Lin, Y. B. and Shen, D. S. *Natural Science Journal of Xiantan Univeristy*, **1997**, 19(2), 49.

Received: 19.11.2012.

Accepted: 28.11.2012.

CHEMICAL WATER QUALITY CHANGES ALONG A STREAM AT AN ABANDONED Pb-Zn MINING SITE

Elza Kovács[a]*, Dario Omanović[b], Ivanka Pižeta[b], Halka Bilinski[b], Stanislav Frančišković-Bilinski[b] and János Tamás[a]

Paper was presented at the 4th International Symposium on Trace Elements on the Food Chain, Friends or Foes, 15-17 November, 2012, Visegrád, Hungary

Keywords: abandoned mining site, heavy metal, surface water

In the present study, chemical water quality changes downstream a pool-riffle type stream located at a former Pb-Zn mining site are discussed. The watershed of the Toka stream (Mátra mountain, Hungary) being under rehabilitation is still continuously affected by a neutralised acidic mine drainage, and temporarily, by an abandoned mine tailing. Upstream the AMD confluence which gives the major part of the water flux in dry season, indeed, the stream is of high water quality, while, directly after that, the electric conductivity is app. quintupled, and the pH as well as the trace element concentrations increase, as expected. However, within the range of 10 kilometres, Fe, Zn and Pb concentrations are all remarkably decreased in relation to the distance from the contamination source, and they almost reach the actual background levels. The electric conductivity does not show significant change along the investigated section of the stream, which would indicate dilution. At the same time, presence of amorphous $Fe(OH)_3$ in the sediment is obvious, based on the pH-Eh relations and geochemical analysis, thus the adsorption processes have considerable role in the decrease of trace element concentrations in solution.

* Corresponding Author
Fax: +3652508456
E-Mail: ekovacs@agr.unideb.hu
[a] Department of Water and Environmental Management, Faculty of Agricultural and Food Sciences, and Environmental Management, Centre of Agriculture and Economy, University of Debrecen, H-4032 Debrecen, Böszörményi 138, Hungary
[b] Division for Marine and Environmental Research, Ruđer Bošković Institute, 10002 Zagreb, POB 180, Croatia

Introduction

At the sulphide-bearing mining sites, potentially toxic elements take part in complex biogeochemical interactions. They have many chemical forms that can readily be transformed into one another, under the dynamically changing environmental conditions. In order to assess the contaminant transport it is inevitable to know the controlling (bio)-chemical and physical mechanisms, such as weathering (*Eq. 1-4*), secondary mineralization, hydrolysis (*Eq. 5-7*), precipitation, dissolution (*Eq. 8*), complexation, and co-precipitation, adsorption, desorption, which all dependent on the species present, their concentrations, and can hardly be measured and monitored simultaneously resulting from the complexity of the system.

$$2\ FeS_2 + 7\ O_2 + 2\ H_2O \rightarrow 2\ Fe^{2+} + 4\ SO_4^{2-} + 4\ H^+ \quad (1)$$

$$4\ Fe_2+ + 10\ H_2O + O_2 \rightarrow 4\ Fe(OH)_3 + 8\ H^+ \quad (2)$$

$$4\ Fe^{2+} + O_2+ 4\ H^+ \rightarrow 4\ Fe^{3+} + 2\ H_2O \quad (3)$$

$$FeS_2 + 6\ Fe^{3+} + 4\ H_2O \rightarrow 7Fe^{2+} + 2\ SO_4^{2-} + 8\ H^+ \quad (4)$$

$$M^{2+} + H_2O \rightarrow M(OH)^+ + H^+ \quad (5)$$

$$M^{2+} + 2H_2O \rightarrow M(OH)_2 + 2H^+ \quad (6)$$

$$M^{2+} + 3H_2O \rightarrow M(OH)_3^- + 3H^+ \quad (7)$$

$$A_pB_{q(s)} \leftrightarrow pA^{v-}_{(aq)} + qB^{v+}_{(aq)} \quad (8)$$

Considering the mines and their drainages, sediments in the affected surface water pose risk of heavy metal remobilisation as a secondary source of pollution.[1-5] As a result of increase in pH (*Eq. 9*), the adsorption, precipitation and co-precipitation specific to heavy metal species take place, and the concentrations in solution show a certain removing order downstream of the discharge point[6-8], although hydrological seasons definitely affect the spatial variation, fate and transport of metals.[8-11]

$$4\ FeS_2 + 8\ CaCO_3 + 15\ O_2 + 6\ H_2O \rightarrow 4\ Fe(OH)_3 + 8\ SO_4^{2-} + 8\ Ca^{2+} + 8\ CO_2 \quad (9)$$

The aim of the present study was to investigate the change in surface water quality and the main governing chemical and physical mechanisms downstream of the Toka stream (Mátra mountain, Hungary) which is affected by an abandoned Pb-Zn mine and its tailing dump, with respect to potentially toxic elements.

Experimental

Site Description and Sampling

According to the Watershed Management Action Plan (WMAP) in Hungary, Toka stream belongs to the class of the silicate-based mountainous small watersheds with gravel stream bed. In the watershed, a Pb-Zn mine and an ore processing plant were operated from 1952 to 1986, however, neutralized acid mine drainage is still led to the stream. There are two discharges, a continuous one from the AMD treated with $Ca(OH)_2$ and settled, and a temporary one from a tailing dump of 2.1 Mm^3, where remediation has not yet been completed. The site has already been investigated from several aspects.[5] Change in surface water quality downstream and the effects of the neutralized AMD discharge were investigated along 10 km, from the source of the Toka to the town Gyöngyös. Site and the sampling points are given in *Fig. 1*.

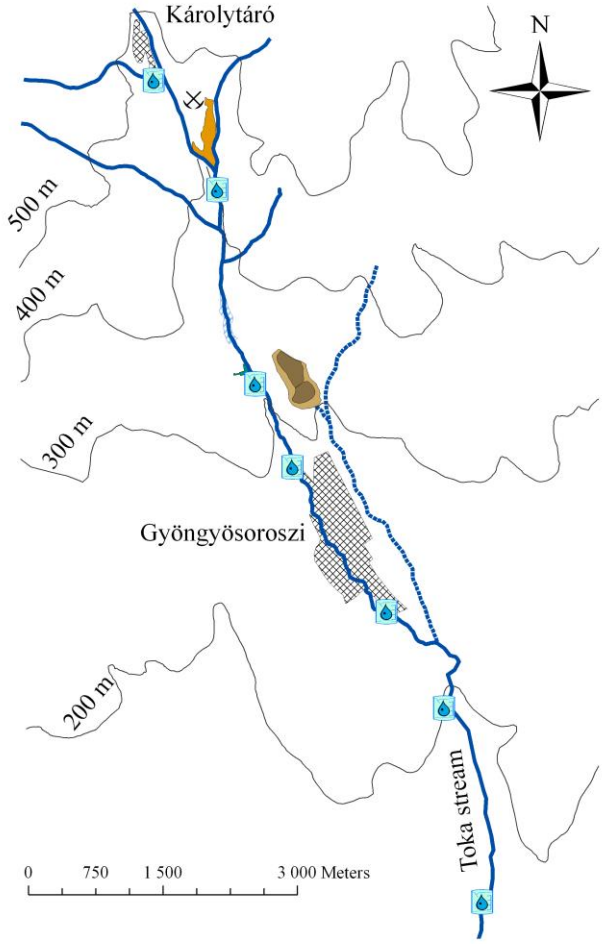

Figure 1. Abandoned Pb-Zn mining site and the sampling points

Sample treatment and analyses

Water samples were taken at 7 different sites along 10 km long transect of the Toka. Sampling was carried in April, 2011, during a dry period. Estimated flow of the river was ca. 0.15 m^3/s upstream, while after the confluence ~ 80% of the water originated from the treated AMD.

Samples for metal analysis were taken by 60 mL pre-cleaned plastic syringe. At each site, before taking final sample, syringe was rinsed at least 5 times by ambient water. Syringe is placed against water flow to avoid contamination of water. For dissolved trace elements, water was filtered by 0.45 µm capsule filters (Sartorius) mounted on syringe into the precleaned (washed with 10% HNO_3 then thoroughly MilliQ water rinsed) HDPE bottles. First few milliliters of filtered sample were discarded to avoid possible contamination from the filter. Blank test of capsule filters and syringes were performed in laboratory and no contamination was found for any element. Samples for metals analysis (total-unfiltered and dissolved-filtered) were acidified in laboratory by addition of concentrated nitric acid (Fluka, *TraceSelect*) - 100 µL on cca 60 mL of water.

Physico-chemical parameters (temperature, pH, dissolved oxygen, conductivity and redox potential) were measured *in-situ* (in the river main body and in each source) by HACH HQ40d portable multi-parameter instrument and associated probes. High Resolution Inductively Coupled Plasma Mass Spectrometer (HR ICP-MS, *Element 2*, Thermo Finnigan, Bremen, Germany) was used for the determination of dissolved element concentrations. The samples for the analyses were prepared in pre-cleaned polyethylene tubes by adding 100 µL of concentrated HNO_3 and 50 µL of indium(115) internal standard (0.1 mg/L) into 5 mL of a sample aliquot. The concentrations of the elements were determined by means of external calibration plots. No special setup of the instrument operating conditions was needed. Quality control (QC) of HR ICP-MS measurements was checked by the determination of elements concentration in "River Water Reference Material for Trace Metals" (SLRS-4, National Research Council Canada). For most elements, a good agreement with the certified data was obtained.

Results and Discussion

General surface water quality

The Water quality along the Toka stream is affected by the neutralized acidic mine discharge as a point of source of heavy metals. Based on previous measurements, despite neutralization, the concentrations of Zn and Cd of the treated AMD itself were found above the environmental permissible levels, though Zn concentration was reported one third of the that in the untreated AMD. Pb concentration was found low for both the untreated and treated effluents.[5,6]

The dissolved element concentrations, measured in filtered samples, and the relevant environmental quality standards for surface water are given in *Table 1*. In the sampling campaign, and for the whole length of the stream, dissolved Pb concentration was significantly below both the standard for annual average provided in Directive 2008/105/EC, and the target value given in the Water Quality Classification for the Danube River Basin[12], as expected. Average Zn concentration was rather high along the whole stream, though it was higher by one order of magnitude compared to the target value even at the source of the stream which might be considered as background since no other sourse upstream was identified, Same was reported by others for similar sites.[13] *Note*: relevant regulation on surface water quality does not give limit value for Zn.

Table 1 Concentrations ± standard deviations of elements in µg L^{-1} determined in water (detection limit for all elements is below 10 ng L^{-1}), pH and the relevant environmental quality standards

Element	Concentration ranges along the stream	EQS*		Target Value for Danube River Basin**
		AA-EQS Inland surface waters	MAC-EQS Inland surface waters	
Fe	73.8 ± 43.6	NG	NG	NG
Mn	1123 ± 829	NG	NG	NG
Zn	264.5 ± 190.2	NG	NG	5
Pb	0.120 ± 0.044	7.2	NA	1
pH	7-8.5	NG	NG	6.5-8.5

* EQS: Environmental quality standards for inorganic micropollutants according to the Directive 2008/105/EC, AA: annual average, MAC: maximum allowable concentration; ** Target values for Danube River Basin according to the Trans National Monitoring Network (TNMN) Yearbook 2001, published by the International Commission for the Protection of the Danube River (ICPDR); NA: not applicable; NG: not given

 DOI: 10.17628/ECB.2013.2.11

Downstream water quality changes

Based on the analytical results, treated AMD has higher pH than the Toka upstream, and even further increase of 1 pH was measured along the stream (*Fig. 2*). It may result from the basic mineralogical composition of the watershed, the riverbed itself and gradual removal (degassing) of CO_2 from the water. Redox potential decreased significantly at the confluence (*Fig. 3*), however, reaching ~340 mV within 1-1.5 km and remained constant thereafter.

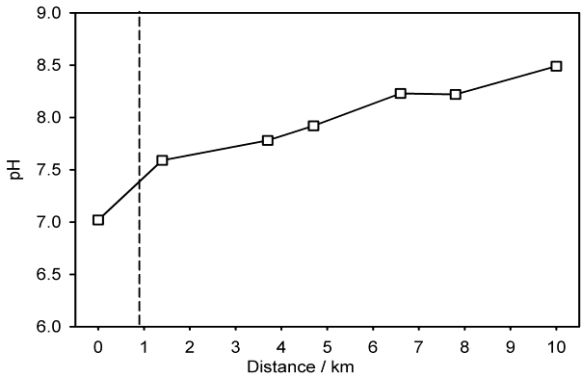

Figure 2. pH profile of the Toka stream, dry season

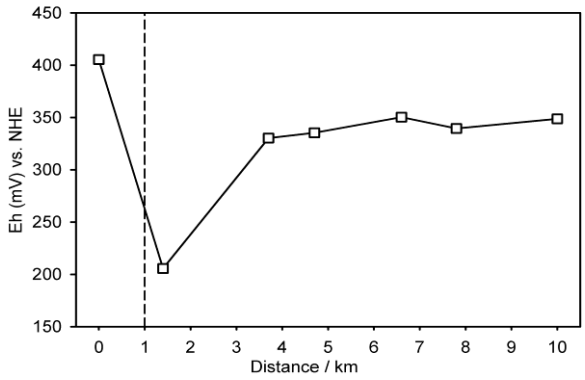

Figure 3. *E*h profile of the Toka stream, dry season

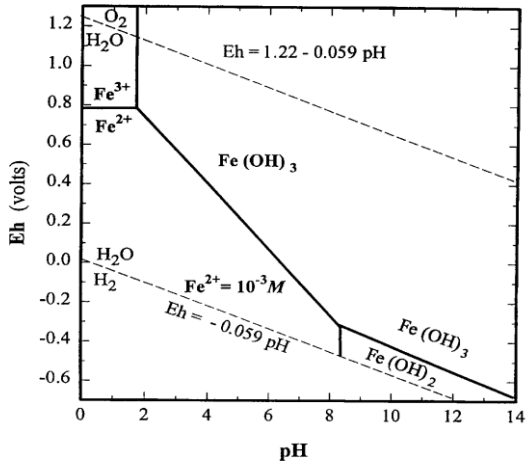

Figure 4. Pourbaix diagram for iron

In the function of pH and Eh relations, metal species can be dynamically transformed into one another. Considering the basic Pourbaix diagram for iron, and taking the measured pH and Eh into consideration, $Fe(OH)_3$ is expected to form instantaneously at the confluence, thus local conversion of dissolved Fe^{2+} to $Fe(OH)_3$ precipitate may have considerable role in co-precipitation mechanisms (*Fig. 4*). Nevertheless, surface water is a highly complex system from chemical point of view, thus presence of carbonate and sulphate ions that are common in treated AMD, cannot be ignored, when heavy metal precipitates are investigated.

Total Fe concentration in water, governing total Pb and Zn concentrations, decreases gradually, indicating settling resulting from flow rates decreasing temporarily at several locations downstream (*Fig. 5*).

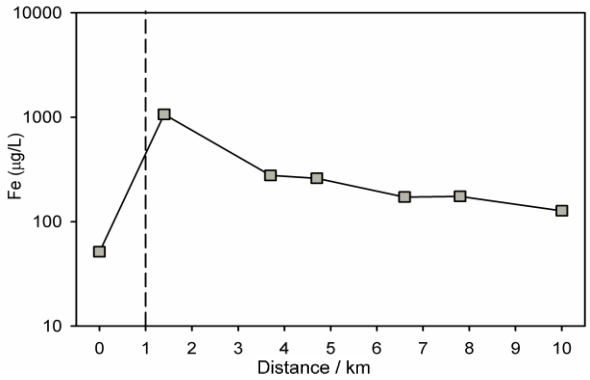

Figure 5. Total Fe concentrations in both solution and colloidal form

Considering the heavy metal concentrations in water, though total Pb concentration is low even in the treated AMD, it decreases further by 5 times downstream (*Fig. 6*). Among its species, thermodynamically $Pb(OH)_2$ is stable above pH 6.5 within the Eh range of the Toka, and dissolved Pb takes part in a further equilibrium, since it is strongly associated with amorphous iron-hydroxide, which results in low, almost constant dissolved Pb concentrations measured along the stream.

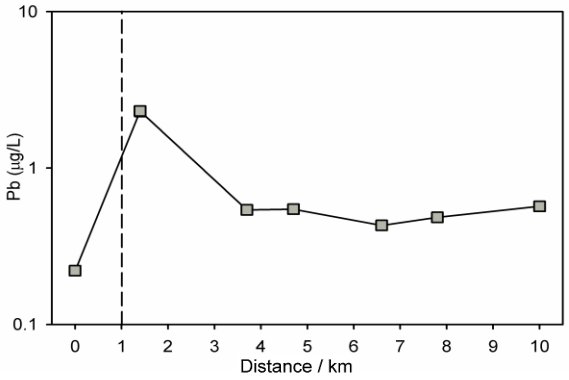

Figure 6. Total Pb concentrations in both solution and colloidal form

Zinc concentration profile is similar to that of Pb (*Fig. 7*), however, Zn prefers dissolved ionic form up to pH 8.5, while $Zn(OH)_2$ is stable in range of pH 8.5-11.5, which explains elevated concentrations along the whole stream[14]. Though, co-precipitation and adsorption on the newly

 DOI: 10.17628/ECB.2013.2.11

formed amorphous iron-hydroxide colloidal particles cannot be ignored[15]. Based on the above experiments, Zn elimination from the AMD requires an additional process to neutralization, such as the application of a passive treatment system[16].

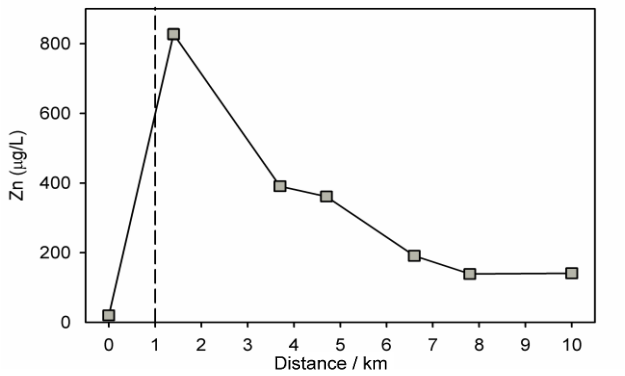

Figure 7. Total Zn concentrations in both solution and colloidal form

Original electric conductivity of the Toka is 200 µS cm^{-1}, which corresponds to the WMAP classification (<300 µS cm^{-1}) while it is app. quintupled at the AMD confluence, as expected (*Fig. 8*). Basically, neutralization agents determine the magnitude of ion concentrations which control conductivity; Fe, Mn and Al concentrations were 465±23, 750±23 and 400±26 µg L^{-1}, respectively, measured previously in dry season in the neutralized AMD, in average.[5] However, major ion concentrations do not show decrease in relation to the distance from the ions' source, which confirms that the gradual decrease in total Fe, Pb and Zn concentrations does not result from dilution, but settling of colloidal adsorbed and co-precipitated species.

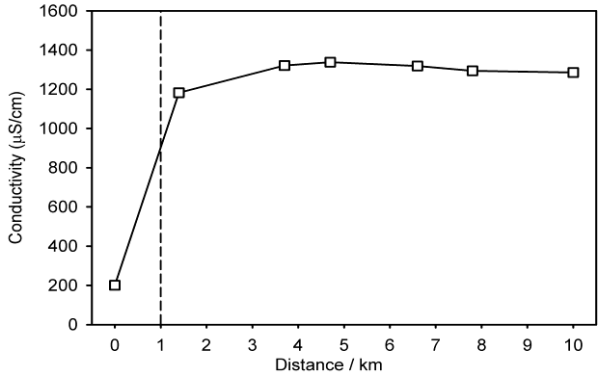

Figure 8. Conductivity profile of Toka stream, dry season

Conclusions

Though, according to WMAP, the watershed of the Toka stream is relatively small, slope of the bed is ~3 %, and the flow rate as well as the stream water discharge can change extremely; rate of the minimum and maximum for the latter one can be up to 1/ 1,000. Thus, solid particles settled continuously from the confluence at the neutralized AMD along the stream bed can be resuspended resulting in increase in the total heavy metal concentrations[13] measurable in unfiltered water samples, however, dissolved concentrations are not expected to increase in case of stable pH and Eh conditions.

At the same time, while Pb and similar elements such as Cu and As are primarily in solid phase under neutral – basic conditions, Zn and similar ones e.g. Cd still have high dissolved concentration. Thus AMD treatment by neutralization cannot result in reaching the target limits[12] for these elements in such surface waters like Toka stream. Though, it defenitely and obviously changes pH that could affect dramatically the ecological systems and the environment, in the acidic range.

Acknowledgement

The research was supported by the Hungarian National Office for Research and Technology, and the Croatian Ministry of Science, Education and Sport, under the Croatian-Hungarian bilateral program, project no. HR-4/2008.

References

[1]Pagnanelli, F., Moscardini, E., Giuliano, V., Toro, L., *Env. Pollut.*, **2004**, *132*, 189.

[2]Cappuyns, V., Swennen, R., Vandamme, A., Niclaes, M., *J. Geochem. Explor.*, **2006**, *88*, 6.

[3]Giuliano, V., Pagnanelli, F., Bornoroni, L., Toro, L., Abbruzzese, C., *Hazard. Mater.*, **2007**, *148*, 409.

[4]Nikolaidis, C., Zafiriadis, I., Mathioudakis, V., Constantinidis, *Bull. Environ. Contam. Toxicol.*, **2010**, *85(3)*, 307.

[5]Kovács, E., Tamás, J., Franciskovic-Bilinski, S., Omanović, D., Bilinski, H., Pižeta I., *Environ. Fres. Bull.*, **2012**, *21(5a)*, 1212.

[6]Horváth, B., Gruiz, K., *Sci. Total. Environ.*, **1996**, 184, 215.

[7]Lee, J.S., Chon, H.T., *Geochem. Explor.*, **2006**, *88*, 37.

[8]Palumbo-Roe, B., Klinck, B., Banks, V., Quigley, S., *Geochem. Explor.*, **2009**, *100*, 169.

[9]Butler, B.A., Ranville, J.F., Ross, P.E., *Sci. Total. Env.*, **2009**, *407*, 6223.

[10]Sarmiento, A.M., Nieto, J.M., Olías, M., Cánovas, C.R., *Appl. Geochem.*, **2009**, *24*, 697.

[11]Pulford, I.D., MacKenzie, A.B., Donatello, S., Hastings, L., *Env. Pollut.*, **2009**, *157*, 1649.

[12]International Commission for the Protection of the Danube River, *Water Quality in the Danube River Basin, TNMN Yearbook, Resch Druck, Vienna*, **2001**.

[13]Gozzard, E., Mayes, W.M., Potter, H. A. B., Jarvis, A. P., *Env. Pollut.*, **2011**, 159, 3113.

[14]Beverskog, B., Puigdomenech, I., *Corros. Sci.*, **1997**, 107.

[15]Zachara, J. M., Cowan, C. E., Resch, C. T., *Geochim Cosmochim Ac*, **1991**, 55(6), 1549.

[16]Nairn, R. W., LaBar, J. A., , Strevett, K. A., Strosnider, W. H., Morris, D., Neely, C. A., Garrido, A., Santamaria, B., Oxenford, L., Kauk, K., Carter, S., Furneaux, B., *Proceedings of IMWA*, **2010**, 255

Received:19.10.2012.
Accepted:28.11.2012.

AN OVERVIEW ON THE CLASSIFICATION AND PREPARATION OF THE EMULSIFYING WAX

Liu Shu[a]* and You Hongjun[b]

Keywords: overview; wax; preparation; emulsion

Classification and preparation of the emulsifying wax have been discussed in the present article. The emulsifying wax is classified into four types of wax such as the cationic emulsified wax, the anionic emulsified wax, the non-ionic emulsifying wax and the amphoteric ionic type emulsified wax based on the properties of surfactant. Further, there are four types of preparation methods for the emulsifying wax are available such as the method of emulsifying agents dissolving in the water, the second in dissolving in the oil, the primary soap method and the taking turns adding method have been introduced also. Effects of the reaction conditions such as choosing the different emulsifying agents, the stirring speed, the emulsifying time and the ratio of emulsifying agents to wax on the emulsifying wax preparation have also been explained.

* Corresponding Author
Fax: 86-24-56860869
E-Mail: liushu-2012@hotmail.com
[a] Liaoning Shihua University, Fushun, Liaoning, P.R. China.
[b] SAIT Polytechnic, Calgary, Alberta, Canada.

Introduction

The emulsifying wax is a cosmetic ingredient. The ingredient name is often conformed by the initials NF, presenting that it follows to the specifications of the National Formulary. The emulsifying wax is produced when a wax material (either a vegetable wax of some kind or a petroleum-based wax) is mixed with a detergent (typically sodium dodecyl sulphate or polysorbates). It makes oil and water mix together into a smooth emulsion. It is a white waxy solid with a low fatty alcohol odour.[1] Wax emulsions do wax distribution evenly into water and change its interfacial tension with additional use of emulsifier. Highly stable wax emulsions are obtained by mechanical energy external forces.[2]

The emulsifying wax is classified into four kinds of wax such as the cationic, anionic, non-ionic and the amphoteric ionic type emulsified wax based on the properties of surfactant.[3] These are having the advantages of melting without heating, evenly becoming a preventive layer, good coverage, easily mixing with other water solutions or emulsion solution. Therefore, the emulsifying wax is widely used in the different areas such as the petroleum industry as a drilling fluid, the wood processing industry as an intensifier, the construction industry as a firming agent, the light and rubber industry as auxiliaries, the textile industry as softening and sizing agents, the medicine industry as auxiliaries of rubber products, the agriculture as an antifreeze of fruit and the paper industry as a pulp sizing agent. [4]

In the present paper, the classification and preparation of the emulsifying wax have been discussed. Four kinds of preparation methods for the emulsifying wax have also been introduced. Effects of the reaction conditions on the emulsifying wax preparation have also been explained.

Discussion

Four types of preparation methods for the emulsifying wax [3]

Four kinds of preparation methods for the emulsifying wax such as the method of emulsifying agents dissolving in the water, dissolving in the oil, the primary soap method and the taking turns adding method have been discussed. The method of emulsifying agents dissolving in the water means that emulsifying agents directly dissolve with water, and then add wax into the water with vigorous stirring. The method of emulsifying agents dissolving in the oil presents that emulsifying agents are added into wax and then the water-in-oil emulsion solution is obtained with additional use of water. When water is continuously added, the water-in-oil emulsion solution is changed to the oil-in-water emulsion solution. This method is called the phase-transfer method. The emulsifying agents dissolving in the oil are firstly transformed to lamellar liquid crystal structure during the process for adding water, and then changed to the oil in water droplets (O/D) gel emulsion structure covered by the continuous phase of surfactant, finally becomes the oil-in-water emulsion solution. The continuous phase of surfactant becomes O/D gel emulsion structure during the process for the emulsifying wax, so a subtle emulsion is obtained because oil droplets evenly distributed and cannot aggregate together to become bigger. The primary soap method describes as the fat and soda are dissolved into wax and water, respectively. When the above two solutions mix together, the primary soap reaction happens. The taking turns adding method presents a little bit of water or wax take turns to be added into emulsifying agents every time. The wax emulsion solution is prepared by the method of emulsifying agents dissolving in the water; however its properties are not stable. On the other hand, the emulsifying wax's properties are very stable by the method of emulsifying agents dissolving in the oil or the primary soap method.

Effects of the reaction conditions on the emulsifying wax preparation

Evaluating the properties of the emulsifying wax includes stability, dispersibility and rheological property, etc. Stability is one of the important properties for the emulsifying wax. The emulsifying wax as an emulsion solution is an unstable

thermodynamic system. They are easily separated after settling at a long time. The instability of the wax emulsion solution shows breaking of emulsion and delamination. The delamination rate (Eqn.1) is given below. Decreasing V value makes an emulsion solution not to separate. In other words, different density between two phases and radius of emulsion solution particles are decreased and viscosity is increased. It is very difficult for the wax emulsion solution to decrease different density between two phases, so it tries to make the emulsion solution particles become smaller and even in shape and size. These are a lot of the reaction conditions having an effect on the stability of the emulsifying wax, such as the different emulsifying agents, the stirring speed, the emulsifying time and the ratio of the emulsifying agents to wax.

$$V = \frac{\Delta\rho d^2 g}{18\eta} \qquad (1)$$

where

V the delamination rate, kg m^{-2} s^{-1}

Δρ- the density difference between two phases, kg m^{-3}

d the radius of emulsion solution particles, cm

g 9.81 m s^{-2}

η the kinematic viscosity, cm^2 s^{-1}

Effects of the different emulsifying agents on the emulsifying wax preparation

Li Guanghui [5] used the conductivity of the emulsion solution to determine the optimized HLB (Hydrophilic-Lipophilic Balance) value of emulsion solution. Figure 1 showed the relationship between HLB and conductivity of emulsion solution. The conductivity of emulsion solution increased with an increase in HLB when HLB values were less than 10. On the other hand, when HLB values were more than 10, the conductivity of emulsion solution almost unchanged. The optimized HLB value for the oil-in-water emulsion solution was determined by its conductivity and HLB value. Table 2 presented the optimized HLB value determined in the system of the emulsifying wax. When HLB values were between 10.25 and 10.75, the wax emulsion solution was very stable based on the below figure 1 and 2.

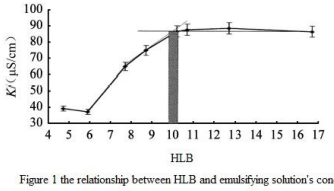

Figure 1 the relationship between HLB and emulsifying solution's conductivity

Figure 1. the relationship between HLB and the emulsion solution's conductivity

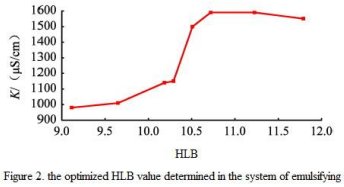

Figure 2. the optimized HLB value determined in the system of emulsifying wax

Figure 2. the optimized HLB value determined in the system of the emulsifying wax

Effects of the different stirring speeds on the emulsifying wax preparation

Li Meng [6] introduced the preparation and application of the wax emulsion solution. Effects of the different stirring speeds on the emulsifying wax preparation have been discussed. Table 1 showed that the stirring speed had an effect on the wax emulsion solution. When the stirring speed is less than 600 rpm, the wax emulsion solution freeze. When the stirring speed is between 600 and 800 rpm, the wax emulsion solution had a good mobility. The wax emulsion solution became extremely thick or become solidify with the stirring speed (more than 1500 rpm).

Table 1. Effects of the different stirring speeds on the emulsifying wax preparation

Stirring speed (rpm)	Emulsion's state
300	Freeze
600	Good mobility
800	Excellent mobility
1500	Extremely thick
1500	Caking

Effects of the different emulsifying time on the emulsifying wax preparation

Li Meng [6] has also studied the different emulsifying time having an effect on the emulsifying wax preparation. Table 2 presented the relationship between the emulsifying time and the properties of the emulsifying wax. The experimental results showed that when the emulsifying time was less than 35 minutes, the properties of the emulsifying wax were very poor. On the other hand, the properties of the emulsifying wax had a good mobility with the emulsifying time (more than 35 minutes). Therefore, the optimized emulsifying time was 35 minutes.

Table 2. the relationship between the emulsifying time and the properties of the emulsifying wax

Emulsifying time (minutes)	Stability (%)	Emulsion's state after settling 24 hours
25	70	Caking
30	80	Good mobility
35	95	Excellent mobility
40	95	Excellent mobility

 DOI: 10.17628/ECB.2013.2.15

Effects of the ratio of the emulsifying agents to wax on the emulsifying wax preparation

Li Meng [5] has also introduced that the ratio of the emulsifying agents to wax had an effect on the emulsifying wax preparation. The ratio of the emulsifying agents to wax was considered to be one of the important methods for producing the emulsifying wax. Patrick Fernandez [7] explained why the critical value of the emulsifying agents/wax ratio was 0.24. When the emulsifying agents/wax ratio was more than 0.24, the submicron's size in the emulsion solution did not almost change and adding water into this system has no effect on the submicron's size. The ratio of oil phase to water phase after settling a long time determined the stability of the emulsion solution. In other words, the sample was kept at a graduated cylinder with plug. The sample's state was checked at any given time. Its stability (Eqn. (2)) was given as follows.

$$R = 100\frac{H_E}{H_T}\ \% \qquad (2)$$

where

R the ratio of the emulsion phase, %

H_E the height of the emulsion phase, cm

H_T the height of the whole system (the height of the emulsion phase and the water phase), cm

Table 3 showed the ratio of the different emulsifying agents to wax having an effect on the emulsifying wax. The height of the emulsion phase increased with an increase in the concentration of the emulsifying agents. The emulsion solution obtained was very stable. The optimized concentration of the emulsifying agents was 8%.

Table 3. the relationship between the ratio of the different emulsifying agents to wax and the stability of the emulsifying wax

Concentration of the emulsifying agents (%)	H_E, cm	H_T, cm	R, %
3	7.9	13.2	59.85
5	9.2	13.3	69.17
8	11.0	13.9	79.14

Conclusion

Based on the above results and discussion, four kinds of preparation methods for the emulsifying wax such as the method of emulsifying agents dissolving in the water, the method of emulsifying agents dissolving in the oil, the primary soap method and the taking turns adding method have been reviewed. The emulsifying wax obtained is very stable by using the method of emulsifying agents dissolving in the oil or the primary soap method. A large number of reaction conditions have an effect on the stability of the emulsifying wax, such as the different emulsifying agents, the stirring speed, the emulsifying time and the ratio of the emulsifying agents to wax. The optimized reaction conditions show that the HLB values, the stirring speed, the emulsifying time and the concentration of the emulsifying agents were 10.25-10.75, 600-800 $r \cdot min^{-1}$, 35 minutes and 8% respectively, the wax emulsion solution obtained was very stable.

References

[1] http://en.wikipedia.org/wiki/Emulsifying_wax.

[2] Yang, S. H. *China Light Industry Press*, **2001**.

[3] Wang, B. F., Zhang, Y. D. and Sun, D. J. *Shandong Chemical Industry*, **2004**, *33*(2), 14.

[4] Hu, W. D. and Yan, C. Y. *Surfactant Industry*, **1997**, *4*, 15.

[5] Li, G. H., Shen, J. W. and Jiang, P. *Drilling Fluid & Completion Fluid*, **2012**, **29**(2), 8.

[6] Li, M. Shang, P. and Liu, M. R. *Tianjing Chemical Industry*, **2010**, *24*(4), 13.

[7] Patrick, F., Valerie, A. and Jens, R. *Colloids and Surfaces A: Physicochem. Eng. Aspects*, **2004**, *251*, 53.

Received: 08.11.2012.
Accepted: 28.11.2012.

EFFECT OF VARIOUS SOIL AMENDMENTS ON THE MINERAL NUTRITION OF *SALIX VIMINALIS* AND *ARUNDO DONAX* ENERGY CROPS

László Simon[a]*, Béla Szabó[b], Miklós Szabó[a], György Vincze[a], Csaba Varga[a], Zsuzsanna Uri[a], József Koncz[c]

Paper was presented at the 4th International Symposium on Trace Elements in the Food Chain, Friends or Foes, 15-17 November, 2012, Visegrád, Hungary

Keywords: soil amendments, mineral nutrition, *Salix viminalis*, *Arundo donax*, energy crops

Basket willow (*Salix viminalis* L., cv. Inger) and giant reed (*Arundo donax* L.) energy crops were grown in open-field experiments. The brown forest soil (loamy sand texture, pH_{KCl} 7.5, humus 1.5%, CEC 10.4 cmolc kg^{-1}; As-38.3, Cd-0.11, Cu-12.7, Pb-13.6, Zn-44.3 mg kg^{-1} in HNO_3 - H_2O_2 extract) was treated with artificial fertilizer and various soil amendments (ammonium nitrate–AN: 100, 150, 300 kg ha^{-1}; municipal sewage sludge compost–MSSC: 15, 25 t ha^{-1}; municipal biocompost–MBC: 20, 25 t ha^{-1}; willow bioash–WB: 600 kg ha^{-1}), and with their combination in 4 or 3 replications. Three months later, in the leaves of treated *Salix* cultures (except WB application) 9.8-23.5% more N was detected than in untreated controls. Most of the treatments enhanced the uptake of K, but concentration of P, Mg, Ca, Fe and Zn in leaves was reduced. Highest As concentrations (1.92-2.11 μg g^{-1}) were found in WB-treated cultures. Cd concentration in treated leaves (0.34-0.57 μg g^{-1}) was lower than in controls (0.99 μg g^{-1}), while Pb concentrations were under the detection limit. Eighteen weeks after first soil treatments with AN, MBC or MSSC mostly MSSC application influenced the accumulation of macro- and micronutrients in the leaves of *Arundo*, however the observed changes were statistically not significant. Concentrations of toxic Cd and Pb were under the detection limits in all treatments. In spite of the repeated soil application of AN, MBC or MSSC, thirty four weeks later statistically significant changes were not observed in the uptake or accumulation most of the elements (including toxic Cd and Pb) in giant reed shoots.

* Corresponding Authors
E-Mail: simonl@nyf.hu
[a] Department of Land Management and Rural Development, College of Nyíregyháza, H-4400 Nyíregyháza, Sóstói str. 31/b. Hungary.
[b] Department of Agricultural Science, College of Nyíregyháza, H-4400 Nyíregyháza, Sóstói str. 31/b. Hungary.
[c] Hungarian Academy of Sciences, Centre for Agricultural Research, Institute of Soil Science and Agricultural Chemistry, H-1022 Budapest, Herman O. str. 15., Hungary.

Introduction

Depletion of fossil fuels and continuously increasing emission of carbon dioxide focus attention on energy production from biomass. Energy crops (e.g. *Agropyron, Arundo, Populus, Robinia, Salix, Sida* sp.) can significantly mitigate carbon dioxide anthropogenic emissions, partially replacing fossil fuels. It was estimated that 1 hectare of energy crop save approximately 5 tons of fossil-carbon[1,2]

Among energy crops, which are cultivated for their high aboveground biomass, the rapidly growing woody basket willow (*Salix viminalis* L.) and herbaceous giant reed (*Arundo donax* L.) are promising. Their annually harvestable shoot wet biomass can achieve 20 or 30 tons per hectare, respectively. Since short rotation coppice (SRC) energy plantations can be cultivated for 15-20 years in the same field, the regular re-supply of plant nutrients in soil is important.[3] One possibility for fertilizing these plants is the field application of municipal sewage sludge, which is rich in nitrogen, phosphorus and various trace elements.[4]

It is well documented that *Salix* sp. (including basket willow) has intensive mineral nutrition, and the Cd and Zn phytoextraction capacity of shoots is high.[5,6,7,8] This phenomenon was confirmed in our pot experiment; shoots of basket willow extracted considerable amounts of Cd and Zn from a galvanic mud contaminated soil.[9] Mineral nutrition of giant reed is less revealed, this plant tolerates well the high concentrations of toxic metals (Cd, Ni, Pb) in soil.[10] It was found in our previous pot and open-field experiments that giant reed shoots principally phytoextracted Zn from a pig slurry or municipal sewage sludge compost amended soil.[11]

The objective of this study was to investigate the inorganic plant nutrient uptake and toxic metal accumulation in basket willow and giant reed aboveground organs. Plants were grown in a brown forest soil treated with ammonium nitrate fertilizer and various amendments (municipal sewage sludge compost, municipal biocompost, and willow bioash).

Experimental

Open-field small-plot experiments were set up with basket willow (cv. Inger) during April 2011 and with giant reed (unidentifiable ornamental plant cultivar originating from Nyíregyháza) during June 2009 in the demonstration garden of the College of Nyíregyháza, located close to Westsik street in Nyíregyháza, Hungary. In one 27 m^2 willows plot 40 plants, and in one 10 m^2 giant reed plot 10 plants were grown.

 DOI: 10.17628/ecb.2013.2.18-21

Table 1. Effect of ammonium nitrate, municipal biocompost, municipal sewage sludge compost and willow bioash on the uptake of essential macro- and microelements in the leaves of basket willow (*Salix viminalis* L., cv. Inger) 12 weeks after treatments (open-field experiment, Nyíregyháza Hungary, September 2011).

Treatments	N	P	K	Ca	Mg	Fe	Cu	Mn	Zn
	m m^{-1} %		mg g^{-1} dry matter			μg g^{-1} dry matter			
Control	2.85a	5.038a	11.906a	10.187bc	5.180a	124a	6.71a	74.9a	104b
	(0.02)	(0.539)	(0.337)	(1.539)	(0.230)	(21)	(0.27)	(9.51)	(12.5)
Ammonium nitrate (AN)	3.33a	3.199ab	13.391a	9.353ab	4.560a	103a	6.87a	82.5a	38.3ab
	(0.19)	(0.214)	(1.171)	(0.294)	(0.408)	(1.1)	0.39	2.60	12.2
Municipal biocompost (MBC)	3.52a	3.143ab	12.695a	7.349a	4.365a	85.7a	6.48a	76.7a	29.4a
	(0.18)	(0.335)	(1.473)	(0.520)	(0.184)	(1.50)	(0.08)	(0.04)	(5.16)
Municipal sewage sludge compost (MSSC)	3.13a	3.411ab	13.698a	8.655ab	4.254a	91.5a	6.39a	73.8a	37.7ab
	(0.29)	(0.040)	(374)	(734)	(428)	(2.9)	(0.54)	(19.2)	(16.0)
Willow bioash (WB)	2.83a	4.026ab	12.414a	9.831abc	4.447a	107a	7.34a	84.5a	77.9ab
	(0.04)	(0.527)	(0.503)	(0.063)	(0.098)	(3)	(0.49)	(14.4)	(34.4)
MBC + AN	3.13a	3.537ab	13.410a	9.287ab	4.392a	86.7a	7.20a	70.9a	28.8a
	(0.47)	(0.538)	(0.762)	(0.483)	(0.280)	(1.48)	(0.08)	(5.1)	(3.7)
MSSC + WB	3.50a	2.822b	14.125a	12.126c	5.034a	99.0a	11.6a	126b	33.6a
	(0.07)	(0.503)	(1.363)	(0.387)	(0.633)	(4.3)	(3.6)	(1.1)	(3.3)
WB + AN	3.19a	3.243ab	13.052a	9.979abc	4.580a	96.6a	6.46a	98ab	46.9ab
	(0.67)	(0.824)	(1.305)	(0.715)	(0.112)	(18.8)	(0.10)	(17)	(29.7)

Data are means of 3 replications, standard deviations are in parenthesis. ANOVA. Tukey's b-test. Means within the columns followed by the same letter are not statistically significant at $P<0.05$.

The uncontaminated brown forest soil (its basic characteristics are in the abstract) of willow plots was treated in June 2011 with ammonium nitrate–AN:100 $kgha^{-1}$ dry weight (producer Nitrogénművek Ltd., Pétfürdő, Hungary); municipal biocompost–MBC: 20 t ha^{-1} wet weight with 75-76% dry matter (producer Térségi Hulladék-Gazdálkodási Ltd., Nyíregyháza Hungary); municipal sewage sludge compost–MSSC:15 t ha^{-1} wet weight with 48-56% dry matter (producer Nyírségvíz Ltd., Nyíregyháza, Hungary); and willow bioash–WB: 600 kg ha^{-1} dry weight (produced at the College of Nyíregyháza by burning of basket willow shoots) with 4 replications. Control plots were untreated. Combined treatments were 20 t ha^{-1} MBC+100 kg/ha AN; 15 t ha^{-1} MSSC+600 kg ha^{-1} WB; and 600 kg ha^{-1} WB+100 kg ha^{-1} AN. Willow leaves were sampled from 20 plants per plot during September, 2011. Leaves were collected from 30-60 cm section of the uppermost section of shoots. [12]

Soil of the giant reed plots was treated in June 2009 with AN (150 and 300 kg ha^{-1}), MBC (25 t ha^{-1}), MBC+AN (25 t ha^{-1} +150 kg ha^{-1}), and MSSC (25 t ha^{-1}) with 3 replications. Control plots were untreated. All treatments were repeated again in July 2010. Eighteen weeks after first soil treatments (in October, 2009) leaf samples, while 34 weeks after second soil treatments (in March, 2011) shoot samples were collected from all experimental plots. First fully developed leaves of the uppermost section of living shoots (from 25 shoots/plot), and middle section of dry shoots (from 10 shoots/plot at approx. 2 m height) were sampled. [12]

Concentration of macro- and microelements in mixed, washed, dried and ground plant samples was determined by ICP-OES technique after HNO_3 - H_2O_2 digestion[12]. Nitrogen concentration of samples was determined by Kjeldahl method. [12]

Statistical analysis of data was conducted with SPSS 18.0 software using analysis of a variance (ANOVA) followed by treatment comparison using Tukey's b-test.

Table 2. Concentration of selected toxic elements in the leaves of basket willow (*Salix viminalis* L., cv. Inger) 12 weeks after soil treatments (open-field experiment, Nyíregyháza Hungary, September 2011).

Treatments	As	Cd	Pb
	μg g^{-1} dry matter		
Control	1.66ab	0.99a	u.d.l.
	(0.50)	(0.35)	-
Ammonium nitrate (AN)	1.86ab	0.57a	u.d.l.
	(0.25)	(0.07)	-
Municipal biocompost (MBC)	1.65ab	0.34a	u.d.l.
	(0.01)	(0.01)	-
Municipal sewage sludge compost (MSSC)	1.86ab	0.57a	u.d.l.
	(0.25)	(0.07)	-
Willow bioash (WB)	1.92ab	0.56a	u.d.l.
	(0.48)	(0.28)	-
MBC +AN	0.66a	0.44a	u.d.l.
	(0.10)	(0.13)	-
MSSC + WB	0.86ab	0.36a	u.d.l.
	(0.48)	(0.05)	-
WB +AN	2.11b	0.55a	0.44
	(0.14)	(0.36)	(0.06)

Data are means of 3 replications, standard deviations are in parenthesis. u.d.l.= under the detection limit: Cd-0.02 μg g^{-1}, Pb-0.30 μg g^{-1}. ANOVA. Tukey's b-test. Means within the columns followed by the same letter are not statistically significant at $P<0.05$.

 DOI: 10.17628/ECB.2013.2.18

Results and Discussion

Table 1 shows the effects of AN, MBC, MSSC, WB and combined treatments on the concentration of essential macro- and microelements in the leaves of basket willow, twelve weeks after soil treatments. Nitrogen concentration was enhanced in basket willow leaves by 9.8-23.5% in all treatments, except WB application. The most pronounced effect was observed at MBC and MSSC+WB treatments, where 23.5% and 22.8% more N was detected than in control culture. All treatments slightly enhanced the potassium content of leaves, while magnesium concentrations were lower than in control. Considering the standard deviation of data, however, the changes in N, K and Mg concentrations were statistically not significant (Table 1).

Treatments lowered the uptake of P, Mg, Fe, Ca (except MSSC+WB application) and Zn concentration in leaves. This phenomenon can be explained by stimulation of the aboveground biomass production of basket willow by most of the treatments.[12] Since higher shoot biomass was formed, the accumulated essential macro- and microelements was more distributed (diluted) in organic matrix. The highest Ca, Cu or Mn concentrations were observed in MSSC+WB-treated cultures.

The Table 2 records the concentration of selected toxic elements (As, Cd, Pb) in willow leaves. The lowest As content (0.66±0.10 μg g^{-1}) was found in MBC+AN-treated culture, while the highest 2.11 (±0.14) was detected in WB+AN treatments. This difference was statistically significant. In the leaves of control cultures 1.66 (± 0.50) μg g^{-1}As was measured. Formerly in MBC 6.26 (± 0.03), in MSSC 20.7 (± 0.60), while in WB 35.4 (± 0.70) mg kg^{-1} arsenic was found in HNO_3 - H_2O_2 extracts.[12] The As concentration in the basic brown forest soil before treatments was relatively high; 38.3 (± 5.5) mg kg^{-1}. [12] In the leaves of control cultures the Cd concentration (0.99±0.35 μg g^{-1}) was the highest; all treatments resulted in lower Cd accumulation. The differences were statistically not significant. Detectable quantity of Pb (0.44 ± 0.06 μg g^{-1}) was present only in WB+AN-treated culture.

Table 3. Effect of ammonium nitrate, municipal biocompost and municipal sewage sludge compost on the uptake of essential macro- and microelements, and accumulation of selected toxic elements in the leaves of giant reed (*Arundo donax* L.) 18 weeks after their first soil application (open-field experiment, Nyíregyháza Hungary, October 2009).

Treatments	N	P	K	Ca	Mg	Cd	Cu	Mn	Pb	Zn
	m m^{-1} %	mg g^{-1} dry matter				μg g^{-1} dry matter				
Control	3.49a	2.649a	17.649a	3.547a	2.822a	u.d.l.	8.59a	99.1a	u.d.l.	24.8a
	(0.01)	(0.048)	(0.606)	(0.223)	(0.072)	-	(0.34)	(10.6)	-	(1.23)
150 kg ha^{-1} ammonium nitrate (AN)	3.47a	2.882a	18.428a	3.040a	2.618a	u.d.l.	9.46a	83.6a	u.d.l.	24.8a
	(0.11)	(0.407)	(3.589)	(0.141)	(0.002)	-	(0.41)	(8.9)	-	(0.68)
300 kg ha^{-1} AN	3.22a	2.347a	17.771a	3.149a	2.017a	u.d.l.	7.77a	80.6a	u.d.l.	21.1a
	(0.29)	(0.076)	(0.295)	(0.124)	(0.091)	-	(0.43)	(1.6)	-	(0.72)
25 t ha^{-1} municipal biocompost (MBC)	3.21a	2.586a	16.997a	3.768a	2.843a	u.d.l.	7.95	99.5a	u.d.l.	24.4a
	(0.02)	(0.102)	(0.630)	(0.301)	(0.150)	-	(0.78)	(4.1)	-	(2.17)
25 t ha^{-1} MBC+ 150 kg ha^{-1} AN	3.49a	2.635a	16.512a	3.713a	2.906a	u.d.l.	8.75a	106.5a	u.d.l.	23.0a
	(0.05)	(0.196)	(2.276)	(0.504)	(0.695)	-	(0.21)	(17.3)	-	(1.11)
25 t ha^{-1} municipal sewage sludge compost (MSSC)	3.57a	2.525a	17.910a	2.942a	1.813a	u.d.l.	8.16a	79.2a	u.d.l.	22.4a
	(0.12)	(0.154)	(1.655)	(0.047)	(0.112)	-	(0.11)	(5.7)	-	(0.78)

Data are means of 3 replications, standard deviations are in parenthesis. u.d.l.= under the detection limit: Cd-0.02 μg g^{-1}, Pb-0.30 μg g^{-1}. ANOVA. Tukey's b-test. Means within the columns followed by the same letter are not statistically significant at $P<0.05$.

In Table 3 the effects of AN, MBC, MSSC and combined soil treatments are presented on the elemental composition of giant reed leaves 18 weeks after soil treatments, at the end of the vegetation period. From the data it is obvious that none of the treatments had significant influence on the macro- and microelement uptake or toxic element accumulation of leaves. It is advantageous that treatment of soil with MSSC have not enhanced the cadmium or lead accumulation in leaves (in all cultures the concentration of these toxic elements remained under the detection limit).

Table 4 shows the elemental composition of giant reed shoots 34 weeks after the second (repeated) soil application of AN, MBC and MSSC. If we compare data in Table 3 and 4, it is evident that in shoots the concentration of macro- and microelements is one order of magnitude lower than in leaves. In spite of the fact that AN, MBC and MSSC were already 2 times applied to the soil, their influence was statistically nor significant for the uptake or accumulation most of the elements (including toxic Cd and Pb) in giant reed shoots. The only exception was Mg uptake, where statistically significant changes were observed.

Conclusions

We can conclude that soil application of the artificial fertilizer ammonium nitrate, or soil amendments as municipal biocompost, municipal sewage sludge compost and willow bioash could influence the uptake of macro- or microelements in basket willow or giant reed energy crops. It is advantageous that it is not a direct short term danger of significant toxic metal (As, Cd, Pb) accumulation in the aboveground plant parts of these species from e.g. MSSC or WB, which can be moderately contaminated with toxic metals. Yield of the *Salix* or *Arundo* energy crops can be stimulated by repeated soil application of biowastes.

 DOI: 10.17628/ECB.2013.2.18

Table 4. Effect of ammonium nitrate, municipal biocompost and municipal sewage sludge compost on the uptake of essential macro- and microelements, and accumulation of selected toxic elements in the shoots of giant reed (Arundo donax L.) 34 weeks after their second soil application (open-field experiment, Nyíregyháza Hungary, March 2011).

Treatments	N	P	K	Ca	Mg	Cd	Cu	Pb	Zn
	m m^{-1} %		mg g^{-1} dry matter			μg g^{-1} dry matter			
Control	0.405a	0.805a	6.742a	0.449a	0.812b	u.d.l.	2.82a	u.d.l.	4.60a
	(0.028)	(0.146)	(0.418)	(0.107)	(0.211)	-	(0.20)	-	(0.55)
150 kg ha^{-1} ammonium nitrate (AN)	0.428a	0.806a	8.436a	0.466a	0.766ab	u.d.l.	2.60a	u.d.l.	4.40a
	(0.041)	(0.130)	(1.917)	(0.133)	(0.279)	-	(0.03)	-	(0.62)
300 kg ha^{-1} AN	0.416a	0.935a	11.967a	0.332a	0.445ab	u.d.l.	2.75a	u.d.l.	4.52a
	(0.058)	(0.110)	(3.930)	(0.021)	(0.028)	-	(0.31)	-	(1.64)
25 t ha^{-1} municipal biocompost (MBC)	0.451a	1.084a	13.816a	0.292a	0.483ab	u.d.l.	2.44a	u.d.l.	6.30a
	(0.054)	(0.264)	(0.123)	(0.093)	(0.089)	-	(0.49)	-	(1.34)
25 t ha^{-1} MBC+ 150 kg ha^{-1} AN	0.343a	0.941a	9.429a	0.308a	0.394a	u.d.l.	3.53a	u.d.l.	3.96a
	(0.035)	(0.148)	(2.744)	(0.011)	(0.037)	-	(1.82)	-	(1.00)
25 t ha^{-1} municipal sewage sludge compost (MSSC)	0.430a	0.979a	11.368a	0.378a	0.628ab	u.d.l.	3.37a	u.d.l.	4.47a
	(0.091)	(0.145)	(3.858)	(0.032)	(0.022)	-	(0.41)	-	(0.98)

Data are means of 3 replications, standard deviations are in parenthesis u.d.l.= under the detection limit: Cd-0.02 μg g^{-1}, Pb-0.30 μg g^{-1}. ANOVA. Tukey's b-test. Means within the columns followed by the same letter are not statistically significant at $P<0.05$.

It is questionable whether there could be a considerable accumulation of toxic metals in the harvested biomass or in bioash, which is formed after its incineration, during 15-20 years long life span of an energy plantation when biowastes (MBC, MSSC, WB) would have been applied 7-10 times to the soil. Further experiments are planned to investigate this phenomenon.

Acknowledgements

This work was sponsored by the Scientific Council of the College of Nyíregyháza and by Nitrogénművek Vegyipari Zrt. (Pétfürdő, Hungary) fertilizer producing company.

References

[1] Blaskó, L., Cultivation of energy plants, site suitability, availability. In: *Renewable Agriculture* (Ed.: Chlepkó, T.). Magyar Katolikus Rádió, Budapest. **2008,** 167-207. (in Hungarian)

[2] Graham, R.L., Wright, L.L., Turhollow, A.F., *Climatic Change*, **1992,** *22*, 223–238.

[3] Gyuricza, Cs., Nagy, L., Ujj, A., Mikó, P., Alexa, L.. *Cereal Res. Commun.*, **2008**, *36*, 279-282.

[4] Kabata-Pendias, A., Pendias, H., *Trace Elements in Soils and Plants (3rd edition)*. Boca Raton, London, New York, Washington, D.C. CRC Press LLC. **2001**.

[5] Tlustoš, P., Pavlíková, D., Száková, J., Fischerová, Z., Balík, J., Exploitation of fast growing trees in metal remediation. In: *Phytoremediation, Rhizoremediation* (Eds.: Mackova, M., Dowling, D., Macek, T.). Springer. Dordrecht, The Netherlands. **2006**, 83–102.

[6] Keller, C. Efficiency and limitations of phytoextraction by high biomass plants: the example of willows. In: *Trace Elements in the Environment. Biogeochem., Biotechnology, and Bioremediation.* (Eds.: Prasad, M.N.V., Sajwan, K.S., Naidu, R.). CRC Press, Taylor and Francis Group. Boca Raton, Florida. **2006**. 611–630.

[7] Máthé-Gáspár, G., Anton, A., *Acta Biol. Szegediensis,* **2005**, *49*, 69–70.

[8] Pulford, I. D., Dickinson, N. M., Phytoremediation technologies using trees. In: *Trace Elements in the Environment. Biogeochemistry, Biotechnology, and Bioremediation.* (Eds.: Prasad, M.N.V., Sajwan, K.S., Naidu, R.). CRC Press, Taylor and Francis Group. Boca Raton, Florida. **2006,** 383-403.

[9] Simon, L., Phytoextraction of heavy metals with *Salix* and *Populus* species. In: *Proceedings of the conference "Competitive Agriculture".* Nyíregyháza, November 29, 2007. (Eds.: Szabó, B., Varga, Cs.). Bessenyei György Book Publisher, Nyíregyháza. **2007,** 197-200. (in Hungarian)

[10] Papazoglou, E. G., Karantounias, G.A., Vemmos, S.N., Bouranis D. L., *Environ. Int*., **2005**, *31*, 243-249.

[11] Simon, L., Kovács, B., Barna, S., Varga, C., Dinya, Z., Accumulation of heavy metals in *Arundo* and *Salix* energy plants treated with pig slurry, municipal sewage sludge and inorganic fertilizers. In: *Proc. 7th Int. Symp. Trace Elements in Human: New Perspectives*. 13-15 October, **2009**. (Ed.: Pollet, E.). University of Athens, Greece. CD-ROM. 258-265.

[12] Simon, L., Szabó, B., Szabó, M., Varga, Cs., Vincze, Gy., *Investigation of the yield and plant mineral nutrient supply of energy crops with special attention to common effect of nitrogen fertilizers and biowastes.* Scientific report prepared for the Nitrogénművek Vegyipari Zrt. (Pétfürdő) fertilizer producer. College of Nyíregyháza, Technical and Agricultural Faculty, Nyíregyháza, Hungary. **2011**. 1-91. (manuscript in Hungarian).

Received: 07.11.2012.
Accepted: 30.11.2012.

MUTUAL SPECTROPHOTOMETRIC DETERMINATION OF MOXIFLOXACIN DRUG AND IRON(III) IONS BY FORMATION OF A COMPLEX COMPOUND

W.F. El-Hawary[a,b]*, Faisal Kh. Al-Gethami[a]

Keywords: Spectrophotometry - Moxifloxacin HCl - Iron(III) ions - Complex.

A simple, new and sensitive spectrophotometric method has been developed for the quantitative determination of the drug Moxifloxacin HCl (MOX), in pure form and in pharmaceutical formulation; and Fe(III) ions. The method was based on the formation of a colored complex between the drug and Fe(III) ions. The maximum absorption wavelength was 450 nm for determination of both MOX and Fe(III) ions. Beer's law was obeyed in the concentration range of 14.45 – 394.2 μg mL^{-1} (r^2 = 0.998) for determination of MOX and 2.8 – 22.4 μg mL^{-1} (r^2 = 0.97) for determination of Fe(III) ions. The conditions for complex formation were studied and optimized to obtain the highest absorbance available. The method was successfully applied for the analysis of commercial tablets (Maxim), and the recovery study reveals that there is no interference from the common excipients that are present in tablets. The results obtained by the proposed method were compared with that obtained by a standard reference one. Statistical comparison of the results was performed with regard to accuracy and precision using student's t-test and F-test at 95% confidence level. The results proved that there no any significant difference, regarding accuracy and precision, between the two compared methods.

*Corresponding Author
E-Mail: waheedfathi@yahoo.com
[a] Chemistry Department, Faculty of Science, Taif University, Taif, Saudi Arabia
[b] Chemistry Department, Faculty of Science, Cairo University, Giza, Egypt

Introduction

Moxifloxacin (MOX) (Scheme 1) is a new fourth generation 8-methoxy fluoroquinolone. Its chemical name is [1-cyclopropyl-7-(S,S)-2,8-diazabicyclo(4.3.0)-non-8-yl-6-fluoro-8-methoxy-1,4-dihydro-4-oxo-3-quinoline carboxylic acid hydrochloride]. The drug was developed primarily for the treatment of community acquired pneumonia and upper respiratory tract infections. It is active against Gram negative pathogens, Gram positive cocci, aerobic intracellular bacteria, atypical organisms and anaerobic bacteria[1]. It has an empirical formula $C_{21}H_{24}FN_3O_4$. HCl with molecular weight 437.89. The drug is an odorless yellow crystalline powder with a melting point in the range 324 – 325 °C. The pH of its 0.1% aq. solution is 4.0 - 5.0. The drug base is sparingly soluble in water, slightly soluble in ethanol (96%) and practically insoluble in acetone; but the hydrochloride form of the drug is fairly soluble in water[2].

Only a little is available in the literature about the analytical determination of MOX, this is may be attributed to the relatively recent abundance of the drug. However, several methods are known for quantitative determination of MOX, including spectral[1,3-12], chromatographic[13-25] and electroanalytical techniques.[9,22,26-29]

The chromatographic method for the determination of MOX requires an automated system, which is not available in many research laboratories. Therefore, it was considered worthwhile to develop rapid and sensitive procedures suitable for the routine quality control analysis of the investigated drug. Spectrophotometric methods still belongs to the most frequently used analytical techniques in pharmaceutical analysis, which gives practical and significant economic advantages over other methods. So, the present study is an investigation and developing a new spectrophotometric method for the determination of MOX in pure form and in its pharmaceutical formulation; and Fe(III) ions, based on the formation of a colored complex compound.

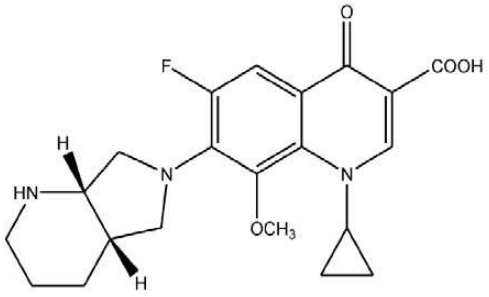

Scheme 1. Chemical structure of moxifloxacin (neutral form).

Experimental

Materials and reagents

All chemicals used in the present investigation were of the highest purity grade chemicals. Ferric oxide was obtained from Sigma-Aldrich products and ferric chloride was obtained from Fluka. Pure MOX was provided by Jamjoom Pharma, Jeddah, KSA. MOX tablets (Maxim) was produced

by Jamjoom Pharma and purchased from local market. The water used for all preparations and washing was freshly prepared deionized water.

Instrumentation

Perkin-Elmer precisely model Lambda 25 – USA, UV-VIS spectro-photometer was used for all spectrophotometric measurements by using quartz cells of 1-cm optical path length. pH - Bench meter model Martini instruments - Romania was used for pH measurements. Millipore (Elix 10) deionizer – USA was used for obtaining deionized water.

Preparation of standard and sample solutions

Preparation of stock standard solution

Stock solution of moxifloxacin.HCl (0.01 M) was prepared by dissolving the accurately weighed amount of the pure drug in the least amount of water, heating until the powder is completely dissolved, then completed to the volume with deionized water. Dilute solutions of the drug were prepared by accurate dilution of the stock 0.01 M solution with deionized water to obtain working concentrations in the range of 14.45 – 394.2 μg mL^{-1}.

Preparation of dosage forms sample solution

Five tablets of MOX drug (Maxim) were ground and mixed well to a fine homogenous powder. An accurately calculated amount of the powder to prepare stock (0.01 M) solution was weighed and dissolved in deionized water with vigorous shaking until complete dissolving of the drug. The solution was centrifuged, filtered, transferred quantitatively to a measuring flask, and completed to the volume with deionized water and shaked well. The solution was standardized spectrophotometrically[4]. Dilute solutions were prepared by accurate dilution whenever needed.

General procedures for determination of MOX

For the determination of MOX using Fe(III) ions, a large excess of Fe(III) ions was added to the drug solution. The absorbance of the formed complex solution was measured at 450 nm against a blank prepared from the same amount of the drug. A calibration curve is constructed between the concentration of the drug and absorbance. All measurements were carried out at room temperature.

General procedures for determination of Fe(III) ions

For the determination of Fe(III) ions using MOX, a large excess of MOX was added to the Fe(III) ions solution. The absorbance of the formed complex solution was measured at 450 nm against a blank prepared from the same amount of the drug. A calibration curve is constructed between the concentration of Fe(III) ions and absorbance. All measurements were carried out at room temperature.

Stoichiometry

The stoichiometric ratios of the formed complexes were determined either by continuous variation or molar ratio methods. In continuous variation method[30], a series of solutions was prepared by mixing equimolecular amounts ($1x10^{-3}$ M) of the Fe(III) ions and drug in varying proportions, while keeping the total molar concentration constant. A plot of the absorbance at the recommended wavelength versus the mole fraction of the drug gave a maximum at the molar ratio of the formed complex. In molar ratio method[31], a series of solutions was prepared by mixing a constant concentration of the drug (3×10^{-4} M and 4×10^{-4} M) with varying concentrations of the Fe(III) ions, then completed with deionized water up to 10 mL. The absorbances of these solution were measured, then plotted versus the ratio between concentration of the iron and total concentration. The plots are straight lines intersect at the most probable molar ratio of the formed complex.

Determination of formation constant for the complex

The formation constant (K_n) of the complex was determined by substituting the data of continuous variation in following equation[32]:

$$K_n = \frac{\frac{A}{A_m}}{\left[\frac{1-A}{A_m}\right]^{n+1} C^n n^n} \qquad (1)$$

where A is the absorbance of the complex at concentration C of the drug, A_m is the maximum absorbance of the complex at full color development which can be obtained from Job's continuous variation curve, and n is the stoichiometric ratio between drug and Fe(III) ions.

Results and discussion

Investigations were carried out to establish the optimal conditions leading to a maximum color development for the quantitative determination of MOX and Fe(III) ions.

Selection of the maximum wavelength

When the spectra of the complex were scanned against deionized water or Fe(III) ions as a blank, it was observed that there is a great absorption in the range 420 – 460 nm; this new absorption may be attributed to the formation of a complex between the drug and Fe(III) ions. The new band of the complex may be obscured by the highly sensitive shoulder of the drug at 360 nm. So, the spectra of the complex were recorded against the pure drug itself as a blank. The results are shown in Fig. 1. It can be shown that a new band at 450 nm appears clearly in this case without any interference from other bands of the drug itself. This new band may be attributed to the formation of a complex between MOX and Fe(III) ions. So, we decided that all of the subsequent measurements will be performed by using the same amount of the drug as a blank.

Effect of solvent

The spectra of the complex were scanned in three solvents; water, acetone and methanol, respectively. The results showed that the absorbance increases slightly in case

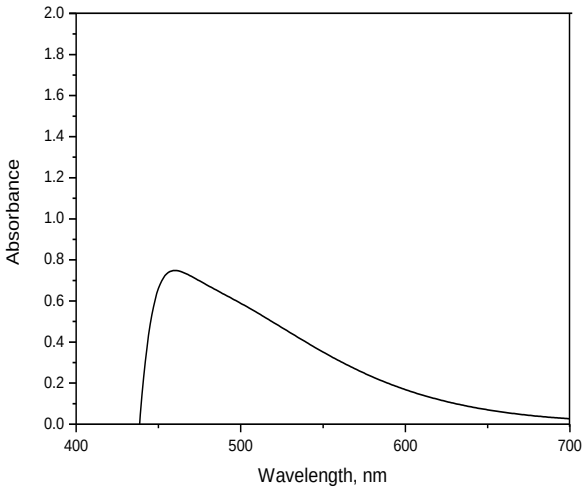

Figure 1. Absorption spectra of the complex in aqueous media against MOX solution as a blank

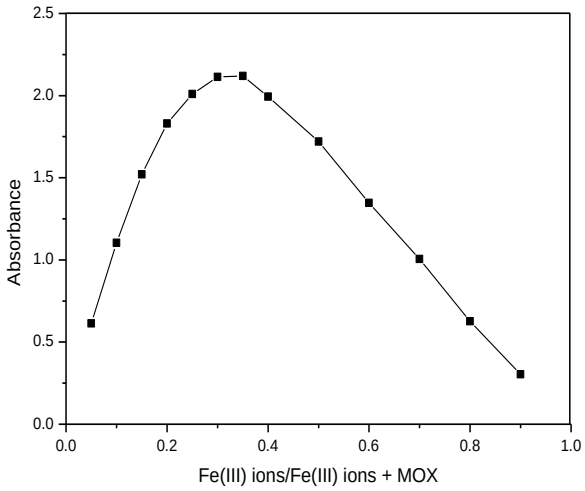

Figure 2. Job's continuous variation method of MOX – Fe(III) ions

of acetone or methanol. But the differences between them and water are not so large. So, all subsequent measurements are performed in aqueous solutions, as water is a widely popular solvent.

Effect of time and temperature

The effect of time on the formation of the complex at room temperature was investigated by allowing the reaction to proceed at different time intervals. The results revealed that the reaction went to completion instantaneously and longer reaction time did not affect the absorbance values. In addition the stability of the complex was studied by following its absorption intensity at different time intervals. The results showed that the absorbance remains stable for more than 48 hours.

The effect of temperature on the reaction and stability of the complex was studied by carrying out the reaction in aqueous medium at different temperatures (25 - 70 ºC). The results revealed that there is no effect of temperature on the reaction of the complex formation.

Effect of pH

The influence of pH on the absorbance of the studied complex was investigated by adding varying amounts of 0.1 M hydrochloric acid or 0.1 M sodium hydroxide to the prepared complex solution. The results revealed that the absorbance in the acidic solutions (pH 2.0 – 3.0), prepared by addition of HCl or without any additions, are very close to each other. Addition of sodium hydroxide with small concentrations (up to pH 3.5), also produces the same absorbance. So, the subsequent measurements are carried out at pH 2 – 3.5 (in presence of the complex only, without addition of neither HCl nor sodium hydroxide).

Stoichiometry of the complex

Under the optimum conditions, the stoichiometry of the reaction between moxifloxacin HCl and Fe(III) ions was investigated by Job's method[30] and molar ratio method[31]. The bell shape of Job's plot (Fig. 2) indicated that the MOX : Fe(III) ions ratio was 2:1.

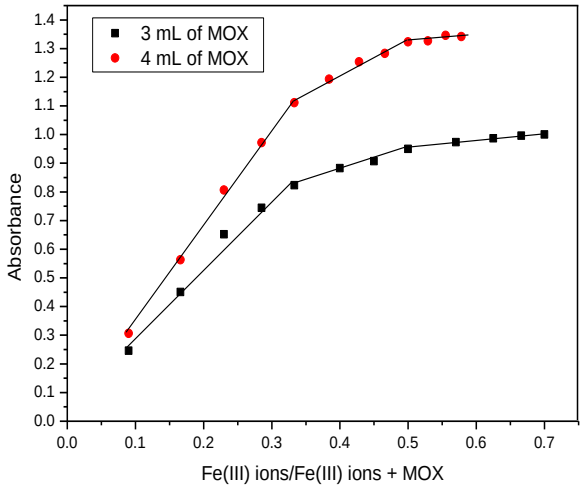

Figure 3. Molar ratio method of MOX – Fe(III) ions complex in aqueous media

The molar ratio method plot (Fig. 3) indicated that the MOX : Fe(III) ions ratio was 2:1 and 1:1.

The Formation Constant of the complex and Free Energy of complexation

The formation constant (K_n) of MOX – Fe(III) ions complex was calculated from the continuous variation data using Eq. (1). The value of K has been determined at several concentration of the drug and the mean value is calculated to be (5.5 ± 0.33) * 10^6 (L $mole^{-1})^2$ (K_{mean} ± SD). It is shown that the value of K is highly enough for complete formation of the complex and to be used in quantitative analysis.

The standard free energy of complexation ΔG^o is related to the formation constant by the following equation:

$$\Delta G^o = -2.303\ RT \log K \qquad (2)$$

where ΔG^o is the free energy change of the complex; R is the general gas constant (1.987 cal mol^{-1} $degree^{-1}$); *T* is the temperature in Kelvin; and K is the formation constant of MOX – Fe(III) ions complex (L mol^{-1}).

 DOI: 10.17628/ECB.2013.2.22

Table 1. Analytical parameters for determination of both MOX using Fe(III) ions, and Fe(III) ions using MOX

Parameter	Determination of MOX	Determination of Fe(III)
λ_{max} (nm)	450	450
Beer's law, µg mL^{-1}	14.45 – 394.2	2.8 – 22.4
Molar absorptivity, L mol^{-1}cm^{-1}	5.74 x 10^{3}	5.46 x 10^{3}
Specific absorptivity, L g^{-1} cm^{-1}	6.12	5.86
Sandell sensitivity, µg cm^{-2}	1.63 x 10^{-4}	1.7 x 10^{-4}
Detection limit (DL), µg mL^{-1}	4.34	1.68
Quantification limit (QL), µg mL^{-1}	14.45	2.8
Ringbom range, µg mL^{-1}	21.9 – 175.2	2.8 – 11.22
Slope of the regression line	6.55 x 10^{-3}	9.77 x 10^{-2}
Intercept of the regression line	-5.5 x 10^{-2}	0.100
Correlation coefficient (r^2)	0.998	0.97
SD of the regression line	0.048	0.227

The value of ΔG^o is equal to (-9.19 ± 0.003) kcal mole^{-1} (ΔG^o ± SD). The negative value of ΔG^o indicates that, the reaction between the drug and Fe(III) ions is spontaneous.

Calibration curve and sensitivity

Under optimum conditions, standard calibration curves for determination of MOX using Fe(III) ions, and for determination of Fe(III) ions using MOX were constructed. The molar absorptivity, specific absoptivity, Sandell's sensitivity and correlation coefficient were determined. Detection limit (DL) and quantification limit (QL)[33] were determined for validation of the analytical method. The regression equation for the proposed procedures are derived using the least squares method and the correlation coefficient was 0.998 for determination of MOX and 0.97 for determination of Fe(III) ions. Table 1 shows the different analytical parameters obtained for determination of MOX and Fe(III) ions.

Reproducibility

The reproducibility of the proposed method was evaluated by performing four replicate analyses of varying concentration covering Beer's law range. The standard deviation and coefficient of variation were determined. The results are show in Table 2 for determination of MOX and Table 3 for determination of Fe(III) ions.

Table 2. Evaluation of precision of the proposed method for determination of MOX using Fe(III) ions

Concentrations, µg mL^{-1}	SD[a]	C.V.[b]
21.9	1.609	8.07
43.8	0.623	1.76
87.6	2.53	3.37
131.4	0.666	0.58
175.2	0.75	0.47
219	3.68	1.82
262.8	0.841	0.34
306.6	0.53	0.18
350.4	2.00	0.593
394.2	1.24	0.327

a: Standard deviation for four replicate measurements;
b: Coefficient of variation for four replicate measurements.

Table 3. Evaluation of precision of the proposed method for determination of Fe(III) ions using MOX

Concentrations, µg mL^{-1}	SD[a]	C.V.[b]
2.8	0.075	2.66
5.6	0.174	2.86
11.2	0.035	0.27
16.8	0.104	0.52
22.4	0.293	1.12

a: Standard deviation for four replicate measurements.
b: Coefficient of variation for four replicate measurements.

Application to Pharmaceutical Preparations

It is evident from the above mentioned observations that the proposed method gave satisfactory results with MOX in pure solution. Thus, its pharmaceutical dosage (Maxim tablets) was subjected to the analysis of its MOX contents by the proposed and a previously reported method[4], which is based on direct measurement of the absorbance of the formed metal complex.

The recovery percentages, using the proposed method, are within the range 100.07 ± 0.52 to 101.99 ± 0.24 (Table 4). These results were compared with that obtained from the previously reported method for pharmaceutical formulation (Table 4). The statistical comparison has been performed with respect to the accuracy (*t*-test) and precision (*F*-test)[34] of the two methods. It was found that there is no significant difference between the calculated and theoretical values of (*t*) and (*F*) at 95% confidence level. This indicated similar precision and accuracy in the analysis of MOX by both methods.

Moreover, to check the validity of the proposed method, the standard addition method was applied by adding small increments of standard MOX to a previously analyzed Maxim solution. The recovery results calculated by comparing the concentrations obtained from the spiked mixtures with those obtained by the reference method[4] were depicted in Table 5. The table, also, includes the standard deviation of the regression lines. The results confirm that the proposed method is not liable to interference by tablet fillers as well as the possibility of determination of lower concentrations using standard addition method.

Table 4. Determination of MOX in pharmaceutical formulation (Maxim tablets) using calibration curve method.

Taken, µg	Found, µg	Recovery±RSD%	F-test[a]	SD	C.V.
14.25	14.45	101.4±4.6	9.54	0.66	4.6
57.8	58.7	101.55±2.74	1.95	1.6	2.74
116.9	117	100.08±0.87	5.13[b]	1.02	0.87
154.2	156.2	101.29±3.14	3.15	4.9	3.14
192.7	194.3	100.83±1.7	1.44	3.32	1.7
270	270.2	100.07±0.52	3.83	1.41	0.52
308.3	312	101.2±1.72	3.78	5.37	1.72
346.9	348.3	100.4±0.46	3.01	1.59	0.46
366.2	371.3	101.39±0.35	4.5	1.3	0.35
385.4	393.1	101.99±0.24	8.94	0.92	0.24

RSD%: relative standard deviation of three replicate analyses except for (b) relative standard deviation of seven replicate analyses; a: Theoretical value for *F* is 19 for two degrees of freedom and 95% confidence limit; b: Theoretical value for *F* is 5.14 for six degrees of freedom for the proposed method and two degrees of freedom for the reference method and 95% confidence limit.

Conclusion

The proposed method for determination of MOX using Fe(III) ions is beneficial over many of the reported methods due to its sensitivity, accuracy, high percentage of recovery, wide application range, low relative standard deviation, and also due to the fact that it doesn't need expensive sophisticated apparatus as the measurements are carried out in the visible region of the spectra. Furthermore, the Fe(III) ions are not expensive and are available in all analytical laboratories. Therefore, the method is practical and valuable and can be used for routine application in quality control laboratories for analysis of MOX. Also, the method can be applied for determination of Fe(III) ions accurately and precisely.

Table 5. Determination of MOX in pharmaceutical formulation (Maxim tablets) using standard addition method

Recovery±SD%[a]	Found, µg	Taken, µg
98.31±0.04	7.01	7.13
101.96±0.03	14.53	14.25
100.1±0.02	57.86	57.8
98.6±0.02	115.26	116.9
100.06±0.01	192.83	192.7

a: SD for regression line.

References

[1]Cirić, A., Jelić, R., Joksović, L., Jelikić-Stankov, M. and Djurdjević, P., *Can. J. Anal. Sci. and Spectroscopy*, **2007**, *52*, 343.

[2]*U.S. Pharmacopeia*, Cat. Nu. 1448606, **2008**, 1.

[3]Misra, M., Misra, A.K., Zope, P., Panpalia, G. M. and Dorle, A. K., *J. Global Pharma Techn.*, **2010**, *2(6)*, 21.

[4]Motwani, S. K., Chopra, S., Ahmad, F. J. and Khar, R. K., *Spectrochim. Acta A*, **2007**, *68*, 250.

[5]Vandana and Chaudhary. A. K., *African J. of Pharm. Sci. and Pharmacy*, **2010**, *1(1)*, 50.

[6]Sahu, S. K., Azam, M.A., Sahu, D. and Banarjee, M., *Pharmacologyonline*, **2011**, *2*, 491.

[7]Dhumal, D. M., Shirkhedkar, A. A. and Surana, S. J., *Der Pharmacia Lettre*, **2011**, *3(3)*, 453.

[8]Sultan, M. A., *Arabian J. Chem.*, **2009**, *2*, 79.

[9]Al-Ghannam, S. M., *Spectrochim. Acta A*, **2008**, *69*, 1188.

[10]Ocaña, J. A., Barragán, F. J. and Callejón, M., *Analyst*, **2000**, *125*, 2322.

[11]Shah, J., Jan, M. R., Inayatullah and Khan, M. N., *African J. of Pharmacy and Pharmacology*, **2011**, *5(5)*, 616.

[12]Ocana, J. A., Barragan, F. J., Callejon, M. and De la Rosa, F., *Microchim. Acta*, **2004**, *144*, 207.

[13]Djurdjevic, P., Ciric, A., Djurdjevic, A. and Stankov, M. J., *J. Pharm. Biomed. Anal.*, **2009**, *50*, 117.

[14]Vishwanathan, K., Bartlett, M. G. and Stewart, J. T., *J. Pharm. Biomed. Anal.*, **2002**, *30*, 961.

[15]Lemoine, T., Breilh, D., Ducint, D., Dubrez, J., Jougon, J., Velly, J.F. and Saux, M.C., *J. Chromatog. B*, **2000**, *742*, 247.

[16]Laban-Djurdjevic, A., Jelikic-Stankov, M.and Djurdjevic, P., *J. Chromatog. B*, **2006**, *844*, 104.

[17]Nguyen, H. A., Grellet, J., Boubakar, B. B., Quentin, C. and Saux, M. C., *J. Chromatog. B*, **2004**, *810*, 77.

[18]Liang, H., Kays, M. B. and Sowinski, K. M., *J. Chromatog. B*, **2002**, *772*, 53.

[19]Boubakar, B. B., Etienne, R., Ducint, D., Quentin, C. and Saux, M. C., *J. Chromatog. B*, **2001,** *754*, 107.

[20]Vu, D.H., Koster, R.A., Alffenaar, J.W.C., Brouwers, J.R.B.J. and Uges, D.R.A., *J. Chromatog. B*, **2011,** *879*, 1063.

[21]Radhakrishna, T., Rao, D. S., Vyas, K. and Reddy, G. O., *J. Pharm. Biomed. Anal.*, **2000,** *22*, 691.

[22]Erk, N., *Anal. Bioanal Chem.*, **2004**, *378*, 1351.

[23]Sultana, N., Arayne, M. S., Akhtar, M., Shamim, S., Gula, S. and Khan, M. M., *J. Chin. Chem. Soc.*, **2010**, *57(4A)*, 1.

[24]Faria, A. F., de Souza, M. V. N. and de Oliveira, M. A. L., *J. Braz. Chem. Soc.*, **2008**, *19(3)*, 389.

[25]Soetebeer, U. B., Schierenberg, M. O., Moller, J.G., Schulz, H., Grunefeld, G., Andresen, P., Blaschke, G. and Ahr, G., *J. Chromatog. A*, **2000**, *895*, 147.

[26]Trindade, M. A. G., Cunha, P. A. C., de Araújo, T. A., da Silva, G. M. and Ferreira, V. S., *Ecl. Quím,* **2006**, *31(1)*, 31.

[27] Trindade, M. A. G., da Silva, G. M. and Ferreira, V. S., *Microchem. J.*, **2005**, *81*, 209.

[28]Radi, A., Wahdan, T., Anwar, Z. and Mostafa, H., *Electroanalysis*, **2010**, *22(22)*, 2665.

[29]Inam, R., Mercan, H. and Yılmaz, E., *Anal. Lett.*, **2007**, *40*, 529.

[30]Job, P., *Ann. Chim.*, **1936**, *6*, 97.

[31]Job, P., *Spectrochemical Methods of Analysis*, Wiley Intersience, New York, **1971**, 346.

[32]Inczedy, J., *Analytical Application of Complex Equilibra*, John Wiley, Budapest **1976**.

[33]Miller, J.C. and Miller, J.N., *Statistics in Analytical Chemistry*, 3rd ed., Horwood, Chichester, UK, **1993**.

[34]Skoog, D. A., West, D. M., Holler, F. J. and Crouch, S. R., *Analytical Chemistry, An Introduction*, 7th ed., Thomson Learning, **2000**, Ch. 7, 149.

Received: 17. 11. 2012
Accepted: 02. 12. 2012.

STUDIES ON THE TRANSPORT RELATED POLLUTANTS IN THE AMBIENT ATMOSPHERE AND THEIR HEALTH IMPACTS ON THE ROAD SIDE VENDERS OF THE INDIAN CITY

A. Mani Prakash[a]*, A.V.V.S. Swamy[a], and R. Hema Krishna[b]

Keywords: transport emissions, air pollution, exposure assessment, roadside vendors, health hazards

The present study "on the transport related pollutants in the ambient atmosphere and their health impacts on the road side venders of the Indian city" has been carried out at Punjagutta station. The ambient air quality was measured in this traffic station and the monthly means were recorded. A 24 h cycle of hourly sampling was also carried out to assess the peak hour traffic concentrations of the ambient air quality parameters. The concentrations of Total Suspended Particulate Matter (TSPM), Respirable Suspended Particulate Matter (RSPM), Sulphur Dioxide (SO_2), Oxides of Nitrogen (NO_x) and Carbon Monoxide (CO) were monitored and compared with the national standards. The behaviour of the quality parameters of this station was described. It has been well established that the time of exposure and dose of the pollutants were positively correlated. The study included vendors who have been staying in the place for not less than three years. Monthly mean concentrations of Respirable Suspended Particulate Matter (RSPM) were highest concentration of 154.16 µg m^{-3} at Punjagutta traffic station during the study period. This concentrations have exceeded the prescribed National ambient air quality (NAAQ) standard for RSPM i.e., 100 µg m^{-3}.Monthly mean concentrations showed a maximum concentration of 6.49 µg m^{-3} of air of SO_2 at Punjagutta. The monthly mean concentrations of oxides of nitrogen (NO_x) were recorded at Punjagutta traffic station has shown maximum concentration of 40.16 µg m^{-3}. Highest traffic volumes were recorded at Punjagutta station (44,954) The present study revealed that the pulmonary functioning decreased among 61.5% of the roadside vendors and a considerable shift of the COHb levels in the blood to the higher side was observed in subject samples.

Corresponding Author:
Tel: 001-647-502-6323
E-mail; hkravuri32@gmail.com
[a]Department of Environmental Sciences, Acharya Nagarjuna University, Nagarjuna Nager-522510, Guntur (Dist.), Andhra Pradesh, India.
[b]Department of Chemistry, University of Toronto, Ontario, Canada. M5S3H6

Introduction

Changes over recent decades in outdoor concentrations of air pollutants were well documented. Human exposure was defined by[1] as 'the event when a person comes into contact with a pollutant of a certain concentration during a certain period of time'. This means that the exposure requires both the pollutant and the person to be present. Most of the epidemiological evidence of the health effects of relatively low concentrations of air pollutants, and in particular of fine particles, uses outdoor concentrations as a surrogate for human exposure. However, the impacts of air pollution on an individual's health actually relate not to these outdoor concentrations but to their personal exposure in the different locations in which they spend time. Although the science of personal exposure assessment, with the associated measurement and modeling techniques, has developed to maturity in North America and Western Europe over the last 50 years, there is an urgent need to apply this science in other parts of the world where the effects of air pollution are now much more serious.[2]

The concentrations of ambient air pollutants which prevail in many urban areas were sufficiently high to cause increased mortality, morbidity, deficits in pulmonary function and cardiovascular and neurobehavioural effects.[3-4] Ambient SPM of anthropogenic origin is emitted into the urban air by a whole host of sources and activities, or it is produced by photochemical processes that lead to the presence of fine aerosols less than 2.5 um in aerodynamic diameter. The anthropogenic SPM is much more toxic than the SPM of natural origin.[5] Motor vehicles, certain industrial processes, and burning of waste also produce and emit particles. High levels of natural wind-blown SPM, albeit less toxic than man made particles, are another feature which complicates this particular air pollution problem. The health effects could be hardly detected by clinical tests. But can be evaluated by the pulmonary function tests. Several studies in such direction were available. Any decrease in the pulmonary function is indicative of the inflammation. The non bacterial inflammations were generally attributed to either occupational or impacts of air pollutants. Roadside vendors generally spend 8-10 hours on the margins of the road and are continuously exposed to the vehicular emissions as well as fugitive dust. The present study has made an attempt to analyze the quality of air in traffic zones and also to record the number of people affected due to traffic pollution in six selected traffic stations in Hyderabad City, Andhra Pradesh, India. Hyderabad is the capital city for the state of Andhra Pradesh. The status of Hyderabad has been recently elevated from 'Municipal Corporation' to 'Greater Hyderabad Municipal Corporation (GHMC)'. With the elevation of status by adjoining rural areas under GHMC, area wise, the GHMC occupied second position after Delhi. This development will lead to further increase of immigrations for employment, increase of vehicles, automobiles and increase traffic volume and density. At such time the impacts of traffic pollution would be multifold .Hence the present work has been carried out with the following specific objectives:

Figure 1. Satellite image of Pun jagutta traffic station

to monitor the ambient air quality at Punjagutta traffic station, by measuring the concentrations of TSPM, RSPM, SO_2, NO_x and Carbon Monoxide.

to ascertain the quality of air in the study area basing on the results of the monitoring and also to compare with the NAAQ Standards.

to correlate the concentrations of the quality parameters with the volume of the traffic and peak hour traffic.

to study the impact of traffic pollution on the health of roadside vendors, through pulmonary function test and carboxyhaemoglobin tests.

Experimental

Punjagutta**:** It is considered as the heart of the city. The roads were fully paved, and devoid of greenery. The vehicular mobility is high and continuous as this is a junction connecting all the four directions. This connects Khairatabad, Banjara hills, Jubilee hills, Hi-tech city, Secunderabad railway station and Bharat Heavy Electricals Limited (BHEL) was shown in Fig.1. Also many contract carriages to all corners of the state will have stopover at this station. There were good numbers of street vendors in this area. But the distribution of push carts like soda sellers, sugarcane juice sellers, fruit sellers and coconut sellers is sporadic because this junction has many radiating roads. As a very important hospital in the State of Andhra Pradesh i.e. Nizam Institute of Medical Sciences (NIMS), is located near to this station, the number of hotels, road side vendors were more. Location of the traffic stations selected for the present study shown in Table.1

Table 1. Location of the traffic stations selected for the present study

Sl.No.	Name of the Traffic Station	Longitude	Latitude
1	Punjagutta	17^0 25’ 36.08” N	78^0 27’ 08.84”E

Sampling of Suspended Particulate Matter (SPM)

The suspended particulate matter was collected in the six selected traffic stations using APM 460 Respirable Dust Sampler (Envirotech Pvt. Ltd., New Delhi). Monthly samples were collected from May 2006 to May 2008 in this station. Both Total Suspended Particulate Matter (TSPM) and Respirable Suspended Particulate Matter (RSPM) were collected and the values were expressed as $\mu g/m^3$. The RSPM was collected using glass fibre filter paper (Whatman GF/A Glass Microfiber Filter, Made in England). The TSPM was collected using the plastic cones supplied along with the sampler by Envirotech pvt. ltd., New Delhi, India. The cones were labelled with the sampling station and date of sampling.

The glass fibre filter paper which was pre-equilibrated for 24 h was taken after ensuring that there were no holes or other visible defects and placed on the mesh. The initial weight of the filter paper was recorded (W1) using an electronic balance (Dhona, 200 D). Final weight of the filter paper was also recorded (W2) after sampling. The initial weight of the cones used for collection of coarse particulates was recorded (C1) before inserting in the cyclone and final weight was recorded (C2) after the completion of the sampling.

Calculations

The concentrations of Respirable Suspended Particulate Matter (RSPM) and Total Suspended Particulate Matter (TSPM) in $\mu g\ m^{-3}$ were calculated using the formulas (1) and (2)

$$RSPM(\mu g\ m^{-3}) = \frac{W_2 - W_1}{Mr\ t} * 10^6 \quad (1)$$

$$TSPM\ (\mu g\ m^{-3}) = \frac{(C_2 - C_1) + (M_2 - M_1)}{Mr\ t} \quad (2)$$

where,

C_1	initial weight of the cone (g)
C_2	final weight of the cone (g)
W_1	initial weight of the filter paper (g)
W_2	final weight of the filter paper (g)
Mr	manometer reading (lpm)
t	total sampling time (minutes)

Sampling and Analysis of Sulphur Dioxide

Thirty ml of 0.04 M potassium tetrachloromercurate (TCM) absorbing solution was taken in a midget impinger and arranged in the gaseous sampling kit attached to the Respirable Dust Sampler. The sampler was allowed to run for 8 hrs (the rotameter set for 0.2 litre / minute) and then the contents of the impinger were transferred to a clean sampling bottle and it is clearly labeled with the date and time of the sampling. The impinger was again filled with 30 ml of TCM solution to continue the sampling procedure. The collected samples were immediately transferred to the laboratory for further analysis.

The contents of the sampling bottle were transferred to a 50 ml volumetric flask. A reagent blank was prepared by adding 25 ml of unexposed absorbing reagent in a 50 ml volumetric flask. To destroy the nitrates from oxides of nitrogen, 1 ml of 0.6% sulfuric acid was added and was allowed to react for 10 minutes. Two ml of 0.2% of formaldehyde and 5 ml Pararosaniline reagent were added. The contents were allowed to stabilize for 30 minutes then the absorbance was measured at a wavelength of 560 nm in a UV-Visible Spectrophotomer (ELICO Model No SL 177, Scanning SPEC).

Aliquots of diluted sodium sulphite solution was added to 0,1,2,3,4 and 5 ml were taken into series of 25 ml volumetric flasks. The contents were made up to 25 ml in the volumetric flask using 0.04 M TCM solution. The absorbances were plotted against concentrations. Concentrations of the SO_2 in the unknowns were drawn from the graph.

Calculations

The SO_2 concentration can be expressed as (Eqn.3):

$$C_{SO_2} = \frac{(A - A_0) * 10^3 \, B V_s}{V_a \, V_t} \qquad (3)$$

where

C_{SO2}	SO_2 concentration in µg_m^{-3}
A	sample Absorbance
A_0	reagent Blank absorbance
10^3	conversion litres to cubic meters
B	calibration factor µg/absorbance
V_a	volume of air sampled in litres
V_s	final volume of sampling solution
V_t	aliquot taken for analysis

Sampling and Analysis of nitrogen oxide

Thirty ml of sodium hydroxide and sodium arsenite absorbing solution was taken in a midget impinger and arranged in the gaseous sampling kit attached to the Respirable Dust Sampler. After the sampling, the contents were taken to the laboratory in the amber colored bottle and subjected to further analysis.

1.5306 g of NaNO*2* was dissolved in double distilled water and made up to 1l. 1 ml of this solution was equivalent to 1000 µg/ml of NO_2. 10 ml of this solution was diluted to 1 l. This contained 10 µg/ml of NO_2. Again 10 ml of this solution was diluted to 100 ml with absorbing solution; this contained 1 µg/ml of NO_2.

25 ml of absorbing solution was taken in ten volumetric flasks and 0.5, 1, 3, 5, 7, 10, 15, 20, 25 ml of 1 µg/ml of NO_2 was placed in each of the flask and made up to 25 ml using absorbing solution. 1ml of H_2O_2, 10 ml of Sulfanilamide solution and 1 ml of NEDA were added to each flask, the contents were thoroughly mixed and left for 30 min for colour development. Then absorbance at 550 nm was measured using a UV-Visible spectrophotometer (Model ELICO Model No SL 177, Scanning Mini SPEC). The absorbance was plotted against concentration to prepare a calibration curve. The concentration of the unknowns were drawn from this calibration curve.

Calculations

The NO_x concentrations can be expressed as:

$$C_{NO_x} = \frac{c_{NO_2} V_s}{0.82 V_a V_t} D \qquad (4)$$

c_{NO2}	NO_2 concentration in analyzed sample (Graph factor x (samples absorbance – blank absorbance)
V_a	volume of air sampled in m^3
0.82	sampling efficiency
D	dilution Factor (D=1 for no dilution; D=2 for 1:1 dilution)
V_s	final volume of sampling solution
V_t	aliquot taken for analysis

Sampling of Carbon Monoxide (CO)

The concentrations of the Carbon Monoxide were recorded using an instrument (Make: Quest technologies)

 DOI: 10.17628/ECB.2013.2.28

that directly gave the read out. The values were recorded exposing the instrument to the ambient condition for one minute. Series of values were recorded and the mean values were tabulated.

The respective concentrations of the ambient air quality parameters were compared at this station with the National Ambient Air Quality (NAAQ) standards.

Sampling and testing of street vendors

For the present study, the vendors were selected using judgment sampling and convenience sampling. The vendors were selected from each sampling station and were subjected to various tests. For all the tests, people who have been living in this area for a minimum of three years were selected. After preliminary interview the vendor was taken to Andhra Pradesh chest hospital, Hyderabad and tested for the parameters initially. The vendor was taken as the item in the sample only when they promised to attend to the tests for the second time. They were financially compensated for the loss of income on the days of tests.

The following tests were performed to the vendors, to identify the impacts of traffic on the health.

Blood pressure test

Pulse oxymetry

Pulmonary function test

Carboxy haemoglobin test

All these tests were performed after recording the age, height (in cm) and weight (in kg) of the vendors. A brief description of each test is given.

a) Blood pressure test

The systole and diastole pressure was measured using a sphygmomanometer. This test was performed only to ascertain the initial health status of the vendors as a cross checks for the information provided by the sample vendor.

b) Pulse oxymetry

The pulse oxymetry was performed for all the vendors to record percent saturation of oxygen in the blood and the pulse rate. The vendors' finger was clipped connecting to the pulse oxymetry (BPL) apparatus. The instrument gave direct reading of percent saturation and the pulse rate of the vendor. The saturation percentage of the individual was compared to the standards available and accordingly the decrease of percent saturation was categorized as normal, mild, moderate and severe, in that order.

c) *Pulmonary Function Test*

PFT test is envisaged to detect whether the vendor has got any breathing problem. This test also helps to detect any obstruction in the trachea of the vendor. The PFT besides tracing out the obstructions, also measures the volume of air that could be held by the lung.

The Pulmonary Function Test was performed to all the vendors. The Pulmonary Function was assessed through two components namely FEV1 and FVC. FEV1 was Forced Expiratory Volume in the first second. The total expiration was measured after a full breathe to record Forced Vital Capacity. The FEV1 and FVC were measured twice at an interval of 20 minutes. The first record of FEV1 and FVC were taken as the base volume and the second record generally was used to prescribe the drug dose basing on the difference. After six months all the vendors were tested for second time. The difference between the two base volumes was considered for the assessment of the impact. The difference between the first FEV1 and second FEV1 (after 6 months) was recorded in ml. The difference between first FVC and value after 6 months was also recorded in ml. The increase of value for FEV1 and FVC over the initial value (when the study was started) was taken as the improvement in the condition and a decrease over the first record was taken as the deterioration of the lung capacity which is referred in the study as 'Affected'.

d) *Carboxy haemoglobin test*

The amount of carbon monoxide in the blood was recorded using a CO meter (Micro Medical CO meter, UK). The vendor was asked to inhale the air to full capacity and hold it for 15-20 seconds and then blow the air out through the mouth piece attached to the CO meter. The CO meter gave a direct read out in percentage COHb. The Carboxy haemoglobin (COHb) test was repeated after six months for all the vendors. The difference between the two records was used to assess the impact. An increase in the value at the second instance was considered to designate the vendor as affected and a decrease for improvement in the condition.

RESULTS AND DISCUSSION

Ambient air quality in the traffic stations

The study included monitoring of TSPM, RSPM, SO_2, NO_x and CO at punjagutta station. The monthly means of the ambient air quality parameters are discussed for this station. Basing on the number of ambient air quality parameters exceeding the standards, the traffic station was assigned a rank to denote the level of air pollution. The hourly means of 24 hours analysis was also made and the concentrations of ambient parameters during peak traffic hours was also determined. A brief description of various AAQ parameters at different traffic zones is furnished here under.

Monthly mean concentrations of ambient air quality parameters at Punjagutta traffic station

a) Total suspended particulate matter (TSPM)

The monthly means of total suspended particulate matter (TSPM) for the study period showed a wide range of concentrations. The minimum TSPM concentration was recorded in August 2006 (347.00 $\mu g/m^3$) and the maximum

was recorded in December 2006 (492.00 µg/m^3), while the mean concentration of the TSPM recorded for the study period was 405.68 µg/m^3. The seasonal distribution of TSPM was similar for the two years. The particles with less than 10 µm diameter were considered as respirable suspended particulate matter or PM_{10}. The developed countries since 1990s have further increased the resolution of this particle diameter to a finest size of $PM_{2.5}$ and $PM_{1.}$ However, the new millennium studies in the developed countries have been monitoring even the 'ultra particulates' or 'nano particulates'. The prime source of these finest particles is the emissions from automobiles. There were supporting evidences by many authors for these sources [6-10] measured the particle size distribution in the range of 11 - 452 nm on the side of a busy Marylebone road in Central London and concluded that 11-30 nm size contained freshly nucleated particles formed as the exhaust gases diluted with ambient air. The summer seasons exhibited moderate concentrations of TSPM and the rainy seasons showed the lowest concentrations, while the highest concentrations of the TSPM were recorded during winter season (Table 2; Fig 2).

b) Respirable suspended particulate matter (RSPM)

The monthly means of respirable suspended particulate matter for the study period showed a wide range of concentrations. The minimum RSPM concentration was recorded in July 2007 (123.50 µg/m^3) and the maximum was recorded in December 2006 (196.80 µg/m^3), while the mean concentration of the RSPM recorded for the whole study period was 154.16 µg/m^3.

The seasonal distribution of RSPM was same for the two years. The summer seasons showed moderate concentrations of RSPM and the rainy seasons showed the lowest concentrations, while the highest concentrations of the RSPM were recorded during winter season. The maximum attention among the traffic pollutants had been focussed on the particulate matter because of it's potential threat to human health particularly in the pulmonary ailments. [11] examined the respirable suspended particulates at 72 locations in 6 urban districts of different land use types in Hong Kong and concluded that the problem of respirable suspended particulates in Hong Kong's roadside environment is quite serious. (Table 2; Fig 2). *c) Sulphur dioxide*

The monthly means of sulphur dioxide for the study period showed a marginal range between 5.90 and 7.10 µg/m^3. The mean concentration of sulphur dioxide for the whole study period was 6.49 µg/m^3. The seasonal variation in the concentrations of sulphur dioxide was not high as there was only marginal difference between the lowest and highest concentrations during the study period. The concentrations of sulphur dioxide were considered as negligible because the recorded concentrations were less than 10% of the prescribed national standard. The sulphur dioxide coupled with particulate matter is known to increase the respiratory and cardio-pulmonary mortality [12]. They have made a study in Vienna, Linz and Graz cities on the effects before and after implementation of standards for TSP and SO_2. (Table 2; Fig 2).

Table 2. Monthly mean concentrations of Ambient air quality parameters at Punjagutta traffic station during the study period.

Month and Year	TSPM, µg m^{-3}	RSPM, µg m^{-3}	SO_2, µg m^{-3}	NO_x, µg m^{-3}	CO, µg m^{-3}
MAY, 2006	404.00	154.70	6.80	37.80	2.70
JUNE, 2006	392.00	156.70	6.60	39.40	2.90
JULY, 2006	360.00	137.80	6.30	36.20	2.20
AUG, 2006	347.00	131.70	6.20	34.90	2.10
SEP, 2006	366.00	129.50	6.10	32.50	2.30
OCT, 2006	364.00	127.80	6.20	36.90	2.10
NOV, 2006	465.00	187.40	6.90	46.20	4.90
DEC, 2006	492.00	196.80	6.90	50.20	4.80
JAN, 2007	483.00	182.90	7.00	49.70	4.60
FEB, 2007	455.00	170.40	6.80	46.30	4.70
MAR, 2007	388.00	154.60	6.40	36.70	2.90
APR, 2007	395.00	147.80	6.30	38.60	2.50
MAY, 2007	407.00	142.70	6.20	39.40	2.50
JUN, 2007	417.00	142.30	6.50	35.90	2.60
JUL, 2007	384.00	123.50	6.10	35.60	2.10
AUG, 2007	370.00	125.50	6.00	34.20	2.00
SEP, 2007	360.00	130.90	5.90	33.10	2.20
OCT, 2007	351.00	128.70	6.00	34.50	2.10
NOV, 2007	445.00	187.70	6.70	43.70	4.90
DEC, 2007	463.00	187.40	6.90	50.70	4.90
JAN, 2008	454.00	177.60	7.10	49.70	4.80
FEB, 2008	438.00	168.60	6.80	47.60	4.70
MAR, 2008	374.00	159.70	6.40	35.80	2.40
APR, 2008	381.00	152.70	6.70	39.70	2.50
MAY, 2008	387.00	148.60	6.50	38.70	2.90
Mean	405.68	154.16	6.49	40.16	3.17
NAAQ Standard	200	100	80	80	2

 DOI: 10.17628/ECB.2013.2.28

Table 3. Hourly parameters at Punjagutta traffic station during the study period

Time of sampling	TSPM ($\mu g/m^3$)	RSPM ($\mu g/m^3$)	SO_2 ($\mu g/m^3$)	NO_x ($\mu g/m^3$)	CO (mg/m^3)
1.00	390.00	145.00	7.00	38.00	3.50
2.00	390.00	155.00	7.50	39.00	4.50
3.00	410.00	155.00	6.50	40.50	3.50
4.00	390.00	145.00	7.50	41.50	4.00
5.00	405.00	155.00	8.00	40.50	5.50
6.00	415.00	165.00	11.00	40.00	7.50
7.00	445.00	195.00	16.50	44.00	8.50
8.00	545.00	260.00	21.50	46.00	13.00
9.00	645.00	280.00	26.50	58.00	16.50
10.00	695.00	395.00	38.00	63.00	25.00
11.00	860.00	260.00	24.50	74.50	12.00
12.00	715.00	230.00	18.00	57.00	8.00
13.00	580.00	185.00	13.00	52.00	7.50
14.00	530.00	210.00	12.00	47.00	7.50
15.00	465.00	255.00	19.00	49.00	13.00
16.00	515.00	310.00	25.50	54.00	18.00
17.00	615.00	395.00	32.00	62.00	20.50
18.00	680.00	440.00	33.50	68.00	28.00
19.00	765.00	340.00	46.00	79.50	18.50
20.00	925.00	255.00	32.00	63.00	14.00
21.00	720.00	210.00	17.50	53.50	11.00
22.00	560.00	180.00	12.00	44.00	8.00
23.00	455.00	170.00	8.00	42.50	6.50
24.00	445.00	170.00	7.50	41.00	4.50
X̄	565.00	235.83	18.77	51.56	11.19
NAAQ Standard	200	100	80	80	2

d) Nitrogen oxide

The concentrations of the oxides of nitrogen for the whole study period ranged between 32.50 and 50.70 µg/m3, with a monthly mean of 40.16 µg/m3. The concentrations of oxides of nitrogen during summer were moderate. The rainy season exhibited less concentration while the concentrations were higher in winter season. However, the highest concentration recorded at Punjagutta (50.70 µg/m3) was a little above 50% of national standard value. The concentrations of NO_x were found to be higher in busy roads and areas with high density of buildings. A study made in Hong Kong on the daily variations of NO_2 at 14 monitoring stations by [13] concluded that the air pollution behaviour was in tune with the variations in the traffic volume and further the dispersion of these pollutants was hindered by the tall buildings and their high density. (Table 2; Fig 2).

e) Carbon monoxide

The carbon monoxide concentrations at Punjagutta ranged between 2.00 and 4.90 mg/m3. The mean concentration for the whole study period was 3.17 mg/m3. Though the difference between the lowest and highest records seemed to be less, a difference of 2.90 mg/m3 would be definitely considerable difference if we take into account the permissible limit for carbon monoxide which stood at 2.00 mg/m3 for 8 h averaging time. The seasonal march of the carbon monoxide was similar to that of any other parameter with trends following, moderate in summer, less in rainy and high in winter, pattern. The concentrations of CO vary widely in different parts of a city[14] conducted a study in Mexico city on in-vehicle carbon monoxide levels to identify the main factors affecting the variation in CO concentrations inside public and private transport vehicles during the winter of 1991. (Table 2; Fig 2).

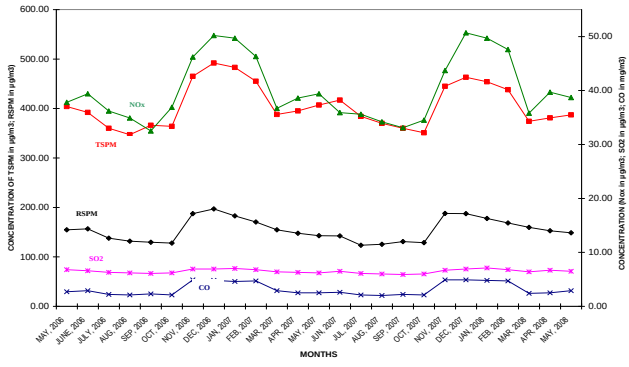

Figure 2. Monthly mean concentrations of ambient air quality parameters at Punjagutta during the study period

Hourly mean concentrations of ambient air quality parameters at Punjagutta traffic station

a) Total suspended particulate matter (TSPM)

The total suspended particulate matter at Punjagutta varied widely between 390.00 and 925.00 $\mu g/m^3$. The TSPM showed two peak concentrations every day corresponding to

 DOI: 10.17628/ECB.2013.2.28

the PTHs. The behaviour of the TSPM dwindled fast with variations in the turbulence due to the traffic.

In a cycle of twenty four hours there was a gradual increase of TSPM concentration with sunrise and reached to the P1 (morning peak) at 11.00 h. Then the concentration of TSPM started to decrease up to 15:00 h followed by a slow increase to reach the P2 (evening peak) at 20:00 h. From 21:00 h in the evening, the concentrations showed a slow decrease till 07:00 h in the morning. The twenty four hour mean of the TSPM at Punjagutta was 565.00 µg/m^3.

The ambient air quality standard specified that the TSPM should not exceed 200.00 µg/m^3 for twenty four hour weighted average for residential, rural and other areas, while for industrial areas, it was 500.00 µg/m^3. The concentrations in the present study have crossed the particular prescribed standards. The lowest values, twenty four hour mean ($\bar{x}$ 24 h = 565.00 µg/m^3) were much higher than the national standard. (Table 3; Fig. 3).

b) Respirable suspended particulate matter (RSPM)

The present study at Punjagutta showed a wide range of RSPM concentrations between 145.00 and 440.00 µg/m^3. However, the hourly mean of twenty four hour cycle was 235.83 µg/m^3, which was well above the national standard. Punjagutta experienced two PTHs during the day. It is interesting from the present study that the concentrations of each parameter reached the peaks independent of other parameters. In other words, the peak concentrations of the AAQ parameters of RSPM reached it's peak at 10:00 h in the morning and at 18:00 h in the evening in a day. The achievement of peak concentration for other parameters was slightly delayed. This was perhaps due to the differences in "settling velocities" and the "diffusion coefficients".

The RSPM was contributed by the automobile emissions as well as the fugitive dust. The highest value of RSPM was recorded at 10:00 h in the morning and at 18:00 h in the evening. As the traffic turbulence decreased, the concentrations of the RSPM also decreased in the night. During early hours the concentrations of RSPM started to increase with the increasing volume of the traffic. After the peak concentration at night, the RSPM concentrations consistently decreased from 21.00 h till 07.00 h. (Table 3; Fig. 3).

c) Sulphur dioxide

The concentrations of sulphur dioxide, in the hourly samples of a twenty four hour cycle revealed excessively high concentrations during the peak hours, 38.00 and 46.00 µg/m^3 at P1 and P2, respectively. The concentrations in the ambient air showed a positive correlation with the volume of traffic. The intensity of traffic was high in the evening compared to the morning times at all the traffic stations. The concentrations of sulphur dioxide also showed a decreasing trend throughout the night and again the concentrations started to rise with the increasing traffic and the hourly sample study recorded an hourly mean of 18.77 µg/m^3. The lowest concentration recorded was 6.50 µg/m^3 at 03:00 h, while the highest 46.00 µg/m^3 was recorded at 19:00 h (Table 3; Fig. 3).

d) Nitrogen oxide

The concentrations of oxides of nitrogen dwindled throughout the day from a minimum concentration of 38.00 µg/m^3 to a maximum of 79.50 µg/m^3. (Table 3; Fig. 3). The traffic at Punjagutta was active from 07:00 h in the morning to 22:00 h. During this period the mobility of the vehicles was not uniform. The volume of traffic would be maximum at least, two times a day during morning and evening. The duration of this maximum volume is more or less consistent throughout the study period. The highest concentration recorded (79.50 µg/m3) at this place was during the peak traffic hour in the evening. In general, the concentrations during the diel peaks were higher and between the two peaks, the evening PTH showed higher values. In a cycle of twenty four hours the concentrations of oxides of nitrogen increased with increased traffic volume. From 23:00 h to 06:00 h the concentrations showed a decrease for nearly eight hours and with the starting of the civil traffic, at 07:00 h the concentrations went up steadily to reach a peak, at 11:00 h then again decreased from noon till 16:00 h. The concentrations then marched towards the evening PTH showed increased values to reach a peak at 19:00 h. The cycle was repeated every day. The national standard prescribed for oxides of nitrogen was 80.00 µg/m3 for residential and other areas, and 120.00 µg/m3 for industrial areas. The concentrations of oxides of nitrogen were very nearer to the maximum permissible limit during the PTH. However, the hourly mean for a twenty four hour cycle at this station, was much less than (51.56 µg/m3) the permissible limit. (Table 3; Fig. 3).

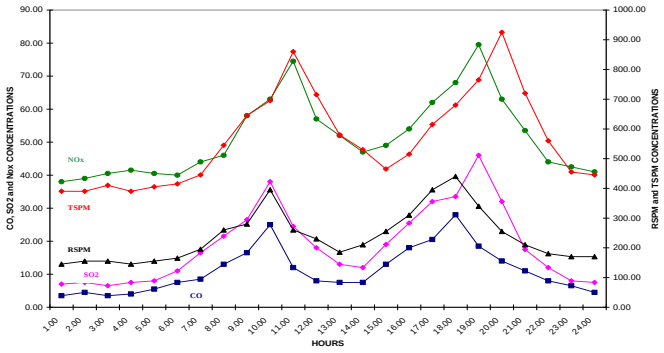

Figure 3. Hourly parameters at Punjagutta traffic station during the study period

e) Carbon monoxide

The concentrations of CO ranged between 3.50 to 28.00 mg/m3 with an hourly mean of 11.19 mg/m3 in a twenty four hour cycle. The concentrations of CO also followed the same path of the increase and decrease as exhibited by the other parameters. During night time, after the evening PTH, the CO concentrations decreased and started increasing from 06:00 h in the morning to reach a peak of 25.00 mg/m3 by 10:00 h. Then, a slight decrease up to 13:00 h to a concentration of 7.50 mg/m3. Again there was a steady increase to reach a peak concentration of 28.00 mg/m3 in the evening PTH. The CO concentrations were almost equal to Sulphur dioxide concentrations during certain hours particularly when the concentrations were on the decrease. The maximum permissible limit as per the national standard

for 8 hourly average was 2.00 mg/m3 and for 1 hour averages it was 4.00 mg/m3. The CO concentrations continued to be higher during the day time and equal to maximum permissible limit during night time. (Table 3; Fig. 3).

Tests for health impact

The vendors were tested twice in a span of six months. The difference between the initial test and final test values were used to record whether the person was affected and if affected the intensity of the impact by comparing with the available standard values.

Blood pressure

The blood pressure of the vendors was initially measured to cross check the information provided by the respondents.. The vendors had normal blood pressure was shown in Table .4.

Table 4. Details of the blood pressure measurement in the beginning of the study for the subject vendors in the study area.

Station	Sample size	Normal B.P.	High B.P.
Punjagutta	11	11(100%)	0 (0%)

Pulse oxymetry

The pulse oxymetry was used to measure percent oxygen saturation in the blood., the vendors have been affected at varied intensities. However, 40.4% of the vendors had the saturation level between 93-95% which was designated as 'mild impact', another 38.5% were affected with moderate impact were shown in Table.5. In these cases the saturation level was between 87-92%. There was no case of 'severe impact'. On the whole, 79% of the roadside vendors were affected and only 21% were normal. This decreased saturation level of oxygen could be taken as a forecasting tool for the future ailments or disorders.

Table 5. Measurement of the percentage oxygen saturation in blood among the subject vendors through pulse oxymetry in the beginning of the study.

Sl.No	Name of the Station	Normal	Mild of impact	Moderate of impact
1.	Punjagutta	3	4	4

Pulmonary function test (PFT)

Pulmonary Function Test is generally considered as the clinical support test of the general health of an individual. The 'Pulmonary Function' varies with not only the bacterial lung infections but also with non bacterial lung infections. Exposure to a deteriorated ambient air quality also lead to the non bacterial lung infections. The periodical testing of lung function helps in prediction of the respiratory allergies, aggravation of already existing respiratory ailments such as Asthma and Bronchitis and also the consistent decrease of lung function forecasts the Chronic Obstructive Pulmonary Disease (COPD). Hence, the pulmonary function test was considered in the present study as the primary indicator of the impact of traffic pollution on the health of roadside vendors.

The Pulmonary function test reveal the air handling capacity of the lungs of an individual. This capacity was measured in two dimensions viz., FEV1 and FVC. The FEV1 was Forced Expiratory Volume in the first second of expiration which was expressed in ml. The FVC was Forced Vital Capacity measures the amount of air one can exhale with force after a full breath, the value of which was expressed in ml. FEV1 and FVC, both were measured to evaluate the pulmonary function of the roadside vendors, in the beginning of the study as well as after six months. The change of value over the first record i.e., in the beginning of the study was noted to denote the impact as "improved" when the second record was higher than the first and the impact was considered as "affected", when the second record was lower than the first. After both the tests, the vendor was considered as "improved" when the second record was higher for both FEV1 and FVC. The vendor was considered as "affected" when the FEV1 and / or FVC have shown a decrease. These values were influenced by many factors such as volume of traffic, duration of exposure, age group, habits of the individual, etc.,

Out of the 11 roadside vendors tested at Punjagutta, six subject vendors have showed a decrease in the Forced Expiratory Volume in first second. The range of decrease of FEV1 from -90.00 to -800.00 ml. Five of the subject vendors showed an improved Forced Expiratory Volume in first second, and this improvement ranged from 60.00 to 370.00 ml. The group which showed improvement included the people shifted their residence to a non traffic zone and some were never smokers. However, this improvement was attributed to shifting to a new place and the resistance capacity of the individual Decreased FEV1 indicated development of obstructions in the respiratory tract of the subject vendors [15] conducted a study to test a hypothesis that children living close to busy roads may have impaired respiratory health. Study concluded that the relation between symptoms and measures of exposure to traffic related air pollution were almost entirely restricted to children with bronchial hyper responsiveness and/or sensitization to common allergens, indicating that these are a sensitive subgroup among all children for these effects.

The Forced Vital Capacity (FVC) indicates total air handling capacity of the lungs, revealed a decrease in six vendors from -20.00 to -1050.00 ml. The decrease in FVC over a period, indicate reduced lung capacity which is a sign of vendor's susceptibility to future infections. Five vendors showed an increase in lung capacity of whom two vendors showed substantial improvement. Among the vendors who showed substantial improvement, one vendor had very less was shown in Table .6, vital capacity in the beginning of the study, later improved health resulted in the overall efficiency and she possessed the lowest vital capacity among the subject samples at Punjagutta. This must be due to a 'recovery' from an ailment.

Table 6. FEV1 and FVC values – Punjagutta

Sl. No	Code of Sample Vendor	FEV1 Initial in ml	FEV1 Final in ml	FEV1 difference in ml	FVC initial in ml	FVC final in ml	FVC difference in ml
1	Pun 1	3000.00	3170.00	170.00	3360.00	3850.00	490.00
2	Pun 2	2980.00	3060.00	80.00	3220.00	3270.00	50.00
3	Pun 3	2410.00	2170.00	-240.00	2700.00	2760.00	60.00
4	Pun 4	2630.00	2540.00	-90.00	2990.00	2720.00	-270.00
5	Pun 5	2850.00	3220.00	370.00	4020.00	3940.00	-80.00
6	Pun 6	3370.00	2570.00	-800.00	3950.00	2900.00	-1050.00
7	Pun 7	1440.00	1500.00	60.00	1520.00	1960.00	440.00
8	Pun 8	2250.00	2130.00	-120.00	3250.00	3230.00	-20.00
9	Pun 9	2450.00	2210.00	-240.00	2850.00	2830.00	-20.00
10	Pun 10	3250.00	3050.00	-200.00	3620.00	3350.00	-270.00
11	Pun 11	2920.00	3170.00	250.00	3490.00	3580.00	90.00

Conclusion

Exposure assessment and epidemiologic studies in the developing world are important and have advantages. On the one hand, increasing exposure data of traffic-related air pollution will provide scientific basis for pollution control in local areas. On the other hand, in-depth human health studies in these countries are necessary for assessing the degree of health outcomes of the public and for setting priorities in taking environmental control measures. In addition, epidemiologic investigations in regions with different metrological and socioeconomic backgrounds are helpful in strengthening scientific evidence about the association or causative relationships between these traffic-generated pollutants and various health endpoints.

In recent years, an increasing number of traffic-related pollution exposure studies and epidemiologic investigations have been reported, many of which are under the collaboration of researchers from developed countries and developing countries. Though the volume of scientific investigation on traffic-related air pollutants is increasing, exposure assessment and epidemiologic data are still not abundant. The differences among measuring methods and a lack of strict quality control in carrying out exposure assessment make it difficult for the findings to be generalized and the comparisons to be made between studies, which is especially true in exposure assessment research on particulate matter. Many of the existing epidemiologic investigations conducted in these underdeveloped regions suffer from inaccurate exposure assessment and insufficient control for potential confounders.

Therefore, future research in the developing world should emphasize the sharing of technical resources and communications between different countries and the use of standard measuring methods. Source-specific exposure assessment studies and studies using source-specific exposure data need to be more widely carried out since this serves directly as the basis for exposure regulations and public health measures. Source-specific studies are particularly crucial for particulate matter for an additional reason: different sources of particulate matter have different physiochemical compositions and thus different biological and environmental potentials.

Acknowledgement

The authors would like to thank to Prof.Z. Vishnuvarthan, Dean and Board of the Studies ,Department of environmental sciences Acharya Nagarjuna University, India., for his co-operation and encouragement. Our special thanks also reserved for our family members and friends who stand always by our side in all our endeavors.

References

[1]Ott, W. *Environ Int.*, **1982**, *7*, 179-196.

[2]Ashmore, M. R. and Dimitroulopoulou, C. Personal exposure of children to air pollution. Atmospheric Environment., **2009,**43 (1): 128-141.

[3]World Health Organization,' 'Air Quality Guidelines for Europe', *WHO Regional Publications*, European Series No. 23, **1987**,WHO Regional Office for Europe, Copenhagen.

[4]J., Douglas W. Dockery and Frank E. Speizer., *Am. J. Respiratory Crit. Care Med.*, **2006**, *173*, 667- 672.

[5]Beck, B. D and Brain, J. D., Prediction of the pulmonary toxicity of respirable combustion products from residential wood and coal stoves. In: *Residential Wood and Coal Combustion*, **1982,** 264-280. Air Pollution Control Association, Louisville, Kentucky.

[6]Roorda-Knape, M.C.R., Nicole A.H. Janssen, Jeroen J. De Hartog, Patricia H.N. Vliet, Hendrik Harssema and Bert Brunekreef., *Atm. Environ.*, **1998**, *32*(11), 1921-1930.

[7]Kumar, A. V., Patil R. S. and Nambi, K. S. V., *Atm. Environ.*, **2001,** *35*(25), 4245-4251.

[8]Saksena, S., Joshi V. and Patil, R. S., *J. Environ. Monit.*, **2003**, *5*(3), 491-499.

[9]Fenger, J., *J. Environ. Monit.*, **2009,** *43*(1), 13-22.

[10]Charron, A., and Harrison, R. M., *Atm. Environ*., **2003,** *37*(29), 4109-4119.

[11]Leung, S. N and Lam, K. C., *Environ. Monitor. Assessment*, **2001**, *72*(3), 235-247.

[12]Neuberger, M. A, and Moshammer, H., *Occupational Environ. Med.*, **2004,** *61*, 157-162.

[13]Lau, J., Hung, W.T. and Cheung, C. S., Atm. Environ., **2009**, *43*(4), 769-777.

[14]Bremauntz, A. A. F and Ashmore, M. R., *Atm. Environ*.. **1995,** *29*(4), 525-532.

[15]Janssen, N. A. H., Brunekreef, B., van Viiet, P., Aarts, F., Meliefste, K., Harssema H. and Fisher, P., *Environ. Health Persp.* **2003,** *111*(12), 1511-1518.

Received: 31.10.2012.
Accepted: 03.12.2012.

POLLUTANT ELEMENTS IN SOIL- PLANT- ANIMAL SYSTEM IN INDIA AND FUTURE THRUST AREAS

R. P. Narwal[a], R. R. Dahiya[a] and R.S. Malik[a]

Keywords: Pollutant elements, toxicity in soil, plant, livestock, management and future strategies

Increasing concentration of pollutant elements due to rapid industrialization and urbanization is now a global problem to soil, plant and animal health and affecting 40 % of the world population. Trace minerals of natural feeds is determined primarily by the mineral composition from the soil and secondly by the actual mineral composition of soil. Widespread deficiencies of Ca, P, Zn and Cu in south Karnataka, excessive Se and Mo in central part of Punjab, Arsenic in lower Indo-Gangetic plains of West Bengal through ground water are causing much toxicity to animal and humans. Clearly, closely linkage of agriculture to animal health must be accomplished if we are to find sustainable solutions to pollutant element deficiencies and associated diet related chronic disease affecting animal health. The deficiency/toxicity of minerals is an area problem. Although, geogenic trace elements toxicities have also caused wide health problems but higher concentration of pollutant elements in soils may lead to an excessive accumulation of metals by plants grown on such soils and may create animal- human health problems. Dysfunctional food systems are mainly responsible for this global crisis in animal- human health. Much of this malnutrition is the result of insufficient intakes of available trace elements in animal's diets. There are several ways in which agricultural factors can contribute to improve animal nutrition and health. Importantly, agricultural systems are the foundation upon which all nutrients enter into the animal food chain. Only through linking agricultural systems to animal nutrition can sustainable solutions. In this paper strategies and future thrust areas for research and for corrective measures of trace elements deficiencies and improvement of animal's health are discussed.

* Corresponding Author
Fax: +91-1662-234952
E-mail: ranbirsinghmalik@gmail.com
[a] Department of Soil Science, CCS Haryana Agricultural University Hisar- 125004, Haryana (India)

Introduction

Heavy metals as environmental contaminants of terrestrial ecosystem are not a recent phenomenon. The concern over environmental pollution and its effect on plant and animal life has brought numerous regulations for waste disposal. In recent years, a great deal of concern has been shown on indiscriminate disposal or use of sewage/industrial effluent in agricultural land may pollute the soil with heavy metals and enter in the food chain and can lead to health hazards in animal and human beings. Trace elements are essential for plants, animal and human health. The deficiency of a nutrient results in non-functionality of an important metabolic activities in agriculture, animals and human lives. These are needed in small amount but are essential and indispensable like other essential nutrients from nutritional point of view.

Use of urban and industrial waste in agriculture processes may pollute the soil with heavy metals and may lead to health hazards in soil, plant, animals and human beings. Soil mineral status keeps on changing due to pressure on land for maximum crop production, fertilizer application and natural calamities, thus altering the mineral contents of feeds and fodders and hence their supply to the animals. Trace elements needed for plants are zinc (Zn), iron (Fe), manganese (Mn), copper (Cu), boron (B), molybdenum (Mo), chlorine (Cl) and nickel (Ni) while animal need Fe, Zn, Cu, Mn, Se, I, Mo and Co.

Soil is the major source of trace elements entering the food chain. It is also a sink for elements from environmental sources.[14] Some localities have deteriorated soils due to the use and movement of groundwater containing heavy metals like As, Se etc to the soil surface. The problem is mainly associated with trace elements very greatly in different localities. For example, selenosis and fluorisis in animals in endemic form has been observed in several countries due to the excessive amount of Se and F in soil, water and agricultural products. Thus, knowledge of the sequence of events affecting the trace elements composition of soil, food and feed is necessary to understand in depth the soil- plant-animal interrelationship in determining the health hazards of animals and human beings. Trace element malnutrition is now a massive and rapid growing public health problem among all societies people below poverty line in many developing nations affecting about 40 % of the world population.[4,9] In view of the above, this paper summarizes the important contributions made by the team of scientist in India on monitoring the effects of heavy metal contamination in soil, plants and animals.

Pollutant elements in soils plants and animals

Zinc (Zn)

Zinc deficiency is widespread in soils of many countries and nearly 50% of the soil in the world is known to be Zn deficient.[16] Total and available Zn content in soils in India ranged between 7- 2960 $mgkg^{-1}$ and 0.1- 24.6 mg kg^{-1}, respectively with an average deficiency of 12 to 87 %.[17] Crops grown in these soils have low Zn content in seed and feeds. 49 per cent soils are deficient in Zn and nearly 1.6 million ha area is receiving 5 kg Zn ha^{-1} Y^{-1}. Zinc soil fertility is a good index of high Zn content in fodder and grains as significant correlation is found between available

Zn content of soils and Zn content in grain. However in many areas hidden deficiency has surfaced. Singh[7] reported that overall Zn deficiency is expected to increase from 48 % found in the year 1970 to 63 % by the year 2025 because more and more areas of marginal land are brought under intensive cultivation with out adequate micronutrient supplementation. The states of Punjab, Haryana, part of Uttar Pradesh and Andhra Pradesh have however shown a build up of Zn and decline in its deficiency. It is estimated that to correct Zn problem in soil and plants India would need 324 tons of fertilizer Zn ha^{-1} $year^{-1}$.

Iron (Fe)

Status of total and available Fe content in Indian soils is high, ranging from 4000- 273000 mg kg^{-1}. Acid and laterite soils still had high available Fe content and its toxicity is common, influencing rice yield during excessive rains.[17] Iron deficiency ranges from 1.0 to 35 % with a mean of 12 % in Indian soils. Its availability is lower in soils in arid and semiarid regions to forage and grains had lower Fe content in these areas and show more chlorosis compared to those grown in soils of humid and sub humid regions. However, Fe soil fertility status is not a good index of high Fe content in fodders as no significant correlation is found between Fe content of soil and Fe content in forage crops.

Manganese (Mn)

Status of manganese in Indian soils is adequate varying from 37 to 11500 mg kg^{-1} and available status 0.6-164 $mgkg^{-1}$ to support optimum growth.[1] Its deficiency in soil ranges from 1.0 to 22% with an average of 5% for the country. In parts of Punjab, Haryana and Uttar Pradesh deficiency of Mn is increasing and as much as 22% soils are reported deficient in areas under rice-wheat cropping system with an average of 5 % for the country. Widespread hidden hunger of Mn in wheat and other summer crops is not only leading to low yields but lead to infertility in cattle due to low Mn content in fodder and grain.

Copper (Cu)

Copper deficiency in Indian soils is not a severe nutritional problem and only about 3-4 per cent soils were found deficient among, 2,50,000 soil samples tested. Total copper content in soil ranged from 1.8-960 mg kg^{-1} and that of available content 0.1 to 32 mg kg^{-1}. Thus by and large most soils do not respond to copper fertilization except peat and mollisol soils having high organic matter contents. Crop management factors do not affect copper concentration in edible parts of plants. Copper toxicity is reported in copper mining areas and field crops continuous application of copper based fertilizers or pesticides. By and large, parent materials and soil character determine the available Cu status: high organic matter and clay content as well as pH causes decrease in its availability. In many parts of the world Cu deficiency in soils, especially sandy or containing large amount of organic matter has been recorded.[2] Its deficiency is prevalent in the Rift valley of Kenya.[6]

Iodine (I)

The rate of return of I is slow and small in quantity and repeated cycles of I in nature leads to its deficiency in soils and the plants grown on such soils contain as low as 10 µg I kg^{-1} in soils having adequate I. Human population largely depended on the food produced in these areas suffer from I deficiency disorder (IDD). This is the reason for the occurrence of wide spread IDD in the population of mountainous or sub-mountainous as well as flood-plains and sandy leached soil tracts of the world such as India, Bangladesh, Nepal, Myanmar etc. Iodine level in the drinking water indicates its content in soil. Its level in the drinking water from severely deficient areas of Nepal is 2.0 µg $L^{-1}$and of India 0.1-1.2 µg L^{-1} as compared to 9.0 µg L^{-1} in mildly I-deficient Delhi areas.

Cobalt (Co)

Cobalt deficiency is wide spread in soil-plant-animal chain in several countries.[3] Cobalt status in Indian soils ranges between 20- 1000 mg kg^{-1} with an available status of 0.5- 10 mg kg^{-1}. Its deficiency occurred on soils containing 4.4 to 47.0 mg Co kg^{-1}; in marginal to deficient areas soils contain 3 to 4 mg kg^{-1}, and in deficient areas 1 to 2 mg kg^{-1} soil.

Molybdenum (Mo)

Most of the Indian soils are adequate in molybdenum (Mo) content but its deficiency was found more in acidic, sandy and leached soils. Total and available Mo in Indian soils ranges between 0.1 to 12 $mgkg^{-1}$ and available Mo content traces to 2.8 mg kg^{-1} soil. About 13% soils of India have tested low. Whereas about 45% samples from acidic soils have tested to be low in Mo in meeting crop requirements.

Fluoride (F)

Fluoride is commonly found in soil mineral as fluorapetite, fluorosilicates and is added through irrigation water and gypsum, phosphogypsum, apetite, phosphoric fertilizers in ample quantities. Fluoride is easily absorbed by plants and its deficiency is not commonly reported.

Chromium (Cr)

Chromium in most of the Indian soils in general found in traces. Plant absorbs chromium though it not an essential elements for completing their growth and reproduction. It uptake is very small in normal unpolluted soils. Chromium concentration in leaf tissue is quite high in vegetable and cereal crops which are grown in soils polluted with sewage, chromite mining areas or industrial waste in peri urban areas. Baring heavily polluted soils with Cr from application of sewage sludge or industrial waste, its toxicity rarely occur.

Trace elements deficiency syndromes and disorders in animals

Diagnosis, assessment and prevention of trace mineral deficiency need a thorough understanding of the factors like age of animal, season, clinical signs, soil profile, and plant mineral content and feeding practices. Based on this preliminary information, further biological diagnostic tests can be followed for its confirmation. In general mineral deficiency is diagnosed by observing the clinical symptoms. But mineral deficiency signs are often confusing as the observed symptoms can be associated with more than one mineral and can be combined with the effect of protein and/or energy inadequacy, various types of parasitism, toxic

plants, infectious disease or with deficiency of other micronutrients. Some minerals like Ca, Mg and P are found in body tissues and their deficiency symptoms are exhibited only after a period of time. Calcium and phosphorous deficiency can be observed more quickly, particularly in high producing animals and fast growing calves. Critical values of certain mineral in soil, plant and animals are provided in Table 1, which will be of much use in ascertaining the material deficiency. Certain naturally occurring mineral deficiency/ toxicity is directly related to soil characteristics as in case of fluoride, Se and Mo, but the level of mineral in soil does not necessarily indicate its availability to plants growing on the soil. Other limitation of plant mineral analysis is the biological availability and factors influencing the utilization like chelating agents, mineral antagonism etc. Therefore analysis of mineral content in body tissues is a better indicator of the mineral adequacy because mineral deficiency result in subnormal concentration of the element and will usually be associated with clinical signs, however for certain minerals due to homeostatic mechanisms the level may remain normal even during deficiency but will respond positively to supplementation. Research is being conducted for using biochemical markers like specific enzymes/tissues to assess the mineral status more precisely.

Diagnosis and assessment of mineral deficiency in animals

Zinc (Zn)

Zn deficiency disorder parakeratosis is associated with bone, joints and skin disorders. It was first detected in 1955 that manifests as thickening, hardening and fissuring of the skin in swine. The deficiency generally results from grazing of animals on forages contained 18 to 40 mg Zn kg^{-1} dry matter. Most of the forages from the Punjab and Haryana states of India contained less than 20 mg Zn kg^{-1} dry matter and their continuous feeding to growing calves and sheep affected growth and resulted in parakerotic skin lesion, poor feed efficiency and shedding of wool.[19] Wool shedding in corriedale sheep also observed at the Central Sheep Breeding Farm, Hisar.[11]

Iron (Fe)

Both in developing and developed countries Fe deficiency is generally recognized as the most common single nutritional deficiency in spite of that it is one of the most abundant minerals on earth. However, Iron deficiency in animals rarely occurs as its concentration in the fodder and feed is generally adequate to meet their requirement. Also fodders and pasture are often contaminated with soil or it is engrossed while grazing and thus supply significant amount of Fe to the animals. Manganese (Mn)

Widespread hidden hunger of Mn in wheat and other summer crops is not only leading to low yields but lead to infertility in cattle due to low Mn content in fodders and grain, glucose intolerance other malfunction which needs more detailed studies from animal and human health point of view. This was evidence by Singh[17] who recorded increased fertility due to Mn deficiency in cattle which were fed on fodder low in Mn grown in highly calcareous soils (free $CaCO_3$ 20-48%) around Pusa, Bihar. These workers found low blood serum Mn, prevalence of infertility and low productivity compared to cattle fed on fodders grown in Mn adequate soils.

Copper (Cu)

In India Cu deficiency or marginal Cu deficiency has been recorded at 60 farms. Its deficiency caused leucoderma (vitilogo), depigmentation of hair and skin around the brisket, neck, face, hind limbs and abdomen in buffaloes in India.[15,18] Also Cu deficiency caused "falling disease" in milch cows. In the livers of affected animals contained low level of Cu 32.6 mg kg^{-1} as compared to the normal concentration of 55.7 mg Cu kg^{-1} in healthy cows.[19]

Table1. Critical values of trace minerals (ppm) for assessment of status

Element	Soil	Feed/Fodder	Animal body	
			Normal level (Serum)	Deficient
Fe	2.5	50	1-2	<1
				<40 (liver-wet weight)
Cu	0.3	8	0.65-1.2	<0.2-0.6
			125-600 (liver, DM)	<33-125 (liver-wet weight)
Zn	1	30	1-2	<0.6-0.8
			25-200 (liver, DM)	<25-40 (liver DM)
Mn	5	40	6-70 ppb	<5 ppb
			>13 (liver, DM)	<7 (liver, DM)
I	-	0.1-0.2	0.1-0.4 total I	<0.05-0.10
			0.04-0.13 (Protein bound)	<0.03-0.05 (protein bound)
			20-100 ppb T 4.	<7-30 ppb T 4
Co	-	0.08-0.1	-	<0.5 mg cm^{-3} (rumen fluid)
				<0.05 (liver)
				Vitamin B12 ,0.1-0.2 ppb
Mo	-	0.5	-	-
Se	-	0.1	0.2-1.2 (whole blood)	<0.2-0.5 (liver, DM)
			1.2-2.5 (liver DM)	<0.06-0.2 (whole blood)
				<0.03

Iodine (I)

Iodine deficiency has been reported in goats in certain districts of Punjab. Deficient levels of I in drinking water have caused endemic goiter in animals and birds[10] in many part of the world also.

Cobalt (Co)

In the chain of soil-plant animal, plant act as accumulator of Co for its conversion into Vitamin B_{12} in ruminants. It is essential for cattle, buffalo, sheep and goat. Ruminants required about 0.1 mg Co kg^{-1}. Under grazing conditions lams are most sensitive to Co deficiency, followed by mature sheep, calves and mature cattle. In cattle its deficiency associated with ground water podzols and gley (low humic or poorly drained) soils of the Atlantic Coastal Plain[8], sandy soils and wet climate. However, very meager information in this respect is available in India.

Molybdenum (Mo)

Molybdenum deficiency in animals is reported more in eastern high rainfall zone of India, where soils are low in Mo content. In north parts of West Bengal hair and hooves falling problem is reported widely in cattle due to low Mo in alluvial leached soils. Molybdenum toxicity in animals and humans is reported in some parts of Punjab, which affects copper utilization in the body due to Mo-Cu interaction.[13]

Chromium (Cr)

Chromium is essential trace elements for human and plays an important role in human and animals mainly in regulation of the glucose tolerance factor, in combination with nicotinic acid and some proteins which are required for every bodily function. In animals sufficient Cr been found to increase growth and longevity. Deficiencies are believed to be a factor in arteriosclerosis and hypertension and possibly in diabetes and cataract. Tetravalent chromium is toxic whereas hexavalent is essential and beneficial to human health.

Fluoride (F)

Fluoride is essential for the normal growth and development of bones in animals. Fluoride toxicity is reported in humans and animals in the form of fluorosis in arid regions mainly in Rajasthan, Gujarat, part of Haryana, Andhra Pradesh and Utter Pradesh where irrigation water containing very high amounts of fluoride than 0.1 mg F L^{-1} in urine.

Effect of trace elements deficiency in soils on animal health

The mineral content of soils depends not only on the parent material but also on the complexity of pedogenic factors like laterization, calcification and salinization of the total mineral concentration in soils, only a small fraction is taken up by plants. The "availability" of minerals in soils depends upon their effective concentration in soil solution. Several factors influence the uptake of minerals by crops and pastures from the soil. These include 1) soil acidity 2) soil moistures 3) soil temperatures 4) plant variety 5) fertilization 6) organic matter and microbial activity of soil. For trace mineral absorption the pH has the most marked effect on the availability. Alkaline soils lead to an increased biological availability of some trace elements such as Se and Mo. With decreasing soil pH, Se is less available, but the uptake of some cationic metals like Cu is increased. Soil leaching, erosion and long duration crops lead to a depletion of trace minerals. Crop management and climatic conditions also influence the eventual trace mineral level in feeds.

Sometimes, the level of Cu, Zn, Mn, Fe and Co in crops is sufficient for optimum yields but is not adequate to meet the needs of livestock animals.[5] Selenium is a trace mineral that is not required by most of the cultivated crops, even then maximum crop yields is obtained on soils with traces of Se. However, if livestock are fed with the low Se feed, they could suffer from serious muscular disorders and other diseases. White muscle disease due to Se deficiency is probably the most common and serious disorder found in calves and lambs.

Survey on micronutrient status in green and dry fodder to support animal health in Vadodara district of Gujarat indicated that though most of the soils are adequate in available Fe, Mn and Cu to support crop yields and need Zn fertilization to get good yields, but these dry fodder were tested and were found low in Fe (61%), Zn (72%) and Cu (87%) and that of Fe (17%), Zn (5%) and Cu (23%) in green fodder respectively, where as concentrations of Fe (90%), Zn (36%) and Cu (9%) mg kg^{-1} dry matter and Fe (70%), Zn (50%) and Cu (45%) for green fodder were considered critical, respectively. Table 2 shows State and zone wise mineral deficiency status for better animal nutrition suggested.

Haryana and most of the other states in the country also have low Zn, P and Fe whereas deficiencies of Mn are emerging fast in intensively cultivated crops in sandy alkaline soils.[12] When feed and fodders produced on such deficient soils were fed to cattle, the animals showed higher percentage of deficiency in their blood serum, hair and milk as given in table 5**.** The deficiency of Ca, P, Cu and Zn was found widespread. Deficiency of minerals commonly ranged from 23 to 57% in Ca, 2 4-69% in P,

20-60% in Zn and 33-64% in Cu in blood serum and milk samples. Animal hair also showed Mn deficiency.[12]

Similar study intended to assess the effect of micronutrient status in soil-plant-animal continuum, revealed that soil of Dahima village of Hisar, Haryana, and found deficiency of 74.45% in Fe, 68.9% in P and 4.8% in Zn and the fodders grown on these soils did not meet the normal mineral requirement of animal body **(**Table 3**).**

Analysis of animal blood plasma serum revealed maximum deficiencies of Cu (37.5%) followed by P (12.5%).

Table 2. Mineral nutrient deficiencies in various states for normal animal nutrition

State	Zone	Mineral deficiency
Arunachal Pradesh	Hilly and Mountain	Na, K, Mg, Cu, Mn
Assam	i) Lower Brahmaputra valley	P
	ii) Upper Brahmaputra valley;	P, Ca, Cu
	iii) Barak valley,	P, Ca, Cu
	iv) Central Brahmaputra valley	Ca, P, Mg, Cu
	v) North Bank Plain	Ca, P, Cu
	vi) Hill zone	Ca, P, Mg, Cu
West Bengal	i) Northern Hill zone	Ca, P, Cu
	ii) Terai zone	Ca, P, Zn, Mn
	iii) New Alluvial zone	Ca, P, Cu, Zn
	iv) old Alluvial zone;	Ca, P, Zn
	v) Red Laterite zone	Ca, P, Zn
	vi) Coastal Saline zone	Ca, P, Cu, Zn, Mn
Jharkhand/ Bihar	i) South-Werstern Semi-arid zone	P, Cu, Zn, Co, Mn
	ii) Central Plain zone	P, Mg, Cu, Zn, Fe
	iii) Eastern Plain Zone	Ca, P, Cu, Co, Mn
Uttar Pradesh	i) Bundelkhand zone	Ca, P, Cu, Zn
	ii) Bhabar and Tarai zone	Ca, Cu, Mn, Co
	iii) Western Plain zone	Ca, P, Cu, Zn, Mn
	iv) Central Plain zone	P, I, S, Zn
	v) Vindhyan zone	P, Zn, Fe
Uttaranchal	i) Hill zone (Rainfed)	Ca, P, Cu, Co
	ii) Tarai-Bhaber zone (Irrigated)	Ca, Cu, Co
Gujarat	i) Rainfed	Ca, Zn
	ii) Irrigated,	Zn
	iii) Arid zone,	Ca, P, Zn
	iv) Semi arid zone	Ca, P, Zn
	v) Hilly	Zn
Punjab	Irrigated	Ca, P, Cu, Zn
Madhya Pradesh	i) Northern Hill zone;	P, Zn
	ii) Kymore Plateau and Satpura Hills zone	P, Zn
	iii) Vindhya Plateau,	P, Zn, Fe
	iv) Central Narmada Valley	P, Zn, Mn
	v) Grid zone,	P, Zn, Fe, Mn
	vi) Bundelkhand zone	P, Zn, Fe, Mn
	vii) Satpura Plateau	P, Zn, Fe
	viii) Malwa Valley,	P, Zn, Fe
	ix) Nimar Valley	P, Zn, Mn
	x) Jhabua Hills zone	Zn, Fe, Mn
Rajasthan	i) Semi arid zone	Ca, P, Zn
	ii) Arid zone	Zn, Cu
Haryana	Irrigated	Ca, P, Cu, Zn, Mn
Himachal Pradesh	i) Shivalik Hill zone	Ca, Zn, K
	ii) Mid Hill zone,	Ca
	iii) High Hill zone	Ca
	iv) Cold Dry zone	Ca, P, Zn, Cu
Maharashtra	i) North Konkan Coastal	Ca, P, Mg, Fe
	ii) Western Ghat	Cu, Zn
	iii) Transition zone-1,	Ca, P, Mg, Cu, Fe, Zn
	iv) Transition zone-II	Ca, P, Mg, Cu, Fe, Zn
Karnataka	i) North East Transition zone	Ca, P
	ii) North East Dry zone	Ca, Zn
	iii) Northern Dry zone;	Ca, P, Mg, Cu, Zn
	iv) Central Dry zone,	Ca, P, Mg, Cu, Zn
	v) Eastern Dry zone	Ca, P, Mg, Cu, Zn
	vi) Southern Dry zone	Ca, P, Zn
	vii) Southern Transition zone	Ca, Cu, Zn
	viii) Northern Transition zone	Ca, P, Cu, Zn, Fe
	ix) Hilly zone	Ca, P, Cu, Zn
	x) Coastal zone	Cu, Zn
Kerala	i) Northern zone,	Ca, P, Mg, Cu, Mn

	ii) Central zone, iii) High Range areas iv) Special problem areas v) Southern zone	Ca, P, Mg Ca, P, Mg Ca, P, Mg, Cu, Mn Ca, P, Mg
Tamil Nadu	i) Rainfed, ii) Coastal iii) Irrigated iv) Arid zone	Ca, P, Cu, Zn Ca, P, Cu, Zn Cu, Zn, Mn P, Cu, Zn
Andhra Pradesh	i) Rainfed zone ii) Coastal zone iii) Arid zone	Ca, P, Cu, Zn, Mn Ca, P, Cu, Zn Cu, Zn, Mn
Bihar	i) Zone-I, ii) Zone-II iii) Zone-IIIA iv) Zone-IIIB	Zn, Fe, Cu, Mn & Co Zn, Fe, Cu, Mn & Co Zn, Fe, Mn & Co Zn, Fe, Cu & Mn

Table 3. Average Percentage of mineral nutrient deficiency in blood serum, hair and milk in cattle in Haryana

Deficiency percentage based on	Ca	P	Cu	Zn	Mn
Serum mineral status	48.1	31.6	40.0		
Hair mineral status basis	30.1			50.3	47.6
Milk mineral status basis	42.8	53.9	29.0	42.9	

None of the human blood plasma samples showed mineral deficiency in the selected farmers and animals. Regular use of Zinc in Haryana by the farmers to rice-based cropping system has resulted in build up zinc fertility and improvement in zinc status in animal and humans. However, in eastern and northeastern regions of India, deficiency of Ca, Zn, Cu and Mo has been widely reported in children and cattle as 25 million h.a. acidic soils had lower status of these elements. Molybdenum deficiency in northern parts of West Bengal caused a drastic fall in hooves and hairs in cattle.

Trace elements fortification in feeds for animals and toxicity

Trace elements toxicity is also causing problems both to human and animals. Among these toxicity of F, NO_3, Mo, As, Se, Ni, Al, Cr and Fe are common in several areas as shown in Figure 1**.** Excessive selenium and molybdenum in certain parts of Punjab, arsenic in lower Indo-Gangetic plains of West Bengal through ground water are causing much toxicity to animal and human.[5,18] Fluoride toxicity, as dental fluorosis, expressed in the form of pigmentation with yellow, brown or black colouration, mottling, irregular wearing, erosion, pitting of enamel on teeth was reported by Sahoo et al. in sheep. 36% out of 1271 sheep monitored around national aluminum company smelter plant in Orissa. Fluoride discharged resulted in contamination of well and pond waters within 5 km of NALCO that ranged from 0.50-1.83 mg L^{-1} and 0.52-3.86 mg L^{-1} above the permissible limits. Fluoride affected sheep blood had significantly higher ceratine, alkaline phosphates in blood serum, but less glucose, cholesterol protein. Fluoride content in the urine, serum, bone, teeth of healthy and fluorotic sheep was 10.02 mg L^{-1} which is 10 times higher than those in healthy animals and critical level of 0.1 mg FL^{-1}, more than 90% of the total fluorides are taken by bony tissues, which however depends upon intake, age, sex, bone type and nature of bone (Table 4).

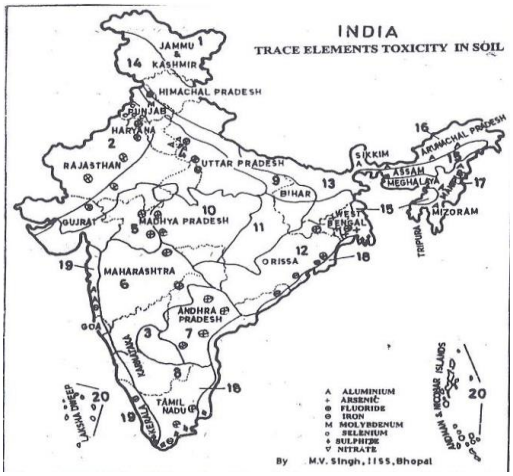

Figure 1. Areas suspecting trace elements toxicity in soil and animals

Thus, for ensuring better nutrition of animals and humans, bio-fortification of micronutrients in staple food crops are urgently needed. Since soils have enough iron, copper and manganese reserves, identifying plant varieties or crop species capable to higher absorption and translocation into seed are highly desired. Influence of micronutrient deficiencies on anatomical changes in plants, mechanisms of uptake and translocation among crop species and varieties need to be studied. Thus, these processes can be used as a tool for identifying efficient and inefficient plants. Besides screening of efficient varieties, agronomic interventions influencing biofortification, balance between micronutrient into shoot for loading higher concentration in seed have immense value for improving bioavailability of trace elements in animal model for reducing malnutrition.

Table 4. Mean fluoride content in the urine, serum, bone and teeth of healthy and fluorotic sheep

Sample	Fluorotic sheep	Healthy sheep
Urine (mg L^{-1})	10.02+-1.19	0.96+-0.13*
Serum (mg L^{-1})	0.61+-0.8	0.09+-0.02
Bone (mg L^{-1})		
Rib	8746+-54.9	658+-38.1*
Radius	7922+-50.4	612+-31.3*
Mandible	9481+-96.9	738+-29.9*
Teeth (mg kg^{-1})		
Incisor	4125+-60.4	320+-18.7*
Molar	4457+-66.6	364+-22.6

Similarly, cattle fed with fodder and concentrate low in Mn in calcareous soil belt had low blood serum than that of the optimum level and suffered more with infertility and low productivity. Thus, from animal health point of view, fodders and feeds need more mineral fortification either at field level keeping in view the soil fertility status or at feeding stall.

Conclusion

In the last few decades our knowledge about pollutant elements problems of soil, plant and animal, related either to the deficiency or toxicity of essential trace elements as well as toxicity of non-essential trace elements, as a result of their movement through the food chain. Their deficiency emanates as a result of their low content in soils and/ or depletion from soil due to high turnover rate with adoption of modern agricultural technologies. The information regarding the endemic diseases resulting specially from the deficiency of I, Zn, Cu, Fe, Se and F with the characteristics of geographic distribution has increased with time. Overcoming the deficiency or imbalances of minerals have improved in the productive efficiency of livestock to a great extent. Though, polluting elements have not received much attention neither in soil nor in the formulating diets, yet their long term practical impact on production, reproduction and immunity should not be ignored.

Thrust areas and Future strategies

- There is need for developing systematic database using GPS to monitoring health hazards from heavy metals pollution and trace elements toxicities in soil, plant, human and animal chain.
- Maps of trace elements deficiency and toxicity need to be produced to create awareness of such areas for taking remedial measures by the people, planners and policy makers.
- Enriching seed and feed with micronutrient for recharging micronutrient malnutrition and enhancing nutritional security of the country.
- To induce deficiency/toxicity symptoms for diagnosis micronutrient and trace elements deficiencies in field crops.
- Developing customized fertilizer for crops. Cropping system and certain agro ecological zones, soils.
- Studying relative supplementation of trace elements from fodders to animal is very much desired.
- Investigations are needed on plant anatomical and rhizoshheric changes responsible for the variability in absorption, translocation and uptake of trace elements by seed and fodder of food crops.
- Creating mass awareness about pollutant elements in soil-plant-animal continuum and remedial measures.
- To establish optimum level of elements for good health of animal and humans.
- A joint multi-disciplinary team consisting of soil scientist, nutrition scientist, physiologists, veterinary and medicine doctors may be constituted to establish definite quantitative association of animal and human health.

References

[1]Alloway, B.J. *Blackie Academic and Professional*, Glasgow. **1995,** 38.0

[2]Baker, D.E.; Senft, J.P. *Blackie Academic and Professional*. Glasgow, **1995,** 177.

[3]Blood, D.C.; Radostitis, O.M. A *Testbook of the diseases of cattle, sheep, pigs, goats and horses.* 7th ed. Bailliere Tindall, London. **1989.**

[4]Buycks, M. *Food Nutr. Agr*. **1993,** *7*, 2.

[5]Combs, G.F.; Welch, Jr.; Duxbury, J.M.; Uphoff, N.T.; Nesheim, M.C. In: *Food-Based Conference on Agricultural Production and Nutrition*. **1997,** 19.

[6]Kang, B.T.; Osiname, O.A. *Fertiliser Res*. **1985,** *17*, 131.

[7]Kiekens, L. *Blackie Academic and Professional*, Glassglow, **1995,** 284.

[8]Kubota, J.; Lemon, E. R.; Alloway, W. H. *Soil Sci. Soc. Am. Proc*. **1963,** *27*, 679.

[9] Lag, J. In: *Geomedicine* (Ed. J Lag). CRC, Boca Raton, **1990,** , 1-24.

[10] Lawrence, C. R.; Johns, M. W. Geomedicine Ist Ed. CRC, Boca Raton. **1990,** 225.

[11] Mandokhot, V. M.; Vasudevan, B.; Mandal, A. B.; Yadav, I. S. In *Proc. Symp. Recent Adv. Miner. Nutr.*, Haryana Agric. Univ. Hisar. **1987,** *?Pp 45-49.*

[12] Narwal, R. P. *AICRP on Micro and Secondary nutrients and pollutant Elements in Soils and Plants*, CCSHAU, Hisar. **2006,** 85.

[13] Nayyar, V. K.; Takkar, P. N.; Singh, R. L.; Kaur, S. P.; Bansal, N. P.; Sadana, U. S. *Res. Bull*. **1990,** 148.

[14] Ramalingaswami, V. *Am. J. Clin. Nutr*. **1995,** *61*, 259- 263

[15] Randhawa, C. S., *PhD Thesis*, PAU, Ludhiana. **1999.**

[16]Robson, A. D. Zinc in Soils and Plants, Kluwer Academic Publishers, London. **1993,** 206.

[17] Singh, M. V. *Micro and Secondary Nutr. Res. India*, **2000,** *23*, 148.

[18] Sinha, B. P.; Jha, J. G. J.; Sinha, B. K. *Indian Vet.* **1976,** *53*, 812.

[19] Vasudevan, V. Proc. Symp. Recent Adv. Mineral Nutr. Haryana agric. Univ., Hisar**. 1987**, Pp 45-49.

Received: 15. 10. 2012.
Accepted: 03. 12. 2012.

THE ROLE OF SELENIUM-ENRICHED FOOD SPROUTS WITH RESPECT TO OUR DAILY SELENIUM NEEDS

Éva Bódi[a], István Fekete[a], Dávid Andrási[a], Béla Kovács[a]*

Paper was presented at the 4th International Symposium on Trace Elements in the Food Chain, Friends or Foes, 15-17 November, 2012, Visegrád, Hungary

Keywords: selenite, selenate, wheat- and pea sprout, ICP-MS

Trace mineral selenium is an essential nutrient of fundamental importance to human biology, therefore it is very important to be in our daily diet. Although it is known that selenium content of foods show wide variety, the most commonly consumed food have low selenium content. The main object of our work is to study the enrichment of selenium during germination of wheat and pea (*Triticum aestivum* and *Pisum sativum*) because we are of the view based on previous studies that the sprouts are able to take up element high in concentration. Sprouting was chosen because it additionally enhances the nutritional value of seeds, for example, by a higher vitamin content, a better quality of protein, and some other parameters. We dicided to combine this with higher selenium content. Inductively coupled plasma mass spectrometry (ICP-MS) was used to determine the total element concentration. After determining the element, we calculated the percent of selenium which was found in sprouts treated with Se, may cover our daily need. With regards to our experiments, we concluded that, selenium are good for the treatment of sprout because the 0.1 mg dm^{-3} selenium treatment contribute to cover our daily need of selenium needs.

* Corresponding Authors
Fax: 36-52-417572
E-Mail: kovacsb@agr.unideb.hu
[a] University of Debrecen,
Centre for Agricultural and Applied Economic Sciences,
Institute of Food Science, Quality Assurance and
Microbiology, H-4032 Debrecen, Böszörményi str. 138.

Introduction

Unlike other seeds, it has been established that sprout seeds, due to its transform protein content, has higher biological value, polyunsaturated fatty acid content, vitamin content and better utilization of minerals has a higher nutritional value. Therefore, germinated seeds are highly nutritious foods. During germination, polysaccharides degrade into oligo- and mono-saccharides, while fats into free fatty acids, whereas the proteins into oligopeptides and free amino acids, which processes support the biochemical mechanisms in our organism.[1]

Different investigations show, that we can further enhance the above high nutritional value of sprouts if we grown the seeds on various trace elements solution, namely they are able to take element high in concentration.[2,3,4]

We studied the enrichment of sprout with selenium during our work. We took into account the fact, we choose micronutrients to our treatment, that selenium can be delivered to the body by a small amount with the most widely consumed food. As a result of which, selenium deficiency affects many inhabitants of European countries, including the Hungarian population.[5] In general we can say that the selenium content of plant raw materials in most fertile soil, the selenium content may be determined.[6] In Hungary, however, selenium soils are quite poor, so that the plant product from selenium supplementation is only a fraction of what is needed.

Selenium deficiency itself usually does not cause disease, but directly or indirectly, by selenium deficiency wide variety of diseases or exacerbation of the disease may play a role, for example: adult-onset diabetes, cystic fibrosis, cerebrovascular disease, colonic ulceration, different types of cancer as well as cardiovascular diseases.[7] In addition, Pappa et al. (2006) noticed, that low Se status was associated with a significantly greater incidence of depression and other adverse effects such as anxiety, confusion and hostility.[8] However, several studies have reported that selenium supplementation reduces the likelihood of developing certain diseases, and increases resistance power of the body. For example the daily extra-dietary supplement of 200 mg Se has been indicated to increase resistance to viral infections and reduce the possibility of cancer.[9] In addition, the importance of selenium is also emphasized by the fact that selenium deactivates the heavy metals (Cd, Hg) which has toxic effect in the body.[10]

Materials and methodes

We used bio wheat (*Triticum aestivum*) and green pea (*Pisum sativum*) for germination. In the experiment, in the case of selenite and selenate 0.1; 1; 10 mg dm^{-3}, selenium concentrations have been applied along with control treatment with distilled water.

For the determination of total selenium concentration a cc. nitric acid – cc. hydrogen peroxide wet digestion sample preparation method was applied. The sample preparation was carried out on the basis of paper made by Kovács et al (1996).[11] For us to completely observe the element concentration, our team used inductively coupled plasma mass spectrometry (ICP-MS). Collision cell technique (7% H_2+93% He) was used to eliminate the polyatomic interferences.

For the statistical analysis we used One-Way analysis of variance (ANOVA) and Tukey-test. Significance was evaluated at the $P<0.05$ level. All statistical analyses were performed using SPSS v.13.0.

Result and Discussion

We monitored the selenium concentration changes of wheat- and pea sprout at increasing concentrations of selenite and selenate treatments in our experiments. The control treatment included distilled water for germination too.

The results of our research are summarized in Table 1-2. These show that on distilled water, grew wheat- and pea sprout had only low selenium concentration. However the concentration of selenium increased significantly the effect of each selenium treatments. Further, this increase was more obvious in the case of wheat sprout.

We measured increased selenium concentrations in sprout at selenate treatment concentrations, in the case of wheat- and pea sprout too, which is known to be in collaboration with the selenite and selenate, their uptake was different. The plants took up selenate actively during sulfur metabolism and accumulated selenite passively.

Table 1. In case of 1x Se (0.1 mg dm^{-3}), 10x Se, 100x Se treatments, the concentration of the 5 days old wheat sprout grown on a solution containing selenium (mg kg^{-1}), (n=3)

Treatments	Wheat sprout			
	Selenite		Selenate	
Control	0.065^a	± 0.017	0.065^a	± 0.017
1x Se	2.18^b	± 0.16	3.55^b	± 0.12
10x Se	15.5^c	± 0.5	18.5^c	± 0.8
100x Se	36.8^d	± 1.2	84.3^d	± 1.6

Table 2. In case of 1x Se (0.1 mg dm^{-3}), 10x Se, 100x Se treatments, the concentration of 4 days old pea sprout grown on a solution containing selenium (mg kg^{-1}), (n=3)

Treatments	Pea sprout			
	Selenite		Selenate	
Control	0.131^a	± 0.014	0.131^a	± 0.014
1x Se	2.50^b	± 0.04	1.43^b	± 0.05
10x Se	4.08^c	± 0.20	4.93^b	± 0.07
100x Se	29.6^d	± 0.6	44.0^c	± 0.9

The practical application of our measurement

In some literature, the daily consumption of the recommended amounts to two or three tablespoons, which approximately corresponds to 15 g. During our investigation, we calculated using this value; how many percent from selenium contain of sprouts treated with Se covers our daily need. Results are summarized in Tables 3-4.

Dietary Reference Intakes (DRIs) defining the value for daily selenium need (2004) was taken into account in calculation. The DRIs selenium is 45 µg/day. This value defines the amount that highly absorbable form the core of a healthy person should.[12]

With regard to the determination of the values, we also evaluated by the germs in our body selenium intake is not utilized 100%. Study of literature by foreign authors outlined that the body of organically bound selenium intake is only up to 80% of the absorbed.[13]

However, this is only an approximate value, since the utilization of selenium in our body also defines a number of factors. For example the health status, age, sex, diet of consumer as well as the distribution of different selenium species.

Table 3. Se content (µg) of wheat sprout mass recommended to daily consumption (15 g) and its Se content rate (%) compared with our daily requirements plotted against control, 1x Se (0.1 mg dm^{-3}), 10x Se, 100x Se treatments

Treat-ments	**Se content of 15 g wheat sprout (µg)**		**The rate of Se content of 15 g wheat sprout compared to daily requirements (%)**
	dry mass calculated	**wet mass calculated**	
	selenite treatments		
Control	0.975	0.244	0.434
1x Se	32.7	8.18	14.5
10x Se	233	59.6	106
100x Se	552	140	248
	selenate treatments		
Control	0.975	0.243	0.433
1x Se	53.25	15.6	27.7
10x Se	278	70.5	125
100x Se	1268	304	541

Table 4. Se content (µg) of pea sprout mass recommended to daily consumption (15 g) and its Se content rate (%) compared with our daily requirements plotted against control, 1x Se (0.1 mg dm^{-3}), 10x Se, 100x Se treatments

Treat-ments	**Se content of 15 g pea sprout (µg)**		**The rate of Se content of 15 g pea sprout compared to daily requirements (%)**
	dry mass calculated	**wet mass calculated**	
	selenite treatments		
Control	1.96	0.432	0.769
1x Se	37.5	9.08	16.1
10x Se	61.2	13.5	23.9
100x Se	444	92.8	165
	selenate treatments		
Control	1,97	0.432	0.769
1x Se	21.5	4.44	7.89
10x Se	74.0	14.9	26.5
100x Se	660	148	262

We recommend tenfold selenite or selenate treatment at wheat germination on the basis of the data in Table 3, because the hundredfold treatment significantly exceed the needs of our daily selenium.

We prefer to keep also 1 mg dm^{-3} concentration treatment also at pea germination on the basis of the results of Table 4, because if the amount of added selenite additional tenfold change, they would expose the 165 respectively 262% of the daily needs of selenium, which is close to the toxic quantity.

The data also shows, that the ratio of daily need of selenium content of sprouts on control treatment is very low (0.5-1%), so we recommend the germination on selenite and selenate solution especially those living in areas of selenium deficiency. In addition, vegetarians may also find useful selenite and selenate enriched sprouts for consumption, mainly because of the domestically produced fruits and vegetables are extremely low in concentrations of selenium. Takács (2001) noted that of 0.01 μg/g.[14] This value is much higher in meats, fish, shellfish, 0.3 μg/g. Animal offar, particularly the liver, kidney have their selenium concentration very high.

Besides this we found it is important to note, however, that in some cases it may be necessary for the daily selenium levels are greater than what our bodies need. For example, investigation has shown that selenium may be used in cancer prevention and treatment, by ensuring that the average level of the body is in excess of this amount must be consumed.[15,16]

Conclusions

With regards to our observations, we concluded that sodium-selenite and sodium-selenate are good for the treatment of sprout, since the wheat- and pea sprouts are able to take up these elements high in concentration, thereby contribute to cover our daily need of selenium requirement.

On the basis of our result we prefer to keep 1 mg dm^{-3} concentration selenite and selenate treatment because the hundredfold treatment significantly exceed the needs of our daily selenium requirement.

Acknowledgements

The publication is supported by the TÁMOP-4.2.2/B-10/1-2010-0024 and TÁMOP-4.2.1./B-09/1/KONV-2010-0007 projects. The projects are co-financed by the European Union and the European Social Fund.

References

[1]Márton, M., Mándoki, Zs., Csapó-Kiss, Zs., Csapó, J. *Acta Univ. Sapientiae, Alimentaria*, **2010,** *3*, 81-117.

[2]Hsu, C. K., Chiang, B. H., Chen, Y. S., Yang, J. H., Liu, C. L., *Food Chemistry*, **2008**, *108*, 633–641.

[3]Liu, C. L., Chen, Y. S., Yang, J. H., Chiang, B. H., Hsu, C. K., *J. Agric. Food Chem*., **2007,** *55*, 8934–8940.

[4]Lintschinger, J., Fuchs, N., Moser, H., Jäger, R., Hlebeina, T., Markolin, G., Gossler, W., in: *Plant Foods for Human Nutrition*. Kluwer Academic Publishers. Printed in the Netherlands, **1997**, 50, 223-237.

[5]Bogye, G., Alfthan, G., Machay, T., Zubovics, L., *Arch. Disease Childhood Fetal and Neonatal Ed*., **1998,** *78*, F225-F226.

[6]Terry, N., Zayed, A. M., Desouza, M. P., Tarun, A. S., *Ann. Rev. Plant Physiol. Plant Mol. Bio*l., **2000,** *51*, 401-432.

[7]Navarro-Alarcón, M., López-Martinez, M. C., *Sci. Total Environ.*, **2008,** *249*, 347-371.

[8]Pappa, E. C., Pappas A., C., Surai P. F., *Sci. Total Environ*., **2006,** *372*, 100–108.

[9]Schrauzer, G. N., Selenium and human health: the relationship of selenium status to cancer and vital disease. *Alltech's 18th Ann. Symp*., **2002,** pp. 263–269.

[10]Sasakura, C., Suzuki, K. T., *J. Inorganic Biochem*., **1998,** *71*(3-4), 159-162.

[11]Kovács B., Győri Z., Prokisch J., Loch J., Dániel P., *Comm. Soil Sci. Plant Anal.*, **1996,** *27*(5-8)1177-1198.

[12]*Dietary Reference Intakes (DRIs) Recommended Intakes for Individuals, Food and Nutrition Board*. Institute of Medicine, National Academies, **2004,** 2.

[13]Rayman, M. P., Infante, H. G., Sargent, M., *Brit. J. Nutr.*, **2008,** *100*, 238–253.

[14]Takács, S., *Környezet, ember, mikroelemek*. Triorg Kft., Budapest **1999**.

[15]Bonelli, L., Camorino, A., Reavelli, P., Missale, G., Bruzzi, P., Aste, H. Reduction of the incidence of metachronous adenomas of the large bowel by means of antioxidants. In: Palmiery Y. (Ed.,): *Proc. 6th Int. Selenium Tellurium Dev. Assoc.*, Scottsdale, Arizona. **1998,** 91-94.

[16]Clark, L. C., Combs, JR. G. F., Turnbull, B. W., Slate, E. H., Chalker, D. K., Chow, J., Davis, L. S., Glover, R. A., Graham, G. F., Gross, E. G., Krongrad, A., Lesher, JR J. L., Park, H. K., Sanders, Jr. B. B., Smith, C. L., Taylor, J. R., *J. Am. Med. Assoc*., **1996,** *276*, 1957-1963.

Received:26.10.2012.
Accepted:03.12.2012.

 DOI: 10.17628/ECB.2013.2.46

VARIETY OF STRUCTURES OF BINUCLEAR CHIRAL SCHIFF BASE Ce(III)/Pr(III)/Lu(III)-Ni(II)/Cu(II)/Zn(II) COMPLEXES

Tomoko Hayashi[a], Haruhiko Shibata[a], Shingo Orita[a] and Takashiro Akitsu[a]*

Keywords: Chirality, Schiff base, Ni(II) complex, Cu(II) complex, Zn(II) complex, Lanthanide complex

We have prepared and characterized several 3d-4f (Ni(II), Cu(II) and Zn(II) transition metal (3d) ions and Ce(III), Pr(III), and Lu(III) lanthanide metal (4f) ions) complexes incorporating chiral Schiff base ligands (abbreviated as **CeNi**, **CeCu**, **CeZn**, **PrNi**, **PrCu**, **PrZn**, **LuNi**, **LuCu**, and **LuZn**, respectively). Solid-state CD spectra and diffuse reflectance electronic spectra exhibited reasonable shift by combination of 3d and 4f ions at charge-transfer region. Magnetic features (antiferromagnetic interactions, if any) also exhibited substitution of 3d-4f ions of diamagnetic or paramagnetic spin numbers. Interestingly, determined crystal structures of some of them exhibited different structural characters about coordination numbers, crystalline solvents, and dimetic (or bridging) features nevertheless of 3d-4f metal substitution in identical organic ligands.

* Corresponding Authors
Tel: +81 3 5228 8271; Fax: +81 3 5261 4361
E-Mail: akitsu@rs.kagu.tus.ac.jp
[a] Department of Chemistry, Faculty of Science, Tokyo University of Science, 1-3 Kagurazaka, Shinjuku-ku, Tokyo 162-8601, Japan

Introduction

In recent years, studies on 3d-4f binuclear metal complexes have gained importance with special interest on photophysical properties[1-4] and magnetic properties[5-12] arising from interactions between metal ions as well as sole metal ion having suitable electronic states or unpaired electrons. For example, some cyanide-bridges 3d-4f metal complexes[13-15] have been studied to elucidate empirical estimation of magnetic interaction including paramagnetic ions for understanding multi-functions.[16] In this context, we have been interested in chiral Schiff base 3d-4f dinuclear complexes incorporating so-called salen-type ligands and investigated structure-property correlation and its variety resulting from metal-substitution and their combination.[16-17] By assembling 3d-4f ions, we are interested in characteristic chiroptical properties of the systems involving superexchange magnetic interactions. Generally, systematic comparison of electronic properties for a series of 3d-4f binuclear metal complexes should be carried out for isostructural ones. Indeed many types of 3d-4f binuclear metal complexes take identical crystal structure nevertheless of substitution of relatively small 3d metal ions and relatively large 4f metal ions showing lanthanide contraction typically. In this work, we prepared new chiral Schiff base Ln(III)-M(II) complexes (abbreviated as **CeNi**, **CeCu**, **CeZn**, **PrNi**, **PrCu**, **PrZn**, **LuNi**, **LuCu**, and **LuZn;** Scheme 1) and characterized with electronic spectra, CD spectra, magnetic properties, and X-ray crystallography. In contrast to common series of 3d-4f metal complexes, the present complexes showed drastic changes of crystal structures as well as molecular structures due to not only ionic radii of 4f ions (the smallest Lu(III), middle Pr(III), and the largest Ce(III)) but also coordination environment of 3d ions especially associated with axial ligands.

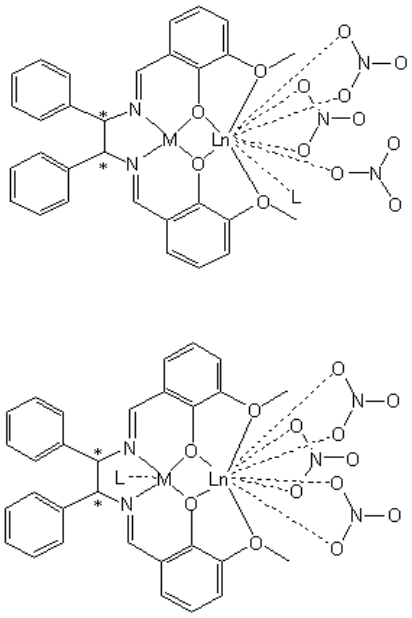

Scheme 1. Molecular structures of 3d-4f complexes representing different coordination modes of potentially bridging nitrate ligands and axial ligands (L).

Experimental

Materials and Instrumentation

Chemicals of the highest commercial grade available (solvents are from Kanto Chemical, organic compounds are from Tokyo Chemical Industry and metal sources from Wako and Aldrich were used as received without further purification. Elemental analyses (C, H, N) were carried out with a Perkin-Elmer 2400II CHNS/O analyzer at Tokyo University of Science. Infrared spectra were recorded using KBr pellets on a JASCO FT-IR 4200 plus spectrophotometer equipped with polarizer in the range of

4000-400 cm^{-1} at 298 K. Diffuse reflectance spectra were measured on a JASCO V-570 UV/VIS/NIR spectrophotometer equipped with polarizer in the range of 800-200 nm at 298 K and were converted from absorbance to reflectance by the Kubelka-Munk method. Circular dichroism(CD) spectra were measured as KBr pellets on a JASCO J-820 spectropolarimeter in a range of 800-300 nm at 298 K. Powder X-ray diffraction patterns were also measured by using synchrotron radiation beamtime at KEK PF BL-8B (2010G511) with 8 keV (λ = 1.54184 Å) with a RIGAKU imaging plate. The $Cu2p_{3/2}$ and $Cu2p_{1/2}$ peaks of XAS (soft X-ray absorption spectra) were measured at KEK PF BL-19B (2010G510) under variable temperature. The spectra were corrected by the standard Au sample. The magnetic properties were investigated with a Quantum Design MPMS-XL superconducting quantum interference device magnetometer (SQUID) at an applied field 1000 Oe in a temperature range 2-300 K. Powder samples were measured in a pharmaceutical cellulose capsule. The apparatus signals and the diamagnetic corrections were evaluated from the analogous diamagnetic **LaZn** complex.

X-ray Crystallography

Orange prismatic single crystals of **CeNi**, purple prismatic single crystals of **CeZn**, light-yellow prismatic single crystals of **CeCu**, red prismatic single crystals of **PrNi**, red prismatic single crystals of **LuNi**, brown prismatic single crystals of **LuCu**, and transparent prismatic single crystals of **LuZn** were glued on top of a glass fiber and coated with a thin layer of epoxy resin to measure the diffraction data. Intensity data were collected on a Bruker APEX2 CCD diffractometer with graphite monochromated Mo Kα radiation (λ = 0.71073 Å). Data analysis was carried out with a SAINT program package. The structures were solved by direct methods with a SHELXS-97[19] and expanded by Fourier techniques and refined by full-matrix least-squares methods based on F^2 using the program SHELXL-97.[19] A multi-scan absorption correction was applied by a program SADABS. All non-hydrogen atoms were readily located and refined by anisotropic thermal parameters. All hydrogen atoms were located at geometrically calculated positions and refined using riding models.

Crystallographic data for ***CeNi***. $C_{30}H_{26}CeNiN_5O_{13}.N_3O_9$, crystal size 0.18 mm × 0.17 mm × 0.12 mm, M_w = 863.39, monoclinic, space group *C2* (#5), *a* = 19.1533(18) Å, *b* = 15.6034(14)Å, *c* = 22.209(2) Å, β = 99.178(2) °, *V* = 6552.2(11) $Å^3$, *Z* = 8, D_{calc} = 1.750 Mg m^{-3}, *F*(000) = 3448, R_1 = 0.0542, wR_2 = 0.1558 (20051 reflections), *S* = 0.847, Flack parameter = 0.00(2). (where $R_1 = \Sigma||F_o|-|F_c||/\Sigma|F_o|$. $R_w=(\Sigma w(|F_o|-|F_c|)^2/\Sigma w|F_o|^2)^{1/2}$, $w=1/(\sigma^2(F_o) + (0.1P)^2)$, $P = (F_{o2} + 2F_{c2})/3$).

Crystallographic data for ***CeCu***. $C_{30}H_{26}CeCuN_2O_4.CH_3O_{10}N_3$ crystal size 0.13 mm × 0.10 mm × 0.07 mm, M_w = 899.25, monoclinic, space group $P2_1$ (#4), *a* = 10.654(8) Å, *b* = 21.113(16) Å, *c* = 15.715(12) Å, β = 101.638(11) °, *V* = 3462(5) $Å^3$, *Z* = 4, D_{calc} = 1.725 Mg m^{-3}, *F*(000) = 1796, R_1 = 0.0538, wR_2 = 0.1631 (18689 reflections), *S* = 0.821, Flack parameter = -0.02(2). (where $R_1 = \Sigma||F_o|-|F_c||/\Sigma|F_o|$. $R_w=(\Sigma w(|F_o|-|F_c|)^2/\Sigma w|F_o|^2)^{1/2}$, $w = 1/(\sigma^2(F_o) + (0.1P)^2)$, $P = (F_{o2} + 2F_{c2})/3$).

Crystallographic data for ***CeZn***. $C_{30}H_{26}CeZnN_2O_4.C_2H_7O_{11}N_3$ crystal size 0.22 mm × 0.12 mm × 010 mm, M_w = 933.12, monoclinic, space group $P2_1$ (#4), *a* = 9.3562(9) Å, *b* = 16.1727(15) Å, *c* = 24.001(2) Å, β = 95.3730(10) °, *V*=3617.3(6) $Å^3$, *Z*=4, D_{calc}=1.713 Mg m^{-3}, *F*(000) = 1872, R_1 = 0.0251, wR_2 = 0.0794 (20128 reflections), *S* = 0.677, Flack parameter = -10(10). (where $R_1 = \Sigma||F_o|-|F_c||/\Sigma|F_o|$. $R_w = (\Sigma w(|F_o|-|F_c|)^2/\Sigma w|F_o|^2)^{1/2}$, $w=1/(\sigma^2(F_o) + (0.1P)^2)$, $P = (F_{o2} + 2F_{c2})/3$).

Crystallographic data for ***PrNi***. $C_{30}H_{26}PrNiN_2O_4.O_9N_3$, crystal size 0.27 mm × 0.18 mm × 0.17 mm, M_w = 864.18, monoclinic, space group *C2* (#5), *a* = 19.173(2) Å, *b* = 15.6164(18)Å, *c* = 22.193(2) Å, β =99.155(2)°, *V*=6560.4(13) $Å^3$, *Z*=8, D_{calc} =1.750 Mg m^{-3}, *F*(000) = 3456, R_1 = 0.0434, wR_2 = 0.0882 (20321 reflections), *S* = 1.012, Flack parameter = -0.001(13). (where $R_1 = \Sigma||F_o|-|F_c||/\Sigma|F_o|$. $R_w=(\Sigma w(|F_o|-|F_c|)^2/\Sigma w|F_o|^2)^{1/2}$, $w = 1/(\sigma^2(F_o) + (0.1P)^2)$, $P = (F_{o2} + 2F_{c2})/3$).

Crystallographic data for ***LuNi***. $C_{30}H_{26}LuNiN_2O_4.O_9N_3$, crystal size 0.09 mm × 0.09 mm × 0.08 mm, M_w = 898.24, monoclinic, space group *C2* (#5), *a* = 19.2462(14) Å, *b* = 15.4932(14)Å, *c* = 21.8129(18) Å, β = 98.9910(10) °, *V* = 6524.4(9) $Å^3$, *Z* = 8, D_{calc} = 1.857 Mg m^{-3}, *F*(000) = 3552, R_1 = 0.0315, wR_2 = 0.0974 (17822 reflections), *S* = 0.679, Flack parameter = -0.015(8). (where $R_1 = \Sigma||F_o|-|F_c||/\Sigma|F_o|$. $R_w = (\Sigma w(|F_o|-|F_c|)^2 / \Sigma w|F_o|^2)^{1/2}$, $w=1/(\sigma^2(F_o) + (0.1P)^2)$, $P = (F_{o2} + 2F_{c2})/3$).

Crystallographic data for ***LuCu***. $2(C_{30}H_{28}LuCuN_2O_4 \cdot CH_3O_{10}N_3)CH_4O$ crystal size 0.19 mm × 0.18 mm × 0.10 mm, M_w = 1900.25, triclinic, space group *P1* (#1), *a* = 9.3607(7) Å, *b* = 14.0284(10) Å, *c* = 15.2948(11) Å, α= 107.9910(10) °, β = 104.5540(10) °, γ = 101.4330(10) °, *V* = 1764.0(2) $Å^3$, *Z* =1, D_{calc} = 1.789 mg/m^3, *F*(000) = 942, R_1 = 0.0193, wR_2 = 0.0433 (9538 reflections), *S* = 0.948, Flack parameter = 0.001(5). (where $R_1 = \Sigma||F_o|-|F_c||/\Sigma|F_o|$. $R_w=(\Sigma w(|F_o|-|F_c|)^2/\Sigma w|F_o|^2)^{1/2}$, $w = 1/(\sigma^2(F_o) + (0.1P)^2)$, $P = (F_{o2} + 2F_{c2})/3$).

Crystallographic data for ***LuZn***. $C_{30}H_{26}LuZnN_2O_4 \cdot O_9N_3$ crystal size 0.19 mm × 0.16 mm × 015 mm, M_w = 904.90, monoclinic, space group $P2_1$ (#4), *a* = 10.2449(4) Å, *b* = 19.1856(8) Å, *c* = 17.2315(7) Å, β = 94.8660(10) °, *V*=3374.7(2) $Å^3$, *Z*=4, D_{calc}=1.781 Mg m^{-3}, *F*(000) = 1784, R_1 = 0.0410, wR_2 = 0.0746 (20711 reflections), *S* = 1.013, Flack parameter = 0.006(8). (where $R_1 = \Sigma||F_o|-|F_c||/\Sigma|F_o|$. $R_w = (\Sigma w(|F_o|-|F_c|)^2/\Sigma w|F_o|^2)^{1/2}$, $w = 1/(\sigma^2(F_o) + (0.1P)^2)$, $P = (F_{o2} + 2F_{c2})/3$).

Preparations

Preparation of ***CeNi***. To a solution of *o*-vanillin (0.305 g, 2.00 mmol) dissolved in methanol (60 mL), (*1R,2R*)-(+)-1,2-diphenylethylenediamine (0.212 g, 1.00 mmol) was added and stirred at 313 K for 2 h to give yellow solution of ligand. Nickel(II) acetate tetrahydrate (0.2551 g, 1.00 mmol) was added to the resulting solution to give muddy brown solution of the complex. After stirring at 313 K for 3 h, cerium(III) nitrate hexahydrate

(0.4375 g 1.00 mmol) was added to the resulting solution and the reaction was refluxed for 4 h at 373 K. After cooling the solution, this orange compound was filtered and recrystallized from methanol/diethyl ether to give orange prismatic single crystals for X-ray analysis.

Yield 0.1288 g (14.92 %). Anal. Found: C, 41.64; H, 2.82; N, 8.05 %. Calc. for $C_{30}H_{26}CeNiN_2O_4.O_9N_3$: C, 41.33; H, 3.24; N, 8.01 %. IR (KBr (cm^{-1})): 669 (s), 694 (s), 735 (s),774 (s), 846 (s), 945 (s), 1021 (s), 1075 (s), 1168 (s), 1071 (s), 1161 (s), 1231 (s), 1383 (w), 1229 (m), 1292 (m), 1368 (m), 1389 (m), 1458 (m), 1608 (m), 1621 (m) (C=N), 1652 (m), 1700 (m), 2339 (s), 3375 (sh). XRD(2q/degree): 7.714, 7.975, 8.700, 9.338, 10.295, 11.31, 11.977, 14.819, 14.848, 16.095, 18.763, 21.025, 21.576, 21.779, 22.765, 23.925, 24.157, 24.650, 26.680, 30.028.

Preparation of ***CeCu***. To a solution of *o*-vanillin (0.305 g, 2.00 mmol) dissolved in methanol (60 mL), (*1R,2R*)-(+)-1,2-diphenylethylenediamine (0.212 g, 1.00 mmol) was added and stirred at 313 K for 2 h to give yellow solution of ligand. Copper(II) acetate hydrate (0.2045 g, 1.00 mmol) was added to the resulting solution to give muddy green solution of the complex. After stirring at 313 K for 3 h, cerium(III) nitrate hexahydrate (0.4375 g 1.00 mmol) was added to the resulting solution and the reaction was refluxed for 4 h at 373 K. After cooling the solution, this purple compound was filtered and recrystallized from methanol/diethyl ether to give crystals containing (nonstoichometric) CH_4O solvent suitable for X-ray analysis.

Yield 0.5415 g (60.22 %). Anal. Found: C, 41.37; H, 2.83; N, 7.74 %. Calc. for $C_{30}H_{26}CeCuN_2O_4.CH_3O_{10}N_3$: C, 41.40; H, 3.25; N, 7.79 %. IR (KBr (cm^{-1})): 604 (s), 640 (s), 668 (m), 701 (s), 741 (m), 754 (s), 778 (s), 813 (s), 852 (m), 951 (m), 993 (s), 1074 (s), 1097 (s), 1165 (s), 1201 (m), 1240 (s), 1288 (m), 1382 (w), 1448 (m), 1453 (m), 1467 (m), 1490 (m), 1555 (s), 1605 (m), 1626 (m) (C=N), 2353 (s), 2360 (s), 2365 (s), 2425 (s), 3352 (sh). XRD(2q /degree): 6.467, 7.743, 9.657, 10.382, 10.962, 11.542, 12.035, 12.644, 12.963, 14.210, 15.022, 15.544, 16.066, 16.385, 17.429, 18.386, 20.097, 20.967, 21.886, 21.982, 23.287, 23.896, 24.969, 25.259, 25.897, 27.144, 28.652, 29.406, 31.146, 32.074, 32.770. XAS: $Cu2p_{3/2}$ 933.3 eV, $Cu2p_{1/2}$ 954.1 eV.

Preparation of ***CeZn***. To a solution of *o*-vanillin (0.305 g, 2.00 mmol) dissolved in methanol (60 mL), (*1R,2R*)-(+)-1,2-diphenylethylenediamine (0.212 g, 1.00 mmol) was added and stirred at 313 K for 2 h to give yellow solution of ligand. Zinc(II) acetate tetrahydrate (0.2217 g, 1.00 mmol) was added to the resulting solution to give light-yellow solution of the complex. After stirring at 313 K for 3 h, cerium(III) nitrate hexahydrate (0.4421 g 1.00 mmol) was added to the resulting solution and the reaction was refluxed for 4 h at 373 K. After cooling the solution, this light-yellow compound was filtered and recrystallized from methanol/diethyl ether to give light-yellow prismatic single crystals containing (nonstoichometric) CH_4O solvent suitable for X-ray analysis.

Yield 0.3279 g (35.75 %). Anal. Found: C, 39.85; H, 2.90; N, 7.47 %. Calc. for $C_{30}H_{26}CeN_2O_4Zn.CH_3O_{10}N_3$: C, 41.91; H, 3.63; N, 7.77 %. IR (KBr (cm^{-1})): 545 (s), 624 (s), 641 (s), 667 (m), 700 (s), 740 (m), 753 (s), 765 (s), 813 (s), 847 (m), 962 (m), 977 (m), 1025 (s), 1072 (m), 1094 (m), 1167 (s), 1219 (m), 1226 (m), 1275 (m), 1316 (m), 1382 (w), 1438 (m), 1449 (m), 1457 (m), 1479 (m), 1554 (m), 1605 (m), 1627 (m) (C=N), 1700 (m), 2357 (s), 2422 (s), 3359 (sh). XRD(2q /degree): 6.438, 7.772, 9.773, 10.237, 11.049, 12.876, 14.181, 15.689, 16.414, 18.270, 20.300, 24.070, 25.027, 25.230, 25.600, 32.016.

Preparation of ***PrNi***. To a solution of *o*-vanillin (0.305 g, 2.00 mmol) dissolved in methanol (60 mL), (*1R,2R*)-(+)-1,2-diphenylethylenediamine (0.212 g, 1.00 mmol) was added and stirred at 313 K for 2 h to give yellow solution of ligand. Nickel(II) acetate tetrahydrate (0.2506 g, 1.00 mmol) was added to the resulting solution to give muddy brown solution of the complex. After stirring at 313 K for 3 h, praseodym(III) nitrate hexahydrate (0.4480 g 1.00 mmol) was added to the resulting solution and the reaction was refluxed for 4 h at 373 K. After cooling the solution, this orange compound was filtered and recrystallized from methanol/diethyl ether to give crystals for X-ray analysis.

Yield 0.3424 g (39.62 %). Anal. Found: C, 41.38; H, 3.20; N, 7.73 %. Calc. for $C_{30}H_{26}PrNiN_2O_4.O_9N_3$: C, 41.70; H, 3.03; N, 8.10 %. IR (KBr (cm^{-1})): 667 (m), 693 (s), 734 (s), 775 (s), 801 (s), 857 (s), 951 (s), 1021 (s), 1074 (s),1171 (s), 1233 (m), 1242 (m), 1290 (m), 1383 (m), 1456 (m), 1486 (m), 1557 (m), 1616 (m) (C=N), 1652 (m), 1700 (m), 2330 (s), 2352 (s), 3386 (sh). XRD(2q/degree): 7.337, 8.004, 8.729, 9.367, 10.324, 11.339, 12.035, 13.311, 13.291, 14.848, 15.138, 16.124, 16.153, 16.588, 170342, 17.516, 18.270, 18.821, 19.952, 22.765, 23.954, 24.186, 24.679, 26.738, 26.796, 27.985, 28.391, 28.971, 29.899, 30.305.

Preparation of ***PrCu***. To a solution of *o*-vanillin (0.305 g, 2.00 mmol) dissolved in methanol (60 mL), (*1R,2R*)-(+)-1,2-diphenylethylenediamine (0.212 g, 1.00 mmol) was added and stirred at 313 K for 2 h to give yellow solution of ligand. Copper(II) acetate hydrate (0.1999 g, 1.00 mmol) was added to the resulting solution to give muddy green solution of the complex. After stirring at 313 K for 3 h, praseodym (III) nitrate hexahydrate (0.4505 g 1.00 mmol) was added to the resulting solution and the reaction was refluxed for 4 h at 373 K. After cooling the solution, this purple compound was filtered and recrystallized from methanol/diethyl ether to give purple prismatic single crystals containing (nonstoichometric) CH_4O solvent suitable for X-ray analysis.

Yield 0.6473 g (72.19 %). Anal. Found: C, 41.72; H, 3.05; N, 8.09 %. Calc. for $C_{30}H_{26}PrCuN_2O_4.CH_3O_{10}N_3$: C, 41.37; H, 3.25; N, 7.78 %. IR (KBr (cm^{-1})): 642 (s), 668 (m), 698 (s), 739 (m), 809 (s), 852 (s), 961 (s), 977 (s), 993 (s), 1019 (s), 1072 (s), 1095 (s), 1166 (s), 1222 (m), 1227 (s), 1289 (m), 1383 (w), 1454 (m), 1471 (m), 1491 (s), 1557 (s), 1605 (m), 1623 (m) (C=N), 1652 (m), 1700 (m), 2336 (m), 2357 (m), 3386 (sh). XRD(2q/degree):

6.467, 7.859, 9.850, 10.295, 11.107, 12.963, 14.268, 15.747, 18.386, 20.445, 21.157, 23.084, 23.519, 23.925, 24.331, 25.201, 25.346, 26.216, 26.825, 27.318, 32.729. XAS: $Cu2p_{3/2}$ 930.9 eV, $Cu2p_{1/2}$ 952.7 eV.

Preparation of ***PrZn***. To a solution of *o*-vanillin (0.305 g, 2.00 mmol) dissolved in methanol (60 mL), (*1R*,*2R*)-(+)-1,2-diphenylethylenediamine (0.212 g, 1.00 mmol) was added and stirred at 313 K for 2 h to give yellow solution of ligand. Zinc(II) acetate tetrahydrate (0.2211 g, 1.00 mmol) was added to the resulting solution to give light-yellow solution of the complex. After stirring at 313 K for 3 h, praseodym (III) nitrate hexahydrate (0.4492 g 1.00 mmol) was added to the resulting solution and the reaction was refluxed for 4 h at 373 K. After cooling the solution, this light-yellow compound was filtered and recrystallized from methanol/diethyl ether to give light-yellow prismatic single crystals containing (nonstoichometric) CH_4O solvent suitable for X-ray analysis.

Yield 0.4836 g (53.61 %). Anal. Found: C, 41.26; H, 3.29; N, 7.81 %. Calc. for $C_{30}H_{26}PrN_2O_4Zn.CH_3O_{10}N_3$: C, 41.37; H, 3.25; N, 7.78 %. IR (KBr (cm^{-1})): 641 (s), 667 (w), 699 (s), 739 (m), 756 (s), 781 (s), 809 (s), 848 (m), 960 (s), 976 (s), 1024 (s), 1071 (s), 1094 (s), 1168 (s), 1219 (m), 1226 (s), 1285 (m), 1309 (s), 1383 (w), 1419 (s), 1436 (m), 1456 (m), 1471 (m), 1506 (m), 1522 (s), 1567(s), 1623 (m) (C=N), 1652 (m), 1700 (s), 2328 (s), 2360 (s), 3392 (sh). XRD(2θ/degree): 6.409, 7.801, 9.744, 10.208, 10.991, 12.847, 14.123, 15.254, 15.602, 18.212, 19.343, 20.242, 21.025, 22.272, 22.881, 23.316, 23.722, 24.099, 24.477, 24.969, 25.114, 26.013, 26.564, 27.057, 27.521, 28.478, 21.319, 30.769, 31.320, 32.323, 32.509.

Preparation of ***LuNi***.To a solution of *o*-vanillin (0.305 g, 2.00 mmol) dissolved in methanol (60 mL), (*1R*,*2R*)-(+)-1,2-diphenylethylenediamine (0.212 g, 1.00 mmol) was added and stirred at 313 K for 2 h to give yellow solution of ligand. Nickel(II) acetate tetrahydrate (0.2545 g, 1.00 mmol) was added to the resulting solution to give muddy brown solution of the complex. After stirring at 313 K for 3 h, lutetium(III) nitrate hexahydrate (0.3642 g 1.00 mmol) was added to the resulting solution and the reaction was refluxed for 4 h at 373 K. After cooling the solution, this orange compound was filtered and recrystallized from methanol/diethyl ether to give crystals.

Yield 0.4921 g (54.85 %). Anal. Found: C, 40.14; H, 2.92; N, 7.75 %. Calc. for $C_{30}H_{26}LuNiN_2O_4.O_9N_3$: C, 40.12; H, 3.02; N, 7.80 %. IR (KBr (cm^{-1})): 583 (s), 591 (s), 667 (m), 695 (m), 736 (m), 779 (s), 809 (s), 863 (s), 952 (s), 1025 (m), 1073 (m), 1171 (s), 1231 (m), 1275 (m), 1314 (m), 1383 (w), 1440 (m), 1474 (m), 1506 (m), 1559 (m), 1610 (m), 1619 (m) (C=N), 1700 (s), 2328 (s), 2922 (s), 3390 (sh). XRD(2θ/degree): 7.377, 8.062, 8.758, 9.388, 10.440, 11.426, 12.093, 13.340, 13.688, 14.065, 14.906, 15.109, 16.240, 16.385, 16.762, 17.574, 18.357, 18.734, 20.157, 21.199, 21.605, 21.808, 22.852, 23.896, 24.218, 24.302, 25.056, 26.709, 28.275, 30.044, 30.218, 30.450, 31.378.

Preparation of ***LuCu***. To a solution of *o*-vanillin (0.305 g, 2.00 mmol) dissolved in methanol (60 mL), (*1R*,*2R*)-(+)-1,2-diphenylethylenediamine (0.212 g, 1.00 mmol) was added and stirred at 313 K for 2 h to give yellow solution of ligand. Copper(II) acetate hydrate (0.2027 g, 1.00 mmol) was added to the resulting solution to give muddy green solution of the complex. After stirring at 313 K for 3 h, lutetium(III) nitrate hexahydrate (0.3610 g 1.00 mmol) was added to the resulting solution and the reaction was refluxed for 4 h at 373 K. The solution was evaporated under reduced pressure, and deep brown compound was yielded. This compound was filtered and recrystallized from methanol/diethyl ether to give crystals containing (nonstoichometric) CH_4O solvent suitable for X-ray analysis.

Yield 0.2852 g (30.54 %). Anal. Found: C, 39.74; H, 3.22; N, 7.53 %. Calc. for $C_{30}H_{26}LuCuN_2O_4.CH_3O_{10}N_3$: C, 39.86; H, 3.13; N, 7.74 %. IR (KBr (cm^{-1})): 649 (s), 667 (w), 698 (m), 742 (m), 854 (s), 955 (s), 1020 (s), 1071 (s), 1093 (s), 1167 (s), 1220 (m), 1239 (s), 1288 (m), 1383 (w), 1464 (m), 1495 (s), 1533 (s), 1557 (s), 1605 (m), 1623 (m) (C=N), 1652 (s), 1700 (m), 2345 (s), 3344 (sh). XRD(2 θ /degree): 6.264, 6.641, 6.699, 7.192, 7.656, 8.236, 9.309, 9.628, 10.237, 10.759, 11.194, 11.803, 12.209, 12.644, 12.934, 13.253, 13.746, 14.355, 15.283, 16.414, 17.023, 18.647, 18.821, 20.184, 21.866, 22.678, 24.447, 24.940, 25.752, 26.245, 27.144, 27.666, 29.000, 30.305, 30.943, 32.074. XAS: $Cu2p_{3/2}$ 933.5 eV, $Cu2p_{1/2}$ 954.1 eV.

Preparation of ***LuZn***. To a solution of *o*-vanillin (0.305 g, 2.00 mmol) dissolved in methanol (60 mL), (*1R*,*2R*)-(+)-1,2-diphenylethylenediamine (0.212 g, 1.00 mmol) was added and stirred at 313 K for 2 h to give a ligand. Zinc(II) acetate tetrahydrate (0.2243 g, 1.00 mmol) was added to the resulting solution to give light-yellow solution of the complex. After stirring at 313 K for 3 h, lutetium(III) nitrate hexahydrate (0.3526 g 1.00 mmol) was added to the resulting solution and the reaction was refluxed for 4 h at 373 K. The solution was evaporated under reduced pressure, and yellow compound was yielded. This compound was filtered and recrystallized from methanol/diethyl ether to give crystals containing (nonstoichometric) CH_4O solvent suitable for X-ray analysis.

Yield 0.5046 g (53.91 %). Anal. Found: C, 39.74; H, 3.12; N, 7.57 %. Calc. for $C_{30}H_{26}LuN_2O_4Zn.CH_3O_{10}N_3$: C, 39.78; H, 3.12; N, 7.48 %. IR (KBr (cm^{-1})): 507 (s), 525 (s), 543 (s), 592 (s), 640 (s), 667 (m), 700 (m), 740 (m), 771 (s), 809 (s), 851 (m), 959 (m), 974 (m), 1024 (s), 1071 (m), 1092 (m), 1165 (m), 1219 (m), 1285 (m), 1382 (w), 1452 (m), 1470 (m), 1557 (s), 1623 (m) (C=N), 1652 (m), 1700 (m), 2424 (s), 3340 (sh). XRD(2θ/degree): 6.206, 7.308, 9.309, 10.005, 11.165, 11.600, 13.195, 14.616, 18.937, 19.169, 21.895, 22.881, 29.58.

Results and Discussion

Solid-state CD and electronic spectra

Figures 1, 2, and 3 show diffuse reflectance electronic spectra and CD (circular dichroism) spectra of Ce-complexes (**CeNi**, **CeCu**, and **CeZn**), Pr-complexes (**PrNi**, **PrCu**, and **PrZn**), and Lu-complexes (**LuNi**,

LuCu, and **LuZn**), respectively. For Ce-complexes, d-d bands (of Ni(II) or Cu(II) moieties) of electronic spectra appeared at about 18300-18600 cm^{-1}, while the corresponding d-d and CT (charge transfer) bands of CD spectra appeared at about 16200-17400 cm^{-1} and 24100-25100 cm^{-1}, respectively. For Pr-complexes, d-d bands (of Ni(II) or Cu(II) moieties) of electronic spectra appeared at about 18300-18400 cm^{-1}, while the corresponding d-d and CT bands of CD spectra appeared at about 16200-17400 cm^{-1} and 24100-25100 cm^{-1}, respectively. For Lu-complexes, d-d bands (of Ni(II) or Cu(II) moieties) of electronic spectra appeared at about 18700-19000 cm^{-1}, while the corresponding d-d and CT bands of CD spectra appeared at about 16000-16300 cm^{-1} and 23300-27100 cm^{-1}, respectively. Therefore, spectral changes, in particular charge transfer bands,[17] are attributed to substitution and/or coordination environment of 3d metal ions.

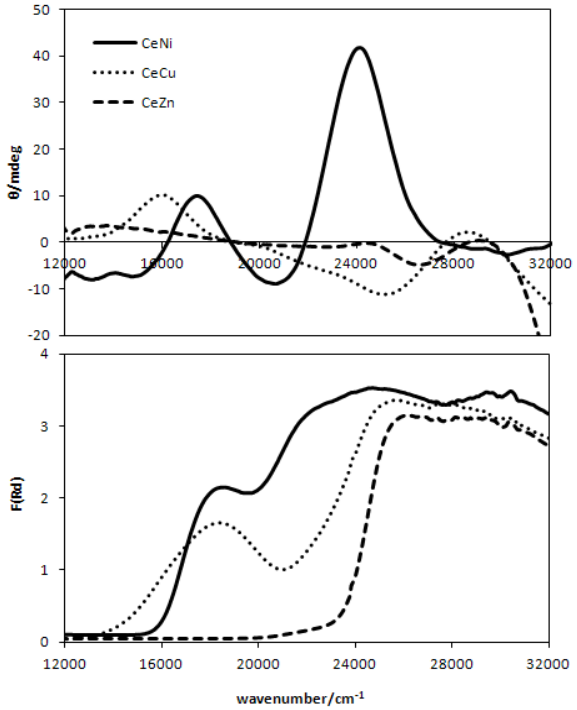

Figure 1. Solid-state CD and diffuse reflectance electronic spectra of **CeNi**, **CeCu**, and **CeZn**.

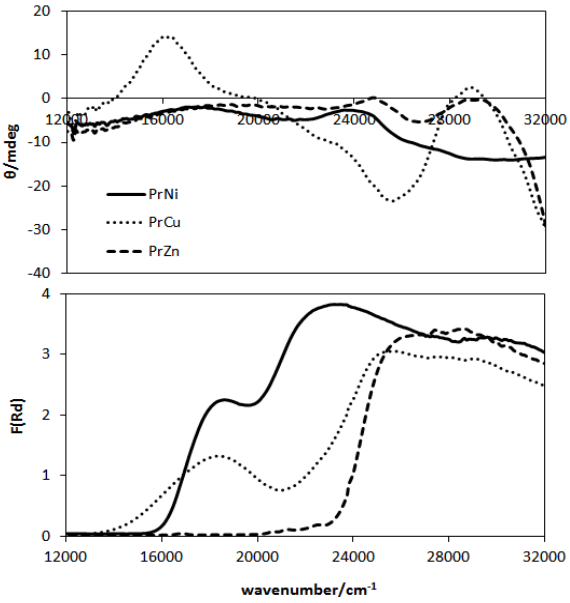

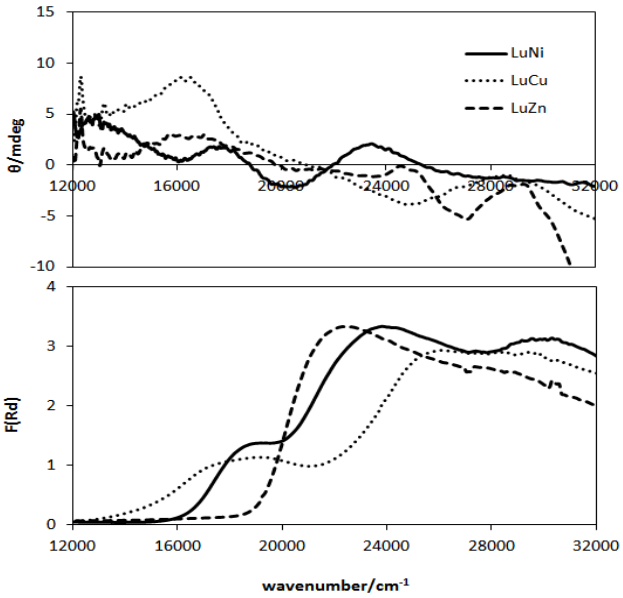

Figure 2. Solid-state CD and diffuse reflectance electronic spectra of **PrNi**, **PrCu**, and **PrZn**.

Figure 3. Solid-state CD and diffuse reflectance electronic spectra of **LuNi**, **LuCu**, and **LuZn**.

Magnetic properties

Figures 4, 5, 6 show the $\chi_M T$ vs T plots for Ce-complexes (**CeNi**, **CeCu**, and **CeZn**), Pr-complexes (**PrNi**, **PrCu**, and **PrZn**), and Lu-complexes (**LuNi**, **LuCu**, and **LuZn**), respectively. For 3d metal ions, Ni(II) ($3d^8$) and Zn(II) ($3d^{10}$) ions are diamagnetic (S = 0) and Cu(II) ($3d^9$) ion is paramagnetic (S = 1/2), while for 4f metal ions, Ce(III) ($4d^1$), Pr(III) ($4d^2$), and Lu(III) ($4d^{14}$) ions are S = 1/2, 1, and 0, respectively. Generally, 4-coordinated square planar and 6-coordinated octahedral Ni(II) complexes exhibit diamagnetism and paramagnetism, respectively, while 5-coordinated square pyramidal ones is not clear. Paramagnetism of Ni(II) ion is in accordance with coordination geometries as their metal complexes. That valence and spin state of Cu(II) ion is kept under the experimental conditions was also supported by the results of XAS. In this way, magnetic interaction between 3d and 4f ions can potentially be observed only for **CeCu** and **PrCu** composed of two paramagnetic ions.

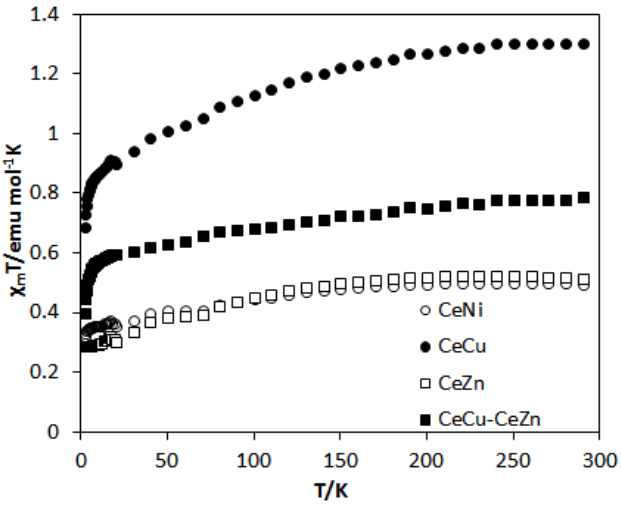

Figure 4. The $\chi_M T$ vs *T* plots for **CeNi**, **CeCu**, and **CeZn**.

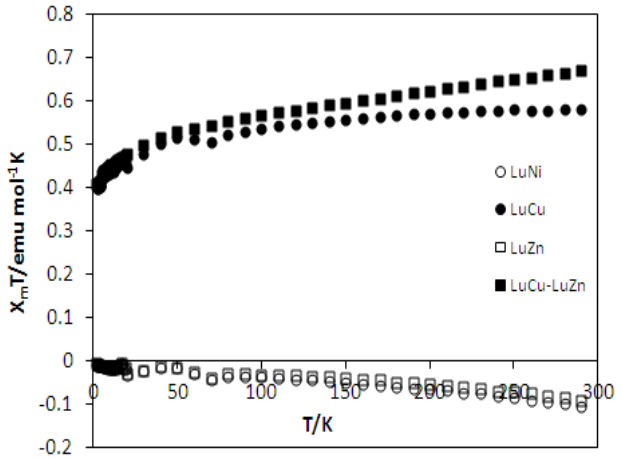

Figure 5. The $\chi_M T$ vs *T* plots for **PrNi**, **PrCu**, and **PrZn**.

Figure 6. The $\chi_M T$ vs *T* plots for LuNi, LuCu, and LuZn.

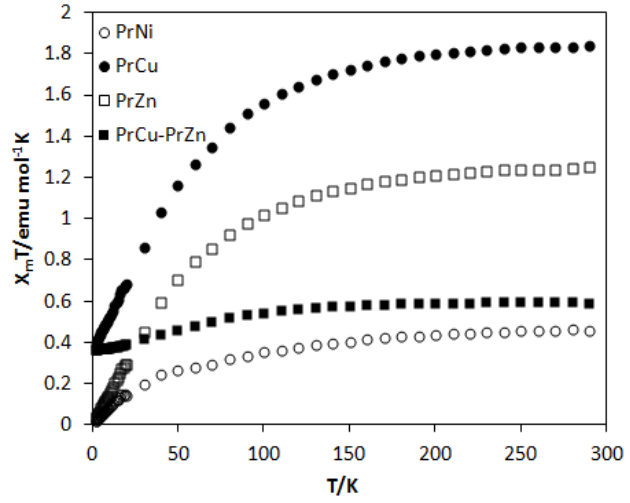

By comparing with the corresponding paramagnetic 4f and diamagnetic 3d complexes, namely CeZn for CeCu and PrZn for PrCu, and evaluating the differences of $\chi_M T$ values, these superexchange interactions via phenolate oxygen atoms are antiferromagnetic ones. It should be noted that discussion above is mentioned based on structural similarity (not isostructure completely) of 3d ion - phenolate oxygen atoms – 4f ion units for all complexes. Judgement for paramagnetic interactions may be impossible according to the way under this condition.[18]

Crystal structures

Crystal structures could be determined for **CeNi**, **CeCu**, **CeZn**, **PrNi**, **LuNi**, **LuCu**, and **LuZn**. According to powder XRD patterns, structural similarity between **LuCu** and **LuZn** and difference to **LuNi** are comparable to the corresponding Pr-complexes. Unfortunately, precise structures of **PrCu** and **PrZn** are not determined. However, one of the three nitrate ions of **CeCu** acts monodentate ligands though XRD patterns are almost similar to **CeZn**. In this way, structural differences between arbitrary two complexes may be reliable, whereas reliable discussion of structural similarity and detailed structure-property correlation are restricted to comparison with only 7 complexes characterized structurally.

Figure 7 depicts structure of **CeNi**. Ni(II) ion affords a 4-coordinated distorted square planar geometry without methanol ligands and Ce(III) ion affords a 10-coordinated environment with distorted square pyramidal from the plane made by two nitrate ligands. Phenyl groups are located under a salen-plane with C40-C39-C54-C55 = 166.6(8) and C10-C9-C24-C25 = 156.3(9) °.

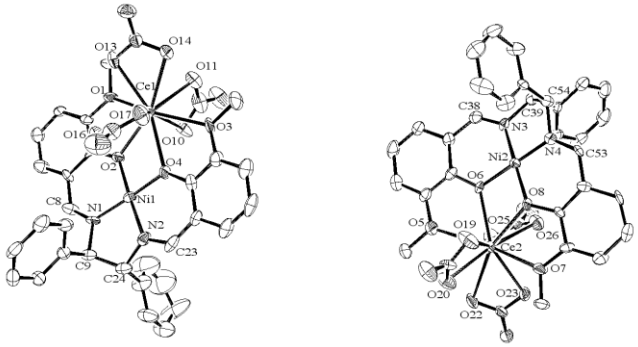

Figure 7. Molecular structures of **CeNi** showing selected atom labeling scheme. Hydrogen atoms are omitted clarity. Selected bond distance (Å) and bond or torsion angles (°): Ni1-N1 = 1.838(9), Ni1-N2 = 1.854(9), Ni1-O2 = 1.844(8), Ni1-O4 = 1.853(8), Ce1-O1 = 2.585(8), Ce1-O2 = 2.485(7), Ce1-O3 = 2.633(8), Ce1-O4 = 2.469(8), Ni2-N3 = 1.823(8), Ni2-N4 = 1.830(9), Ni2-O6 = 1.846(7), Ni2-O8 = 1.846(8), Ce2-O5 = 2.615(8), Ce2-O6 = 2.429(7), Ce2-O7 = 2.612(8), Ce2-O8 = 2.497(7), N1-Ni1-N2 = 86.4(4), O2-Ni1-N1 = 94.7(3), O2-Ni1-N2 = 175.8(3), O2-Ni1-O4 = 84.6(3), O4-Ni1-N1 = 175.2(4), O4-Ni1-N2 = 94.6(4), N3-Ni2-N4 = 85.9(4), O6-Ni2-N3 = 94.8(3), O6-Ni2-N4 = 177.5(3), O6-Ni2-O8 = 84.4(3), O8-Ni2-N3 = 176.9(3), O8- Ni2- N4 = 95.0(3), O1-Ce1-O2 = 60.8(3), O1-Ce1-O3 = 157.4(2), O1-Ce1-O4 = 120.0(3), O2-Ce1-O3 = 120.2(3), O2-Ce1-O4 = 60.3(3), O3-Ce1-O4 = 61.5(3), O5-Ce2-O6 = 61.4(2), O5-Ce2-O7 = 158.9(3), O5-Ce2-O8 = 118.2(3), O6-Ce2-O7 = 120.8(2), O6-Ce2-O8 = 60.4(3), O7-Ce2-O8 = 60.5(3).

Figure 8 depicts structure of **CeCu** of a dimer bridged via a nitrate ligand (see Scheme 1 [up]). Cu(II) ion affords a 4-coordinated almost square planar geometry, and Ce(III) ion affords a 10-coordinated envitonment with distorted square pyramidal towards a bridging nitrate ligand. Phenyl gruops indicate slight distortion with C40-C39-C54-C55 = 65.8(14) and C25-C24-C9-C10 = 59.2(13) °. Figure 9 depicts structure of **CeZn**. Zn(II) ion affords a 5-coordinated square pyramidal geometry lifted up towards axial methanol ligands and Ce(III) ion affords a 10-coordinated environment with distorted square pyramidal from the plane made by two nitrate ligands. Phenyl gruops connected to asymmetirc carbon atoms indicate slight distortion with C40-C39-C54-C55 = 59.9(4) and C25-C24-C9-C10 = 58.0(4) °.

 DOI: 10.17628/ECB.2013.2.49

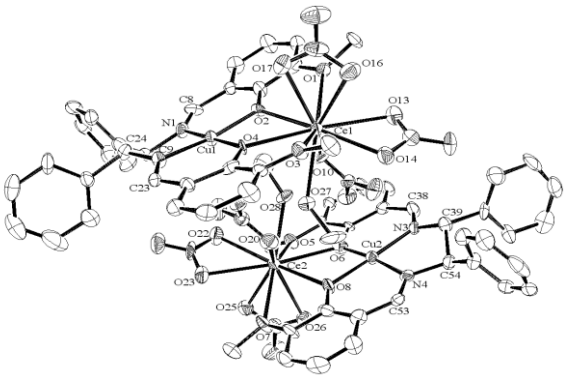

Figure 8. Molecular structures of **CeCu** showing selected atom labeling scheme. Hydrogen atoms are omitted clarity. Selected bond distance (Å) and bond or torsion angles (°): Cu1-N1 = 1.910(10), Cu1-N2 = 1.932(9), Cu1-O2 = 1.897(7), Cu1-O4 = 1.909(8), Ce1-O1 = 2.677(10), Ce1-O2 = 2.453(9), Ce1-O3 = 2.705(9), Ce1-O4 = 2.508(7), Cu2-N3 = 1.928(9), Cu2-N4 = 1.908(11), Cu2-O6 = 1.898(10), Cu2-O8 = 1.908(8), Ce2-O5 = 2.718(9), Ce2-O6 = 2.497(9), Ce2-O7 = 2.693(11), Ce2-O8 = 2.478(9), N1-Cu1-N2 = 85.8(4), O2-Cu1-N1 = 95.8(4), O2-Cu1-N2 = 170.2(4), O2-Cu1-O4 = 83.4(3), O4-Cu1-N1 = 178.9(4), O4-Cu1-O2 = 95.1(4), N3-Cu2-N4 = 86.5(4), O6-Cu2-N3 = 95.7(4), O6-Cu2-N4 = 171.3(4), O6-Cu2-O8 = 83.3(4), O8-Cu2-N3 = 178.1(4), O8-Cu2-N4 = 94.8(4), O1-Ce1-O2 = 59.5(3), O1-Ce1-O3 = 145.9(3), O1-Ce1-O4 = 117.0(3), O2-Ce1-O3 = 118.2(3), O2-Ce1-O4 = 61.4(2), O3-Ce1-O4 = 58.9(3), O5-Ce2-O6 = 59.1(3), O5-Ce2-O7 = 145.5(3), O5-Ce2-O8 = 117.8(3), O6-Ce2-O7 = 117.5(4), O6-Ce2-O8 = 61.1(3), O7-Ce2-O8 = 60.0(3).

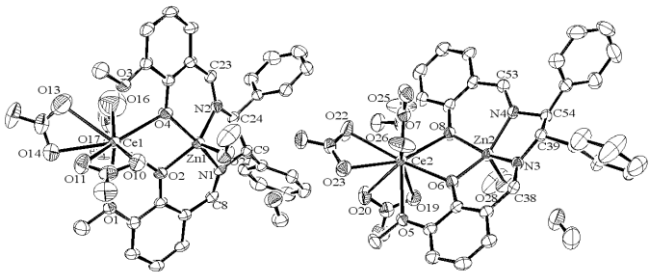

Figure 9. Molecular structures of CeZn showing selected atom labeling scheme. Hydrogen atoms are omitted clarity. Selected bond distance (Å) and bond or torsion angles (°): Zn1-N1 = 2.005(3), Zn1-N2 = 2.043(4), Zn1-O2 = 1.997(3), Zn1-O4 = 1.996(3), Ce1-O1 = 2.674(3), Ce1-O2 = 2.408(3), Ce1-O3 = 2.758(3), Ce1-O4 = 2.407(3), Zn2-N3 = 2.053(3), Zn2-N4 = 2.043(3), Zn2-O6 = 2.005(3), Zn2-O8 = 1.975(3), Ce2-O5 = 2.678(3), Ce2-O6 = 2.428(3), Ce2-O7 = 2.681(4), Ce2-O8 =2.432(3), N1-Zn1-N2 = 83.21(14), O2-Zn1-N1 = 92.21(13), O2-Zn1-N2 = 141.52(14), O2-Zn1-O4 = 80.89(11), O4-Zn1-N1 = 160.41(14), O4-Zn1-O2 = 90.81(12), N3-Zn2-N4 = 81.81(13), O6-Zn2-N3 = 90.29(13), O6-Zn2-N4 = 149.33(14), O6-Zn2-O8 = 80.67(11), O8-Zn2-N3 = 149.26(14), O8-Zn2-N4 = 91.11(12), O1-Ce1-O2 = 60.43(9), O1-Ce1-O3 = 152.3(1), O1-Ce1-O4 = 123.82(9), O2-Ce1-O3 = 121.0(1), O2-Ce1-O4 = 65.09(9), O3-Ce1-O4 = 58.4(1), O5-Ce2-O6 = 59.87(9), O5-Ce2-O7 = 154.33(12), O5-Ce2-O8 = 122.34(8), O6-Ce2-O7 = 121.76(10), O6-Ce2-O8 = 64.03(9), O7-Ce2-O8 = 59.74(10).

Figure 10 depicts structure of **PrNi**. Ni(II) ion affords a 4-coordinated distorted square planar geometry without methanol ligands and Pr(III) ion affords a 10-coordinated environment with distorted square pyramidal from the plane made by two nitrate ligands. Phenyl groups are located under a salen-plane with C40-C39-C54-C55 = 154.1 (5) and C10-C9-C24-C25 = 165.6(5) °.

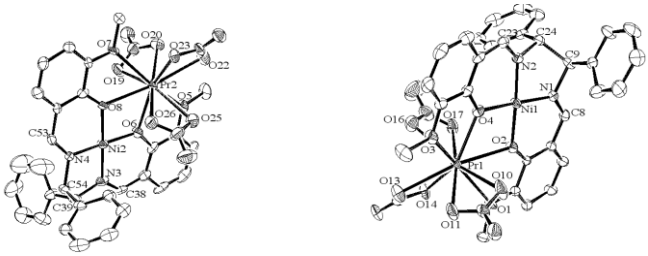

Figure 10. Molecular structures of **PrNi** showing selected atom labeling scheme. Hydrogen atoms are omitted clarity. Selected bond distance (Å) and bond or torsion angles (°): Ni1-N1 = 1.851(5), Ni1-N2 = 1.836(5), Ni1-O2 = 1.857(6), Ni1-O4 = 1.856(5), Pr1-O1 = 2.601(5), Pr1-O2 = 2.490(4), Pr1-O3 = 2.615(5), Pr1-O4 = 2.417(5), Ni2-N3 = 1.850(6), Ni2-N4 = 1.843(5), Ni2-O6 = 1.861(5), Ni2-O8 = 1.833(5), Pr2-O5 = 2.624(5), Pr2-O6 = 2.444(5), Pr2-O7 = 2.576(5), Pr2-O8 = 2.470(4), N1-Ni1-N2 = 86.5(2), O2-Ni1-N1 = 94.8(2), O2-Ni1-N2 = 176.7(2), O2-Ni1-O4 = 84.4(2), O4-Ni1-N1 = 177.6(2), O4-Ni1-N2 = 94.4(2), O1-Pr1-O2 = 60.33(17), O1-Pr1-O3 = 57.57(16), O1-Pr1-O4 = 121.34(16), O2-Pr1-O3 = 118.62(7), O2-Pr1-O4 = 61.11(17), O3-Pr1-O4 = 61.30(16), N3-Ni2-N4 = 86.9(2), O6-Ni2-N3 = 94.7 (3), O6-Ni2-N4 = 74.0(2), O6-Ni2-O8 = 83.9(2), O8-Ni2-N3 = 175.5(2), O8-Ni2-N4 = 95.00(2), O5-Pr2-O6 = 62.03(18), O5-Pr2-O7 = 156.34(16), O5-Pr2-O8 = 120.45(18), O6-Pr2-O7 = 120.50(17), O6-Pr2-O8 = 60.32(17), O7-Pr2-O8 = 61.15(17).

Figure 11 depicts structure of **LuNi**. Ni(II) ion affords a 4-coordinated distorted square planar geometry without methanol ligands and Lu(III) ion affords a 10-coordinated environment with distorted square pyramidal from the plane made by two nitrate ligands. Phenyl groups connected to the asymmetric carbon atoms are located under a salen-plane with C40-C39-C54-C55 = 166.2(5) and C10-C9-C24-C25 = 155.5(6) °.

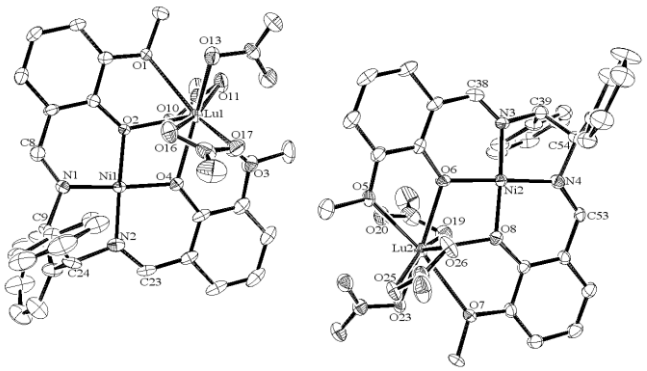

Figure 11. Molecular structures of LuNi showing selected atom labeling scheme. Hydrogen atoms are omitted clarity. Selected bond distance (Å) and bond or torsion angles (°): Ni1-N1 = 1.835(6), Ni1-N2 = 1.834(6), Ni1-O2 = 1.833(5), Ni1-O4 = 1.846(5), Lu1-O1 = 2.522(5), Lu1-O2 = 2.313(4), Lu1-O3 = 2.508(5), Lu1-O4 = 2.275(5), Ni2-N3 = 1.837(6), Ni2-N4 = 1.829(6), Ni2-O6 = 1.835(5), Ni2-O8 = 1.828(6), Lu2-O5 = 2.484(5), Lu2-O6 = 2.271(5), Lu2-O7 = 2.530(5), Lu2-O8 = 2.363(4), N1-Ni1-N2 = 86.9(3), O2-Ni1-N1 = 96.1(2), O2-Ni1-

N2 = 175.0(2), O2-Ni1-O4 = 81.5(2), O4-Ni1-N1 = 172.8(2), O4-Ni1-N2 = 96.1(2), O1-Lu1-O2 = 60.10(18), O1-Lu1-O3 = 150.47(16), O1-Lu1-O4 = 124.11(17), O2-Lu1-O3 = 125.41(19), O2-Lu1-O4 = 63.10(18), O3-Lu1-O4 = 64.96(19), N3-Ni2-N4 = 86.9(2), O6-Ni2-N3 = 94.6 (2), O6-Ni2-N4 = 178.2(2), O6-Ni2-O8 = 82.9(2), O8-Ni2-N3 = 176.8(2), O8-Ni2-N4 = 95.6 (2), O5-Lu2-O6 = 64.83(17), O5-Lu2-O7 = 151.07(16), O5-Lu2-O8 = 122.70(19), O6-Lu2-O7 = 125.10(17), O6-Lu2-O8 = 63.09(19), O7-Lu2-O8 = 62.33(18).

Figure 12 depicts structure of **LuCu** containing diffrent two types of molecules in an asymmetirc unit**.** Cu(II) ion affords a 4-coordinated compressed tetrahedral geometry, and Lu(III) ion affords 9- and 10-coordinated envitonments with distorted square pyramidal towards a coordinated methanol ligand or a bridging nitrate ligand.

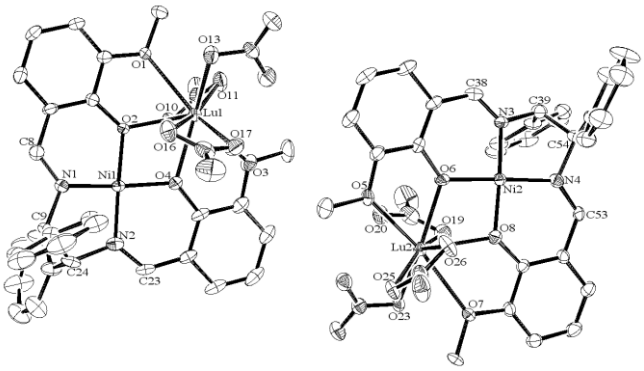

Figure 12. Molecular structures of **LuCu** showing selected atom labeling scheme. Hydrogen atoms are omitted clarity. Selected bond distance (Å) and bond or torsion angles (°): Cu1-N1 = 1.835(6), Cu1-N2 = 1.834(6), Cu1-O2 = 1.833(5), Cu1-O4 = 1.846(5), Lu1-O1 = 2.522(5), Lu1-O2 = 2.313(4), Lu1-O3 = 2.508(5), Lu1-O4 = 2.275(5), Cu2-N3 = 1.837(6), Cu2-N4 = 1.829(6), Cu2-O6 = 1.835(5), Cu2-O8 = 1.828(6), Lu2-O5 = 2.484(5), Lu2-O6 = 2.271(5), Lu2-O7 = 2.530(5), Lu2-O8 = 2.363(4), N1-Cu1-N2 = 86.9(3), O2-Cu1-N1 = 96.1(2), O2-Cu1-N2 = 175.0(2), O2-Cu1-O4 = 81.5(2), O4-Cu1-N1 = 172.8(2), O4-Cu1-N2 = 96.1(2), O1-Lu1-O2 = 60.10(18), O1-Lu1-O3 = 150.47(16), O1-Lu1-O4 = 124.11(17), O2-Lu1-O3 = 125.41(19), O2-Lu1-O4 = 63.10(18), O3-Lu1-O4 = 64.96(19), N3-Cu2-N4 = 86.9(2), O6-Cu2-N3 = 94.6 (2), O6-Cu2-N4 = 178.2(2), O6-Cu2-O8 = 82.9(2), O8-Cu2-N3 = 176.8(2), O8-Cu2-N4 = 95.6 (2), O5-Lu2-O6 = 64.83(17), O5-Lu2-O7 = 151.07(16), O5-Lu2-O8 = 122.70(19), O6-Lu2-O7 = 125.10(17), O6-Lu2-O8 = 63.09(19), O7-Lu2-O8 = 62.33(18).

Figure 13 depicts structure of **LuZn**. Zn(II) ion affords a 5-coordinated square distorted pyramidal geometry lifted up towards axial methanol ligands and Lu(III) ion affords a 9-coordinated environment with distorted square pyramidal towards bridging nitrate ligands. Phenyl gruops connected to asymmetirc carbon atoms indicate slight distortion with C40-C39-C54-C55 = 56.0(8) and C25-C24-C9-C10 = 65.4(8) °.

Conclusion

In summary, we have prepared and structurally characterized seven 3d-4f binuclear complexes incorporating chiral salen-type Schiff base ligands. According to lanthanide contraction, the order of ion radii for the present 4f ions are Lu(III) ($4f^{14}$) < Pr(III) ($4f^{2}$) < Ce(III) ($4f^{1}$). For 4f ions, Ce-complexes and Pr-complexes adopted coordination number 10, which are

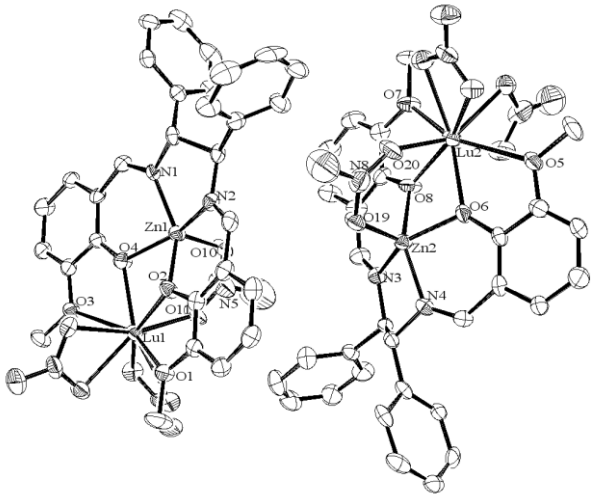

Figure 13. Molecular structures of **LuZn** showing selected atom labeling scheme. Hydrogen atoms are omitted clarity. Selected bond distance (Å) and bond or torsion angles (°): Zn1-N1 = 2.004(6), Zn1-N2 = 2.021(6), Zn1-O2 = 1.999(5), Zn1-O4 = 2.014(5), Lu1-O1 = 2.562(5), Lu1-O2 = 2.282(5), Lu1-O3 = 2.603(5), Lu1-O4 = 2.229(6), Zn2-N3 = 2.041(6), Zn2-N4 = 2.016(6), Zn2-O6 = 2.019(5), Zn2-O8 = 2.011(5), Lu2-O5 = 2.627(6), Lu2-O6 = 2.232(5), Lu2-O7 = 2.568(5), Lu2-O8 = 2.238(5), N1-Zn1-N2 = 83.2(2), O2-Zn1-N1 = 143.7(2), O2-Zn1-N2 = 91.5(2), O2-Zn1-O4 = 77.4(2), O4-Zn1-N1 = 91.0(2), O4-Zn1-N2 = 152.6(2), O1-Lu1-O2 = 61.9(2), O1-Lu1-O3 = 151.5(2), O1-Lu1-O4 = 127.8(2), O2-Lu1-O3 = 127.7(2), O2-Lu1-O4 = 67.6(2), O3-Lu1-O4 = 62.7(2), N3-Zn2-N4 = 82.2(2), O6-Zn2-N3 = 141.7(2), O6-Zn2-N4 = 90.6(2), O6-Zn2-O8 = 77.4(2), O8-Zn2-N3 = 89.9(2), O8-Zn2-N4 = 149.3 (2), O5-Lu2-O6 = 61.6(2), O5-Lu2-O7 = 149.9(2), O5-Lu2-O8 = 124.6(2), O6-Lu2-O7 = 130.1(2), O6-Lu2-O8 = 68.6(2), O7-Lu2-O8 = 62.0(2).

similar to analogous 3d-4f complexes previously reported.[17-18,20-21] However, Lu-complexes are 10-coordinated for **LuNi**, 9- and 10-coordinated for **LuCu**, and 9-coordinated for **LuZn**. Moreover, bridging modes of nitrate ligands of **CeCu** and **LuCu** (and resulting dimeric structure) are different from other complexes. For 3d ions, axial coordination of methanol ligands and degree of distortion from planar basal plane exhibited variety among the complexes. Therefore, the present examples of appropriate combination of 3d-4f ions only by substituting three 3d ions and three 4f ions indicated drastic variety of crystal structures including crystalline solvents nevertheless of the identical chiral organic ligands.

Supplementary data

CCDC 864541 - 864545 contain the supplementary crystallographic data. These data can be obtained free of charge *via* http://www.ccdc.cam.ac.uk/conts/retrieving.html, or from the Cambridge Crystallographic Data Centre, 12 Union Road, Cambridge CB2 1EZ, UK; fax: (+44) 1223-336-033; or e-mail: deposit@ccdc.cam.ac.uk.

Acknowledgements

This work was supported by Research Foundation for Opto-Science and Technology.

References

[1]Yang, X.-P., Jones, R. A., Wong, W.-K., Lynch, V., Oye, M., M., Holmes, A. L., *Chem. Commun.*, **2006**, 1836.

[2]Burrow, C. E., Burchell, T. J. Lin, P.-H. Habib, P., Wernsdorfer, W. Clerac, R., Murugesu, M.,*Inorg. Chem.*, **2009**, *48*, 8051.

[3]Wong, W.-K. Yang, X., Jones, R. A., Rivers, J. H., Lynch, V., Lo, W.-K., Xiao, D., Oye, M. M., Holmes, A. L., *Inorg. Chem.*, **2006**, *45*, 4340.

[4]Pasatoiu, T. D., Madalan, A. M., Kumke, M. U., Tiseanu, C., Andruh, M., *Inorg. Chem.*, **2010**, *49*, 2310.

[5]Andruh, M., Costes, J.-P., Diaz, C., Gao, S., *Inorg. Chem.*, **2009**, *48*, 3342.

[6]Colacio, E., Ruiz, J., Mota, A. J., Palacios, M. A., Cremades, E., Ruiz, E., White, F. J., Brechin, E. K., *Inorg. Chem.*, **2012**, *51*, 5857.

[7]Yan, P.-F., Lin, P.-H. Habib, F. Aharen, T. Murugesu, M. Deng, Z.-P. Li, G.-M., Sun W.-B., *Inorg. Chem.*, **2011**, *50*, 7059.

[8]Colacio, E., Ruiz-Sanchez, J., White, F. J., Brechin, E. K.., *Inorg. Chem.*, **2011**, *50*, 7268.

[9]Jana, A., Majumder, S., Carrella, L., Nayak, M., Weyhermueller, T., Dutta, S. Schollmeyer, D., Rentschler, E., Koner, R. Mohanta, S., *Inorg. Chem.*, **2010**, *49*, 9012.

[10]Feltham, H. L. C., Clerac, R., Ungur, L. Vieru, V. Chibotaru, L. F., Powell, A. K., Brooker, S., *Inorg. Chem.*, **2012**, *51*, 10603.

[11]Margeat, O., Lacroix, P. G., Costes, J. P., Donnadieu, B., Lepetit, C., *Inorg. Chem.*, **2004**, *43*, 4743.

[12]Gomez, V., Vendier, L., Corbella, M., Costes, J.-P., *Inorg. Chem.*, **2012**, *51*, 6396.

[13]Figuerola, A., Diaz, C., Ribas, J., Tangoulis, V., Granell, J., Lloret, F., Mahia, J., Maestro, M., *Inorg. Chem.*, **2003**, *42*, 641.

[14]Li, G., Akitsu, T., Sato, O., Einaga, Y., *J. Am. Chem. Soc*., **2003**, *125*, 12396.

[15]Svendsen, H., Overgaard, J., Chevallier, M., Collet, E., Iversen, B.B., *Angew. Chem. Int. Ed.*, **2009**, *48*, 2780.

[16]Akitsu, T., *Asian Chem. Lett.*, **2010**, *14*, 53 and references therein.

[17]Akitsu, T., Hirarsuka, T., Shibata, H., *Magnets: Types, Uses and Safety*, *Nova Science Publishers*, **2012** and references therein.

[18]Hirarsuka, T., Shibata, T. Akitsu, H., *Crystallography: Research, Technology and Applications*, *Nova Science Publishers*, **2012** and references therein.

[19]Sheldrick, G. M., *Acta Cryst*., **2008**, *A64*, 112.

[20]Bi, W.-Y., Lu, X.-Q., Chai, W.-L., Song, J.-R., Wong, W.-Y., Wong, W.-K., Jones, R. A., *J. Mol. Struct.*, **2008**,*891*, 450.

[21]Bi, W.-Y., Lu, X.-Q., Chai, W.-L., Jin, W.-J., Song, J.-R., Wong, W.-K., , *Inorg. Chem. Commun.*, **2008**, *11*, 1316.

Received: 23.11.2012.
Accepted: 04.11.2012.